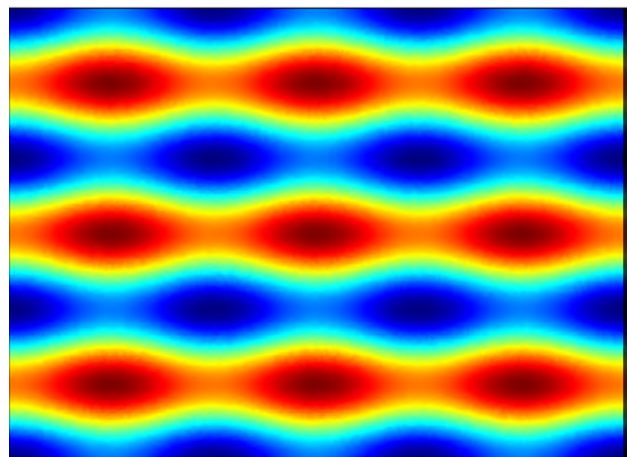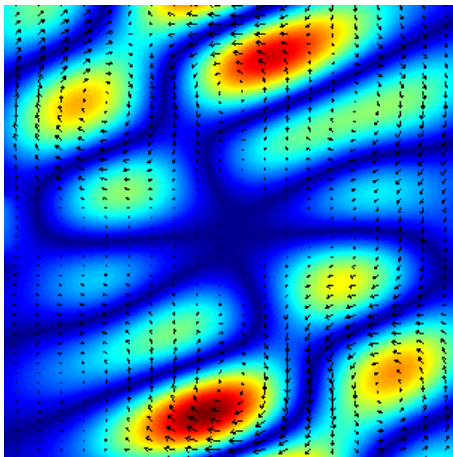Bachelor Thesis

Acoustofluidics in mirosystems: Theory and simulation

Torben Nielsen, s052614
Alan Wiinberg, s050294

Supervisor: Henrik Bruus

DTU Nanotech – Department of Micro and Nanotechnology
Technical University of Denmark

June 23, 2008

Abstract

In the recent years lab-on-a-chip devices have won seriously commercial recognition within various application fields. The evolving field of lab-on-a-chip systems has caused an increasing interest in fields like microfluidics and demanded a better theoretical insight. A subset of microfluidics is the field of acoustofluidics which provide the theoretical background for several lab-on-a-chip applications like pumping, separation, sorting, cleaning and mixing.

One of the interesting phenomenons observed in acousto fluidic microsystems is acoustic streaming. In earlier studies the fluid viscosity and the boundary layer effect have been investigated as potential sources of streaming but could not account for experimental results. Therefore the attention has turned to energy dissipation to the surroundings as a possible source of streaming. The main goal of this thesis is to investigate how the streaming phenomenon depends on the latter source.

The analytical approach is perturbation theory of second order which is applied to the continuity and Navier–Stokes equations. To handle more complex systems numerical computations in COMSOL have been executed.

A term coupled to the actual streaming velocity is derived. A comprehensive analysis of this term strongly indicates that energy dissipation to the surroundings in fact is a source of acoustic streaming. Furthermore, numerical calculations indicates how the amount of streaming depends on the energy dissipation. These results have contributed to a better understanding of the streaming phenomenon.

Resumé

I de seneste år har lab-on-a-chip systemer fået stor kommerciel anerkendelse indenfor forskellige anvendelsesområder. Det voksende felt indenfor lab-on-a-chip systemer har øget interessen indenfor felter som mikrofluidik og medført behov for en bedre teoretisk indsigt. Akustofluidik hører som forskningsområde under mikrofluidik og har leveret den teoretiske baggrund for adskillige anvendelser af lab-on-a-chip systemer som for eksempel pumpning, separation, sortering, rensning og blanding.

Akustisk strømning er en af de interessante fænomener, som er observeret i akustofluide mikrosystemer. I tidligere studier er fluidens viskositet og grænselagseffekten blevet undersøgt som potentielt ophav til akustisk strømning, men disse kunne ikke redegøre for eksperimentelle resultater. Derfor er opmærksomheden blevet rettet mod energitab til omgivelserne som et muligt ophav til den observerede akustiske strømning. Hovedformålet med denne afhandling er at undersøge, hvordan strømningsfænomenet afhænger af energitab til omgivelserne.

Den analytiske tilgang er perturbations teori til anden orden, som er blevet anvendt på kontinuitetsligningen og Navier–Stokes' ligning. For at kunne håndtere mere komplekse systemer er numeriske beregninger blevet udført i COMSOL.

Vi udleder et led, som er koblet til den faktiske strømningshastighed. En omfattende analyse af dette led indikerer stærkt, at energitab til omgivelserne faktisk giver ophav til akustisk strømning. Yderligere har numeriske beregninger indikeret, hvordan mængden af strømning afhænger af energitabet. Disse resultater har bidraget med en bedre forståelse af strømningsfænomenet.

Preface

The thesis hereby presented is titled "Acoustofluidics in mirosystems: Theory and simulation". It has been submitted in order to obtain 15 ECTS points and the Bachelor of Science degree at the Technical University of Denmark (DTU). The thesis documents the work done by Torben Nielsen (s052614) and Alan Wiinberg (s050294) during the spring semester from the 4th of February 2008 to the 23th of June 2008.

This bachelor thesis is written in the field of theoretically microfluidics and covers the area of acoustofluidics. The aim of this thesis is to continue the effort done by P. Skafte-Pedersen in his master thesis and explain the streaming phenomenon seen in resonant micro systems actuated by frequencies in the low MHz range.

Finally, we would like to thank our supervisor Professor Henrik Bruus for his inspiring guidance and long lasting patience. Secondly, thanks to M. Hagsäter for providing the experimental basis from which this project was inspired. Last we would like to express our gratitude to Ph.D. student P. Skafte-Pedersen for providing us with the results from his master project, and always being ready to help.

Acknowledgements

Torben Nielsen
Alan Wiinberg
DTU Nanotech – Department of Micro and Nanotechnology
Technical University of Denmark
June 23, 2008

Contents

List of Figures

List of Tables

List of symbols

Symbol	Description	Unit
ρ	Mass density	kg m^{-3}
$\boldsymbol{r}$	Position vector	m
$\boldsymbol{v}$	Velocity vector	m s^{-1}
v	Velocity	m s^{-1}
U	Velocity amplitude	m s^{-1}
$\boldsymbol{g}$	Gravity	N kg^{-1}
ℓ	Actuator amplitude	m
γ	Momentum diffusion length	m
λ	Wave length	m
k	Wave number	m^{-1}
k_0	Inviscid wave number	m^{-1}
c_a	Speed of sound	m s^{-1}
p	Pressure	N m^{-2}
f	Frequency	Hz
ω	Angular frequency	rad s^{-1}
ν	Kinematic viscosity	m^2 s^{-1}
μ	Dynamic viscosity	kg m^{-1} s^{-1}
T	Temperature	K
I_{aco}	Acoustic intensity	Kg m^{-3}
Z	Acoustic impedance	Kg m$^{-4}s^{-1}$
$\boldsymbol{n}$	Surface outward normal vector	
u	Solution to scalar problem	
h	Mesh size	
Re	Reynolds number	

Chapter 1

Introduction

In the recent years lab-on-a-chip devices have won seriously commercial recognition within various application fields. The evolving field of lab-on-a-chip systems has caused an increasing interest in fields like microfluidics and demanded a better theoretical insight. Lab-on-a-chip systems is more thoroughly described in section 1.1.

This bachelor thesis is written in the field of theoretically microfluidics and covers the area of acousto-fluidics. The work is among others motivated by the experimental results reported by Melker Hagsäter who observed radiation forces and streaming phenomenon in microfluidic systems. The description of his experimental setup and results is seen in section 1.3. The observed radiation force in his experiments has been thoroughly investigated and explained by Jensen [7]. The observed streaming has, however, found to be harder to account for. This thesis follows up on the work done by Peter Skafte-Pedersen [2], trying to give a reasonable explanation for the streaming seen in experiments. In this thesis the treatment of acousto-fluidics as a whole is restricted to involve theory and investigation which can be used to gain an understanding of the streaming phenomenon.

In the remaining of this chapter we will give a short introduction to lab-on-a-chip systems, acousto-fluidics, the experimental setup and results. Finally, we will make a short outline for the rest of the thesis.

1.1 Lab-on-a-chip systems

Lab-on-a-chip research is a relatively new area of research which started to grow seriously two decades ago. The basic idea is to integrate one or multiple laboratory functions on a single chip where the laboratorial setup is on a 100μm scale. Lab-on-a-chip is especially well-suited for areas like medical diagnostics and biochemical measurements. An advantage is that provides a fast analysis which only requires a very small sample to be available. Furthermore, lab-on-a-chip systems are cheap and flexible due to their small size. Lab-on-a-chip systems are already widely in use and have a broad range of applications, e.g. measurement of blood sugar for diabetes patients, DNA analysis and drug testing.

Shrinking a laboratory setup to a 100μm scale also have some consequences which one have to take into account. When the system is minimized the ratio of surface compared to volume will increase significantly and thus surface forces, as surface tension, will become more important. On the contrary volume forces, like gravity and inertia, will become less dominating.

1.2 Fluid description

All liquids and all gases are fluids. The problem at hand does however only involve liquid flow. Some important physical properties of liquids to be used throughout this thesis is the mass density and the sound velocity. The value of all the material parameters used is listed in appendix A.

Liquids such as water have relatively high mass density. This is caused by the fact that the molecules is packed with an average intermolecular distance of 0.3 nm [1]. The fact that the molecules are packed so densely in most liquids implies that the compressibility of liquids is quite low. Thus for many practically purposes most liquids can be treated as being incompressible. However, when dealing with sound propagation in liquid

systems the compressibility is, no matter how small, necessary to take into account. The reason is that sound is transmitted through fluids as longitudinal waves, also called compression waves. Longitudinal sound waves are waves of alternating pressure deviations from the equilibrium pressure, causing local regions of compression and rarefaction.

As we in this thesis will not be working with liquid on a length scale smaller than about 0.5 mm, which is a macroscopic length scale, we can safely assume that the continuum hypothesis holds. In short the continuum hypothesis states that even though a liquid consist of molecules, it can be treated as having a perfectly continuous structure. The continuum hypothesis also leads to the concept of fluid particles which have a finite size. The fluid particles should big enough for the continuum hypothesis to hold but small enough to keep the fluid properties unchanged by the influence of external forces. Thus the size of such a fluid particles should have a length scale about $10\,\mathrm{nm}$ to $10\,\mu\mathrm{m}$ [1]. Notice that the given length scale is not a perfectly well-defined size. Because of the continuum hypothesis it is natural to work with physical properties per volume such as mass density and momentum density.

When describing the behavior of a fluid, e.g. the flow, one commonly makes use of a Eulerian description. In the Eulerian description one consider any field variable at a fixed position $\mathbf{r}$, independent of the time t, for all times t. In other words the coordinate system is fixed for all times when the Eulerian description is used. Therefore one can observe how the fields at certain observation points evolve in time.

1.3   Acousto-fluidics and experimental data

Acoustic forces can be utilized for several lab-on-a-chip applications, including basic functionalities such as pumping, separation, sorting, cleaning and mixing [8]. This has motivated the experimental studies by Melker Hagsäter [8] of acoustic radiation forces and acoustic streaming in microfluidic chambers under piezo-actuation in the MHz range. The study was, among other things, based on a square chamber with a side-length of 2 mm, etched in a silicon wafer. The chamber was connected to 400 μm wide inlet and outlet channels, and the depth was 200 μm throughout. The chamber was filled with water and tracer particles. The size of the tracer particles was in the experiments variated in order to show the different acoustic effects. The piezo-actuator was pressed to the backside of the silicon wafer. The area of the actuator was of such size that the entire chamber was easily covered. In figure 1.1 a top-view photograph of the chip is shown.

Figure 1.2 shows some of the experimental results captured by particle image velocimetry (PIV). The two images show both streaming drag and radiation forces occurring at the same resonance frequency. The radiation force, which depends on the pressure, is seen to dominate for large particles, and the viscous streaming drag is likewise seen to dominate for the small particles. The streaming drag on the water is seen to manifest itself as a characteristic 6×6 pattern of vortices.

Acoustic streamning is a non-linear phenomenon that occurs when sound waves transmitted through a viscous fluid give rise to a time-independent movement of the bulk fluid with a given streaming velocity. The acoustic radiation force is a non-linear, time-independent phenomenon arising in a sound field when particles or other obstacles are present and get affected by the radiation force. The radiation force on larger particles results in particle accumulation at the pressure nodal lines [2].

In order to fully understand the dynamics in the system a theoretical explanation of the streaming patterns in figure 1.2 has been sought. A theoretical study of the streaming phenomenon in the system, e.g. seen in figure 1.2 (b), has been made by Peder Skafte-Pedersen. Viscous damping and the boundary layer effect in the system were proposed as potential sources of the streaming pattern but turned out not to provide a satisfying explanation for the experimental observations [2]. A third alternative explanation was proposed to be the transmission loss to the surroundings, however, this potential source of streaming has not been fully investigated yet.

1.4   Project aim

The aim in this thesis is to continue the effort done by P. Skafte-Pedersen in his master thesis to explain the streaming phenomenon seen in resonant microsystems actuated at frequencies in the low MHz range. The frame of reference is the experimental results obtained by M. Hagsäter during his Ph.D. work. The main focus
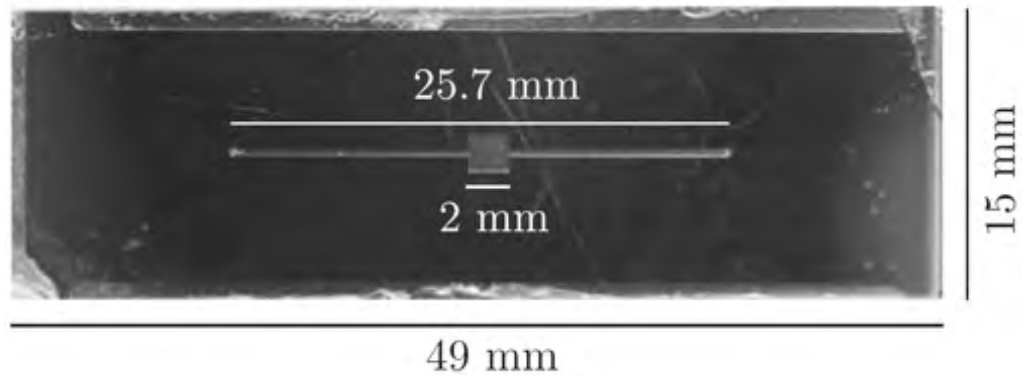
Figure 1.1: The figure shows a top-view photograph of the silicon chip (dark gray) containing a square chamber with straight inlet and outlet channels (light gray). Courtesy of M. Hagsäter.
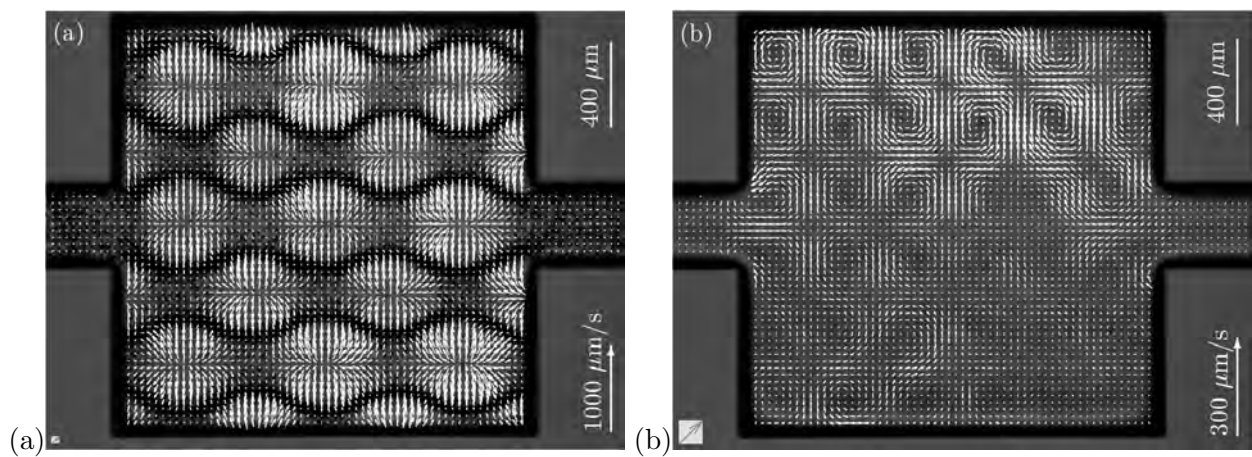
Figure 1.2: Experimental results obtained by particle image velocimetry (PIV) of (a) acoustic streaming with 1 μm tracer beads and (b) radiation forces on 5 μm beads. The acoustic streaming of the water is seen to manifests itself as a characteristic 6×6 pattern of vortices. Experimental pictures courtesy of M. Hagsäter.

will here concern the energy dissipation to the surroundings as a source of streaming. However, also general acousto-fluidic problems will be considered, and other sources of streaming will be presented.

Chapter 2

Generel fluid theory

In this chapter we will account for the basic theory which can be used to gain an understanding of acoustofluidic problems in general and the streaming phenomonen in particular. First the governing equations will be introduced and the basic approach of perturbation theory will be treated. Pertubation theory will be used in order to give an expression for the acoustic streaming. The wave equation will be derived for both undamped and damped systems. Finally, the basics of boundary layer theory will be presented.

2.1 Governing equations

For the treatment of fluid dynamic problems two main equations are used. These are the continuity equation which express the conversation of mass, and the Navier–Stokes equation which express the conversation of momentum. Also a third equation, the heat transfer equation, which governs the conversation of energy exists. However, as we will not be considering thermal effects this equation will not be treated.

In many fluid dynamic problems the fluid is considered to be inviscous and incompressible. However, compressibility is a fundamental condition for the propagation of sound, and viscousity gives rise to many acousto-fluidic phenomonon, and thus both compressibility and visousity will be taken into account in the following chapters of this thesis.

The continuity equation is derived in appendix C and for a compressible fluid it reads

$$\partial_t \rho(\mathbf{r}, t) = -\boldsymbol{\nabla} \cdot (\rho \mathbf{v}) \tag{2.1}$$

We see that the continuity equation is a linear, partial differential equation of first order. As mentioned the continuity equation describes the conversation of mass. It arises when an arbitrary volume is considered, and one equals the change in mass with the mass flux through the volume surface.

The Navier–Stokes equation for a compressible, viscous, Newtonian fluid is derived in appendix D is given by

$$\rho[\partial_t \mathbf{v} + (\mathbf{v} \cdot \boldsymbol{\nabla})\mathbf{v}] = -\boldsymbol{\nabla} p + \eta \nabla^2 \mathbf{v} + \left(\zeta + \frac{\eta}{3}\right) \boldsymbol{\nabla}(\boldsymbol{\nabla} \cdot \mathbf{v}) \tag{2.2}$$

The Navier–Stokes equation is a unlinear, partial differential equation of second order. It can be derived considering an arbitrary volume, and the change of momentum is expressed by the sum of convection through a volume and forces acting on the volume. The forces that needs to be considered is pressure forces and viscous forces.

The Navier–Stokes equation can be given a physical interpretation. The first term on the left hand side is the usual acceleration times mass per volume which is known from Newtons second law. As we are using the Eulerian description the second term on the right hand side is added. The first term on the left hand side occurs from pressure forces acting on the fluid. The last two terms on the right hand side express the viscous forces affecting the fluid. The first viscous term express the internal friction due to shear stress, and

the second viscous term express the internal frition due to compression. η and ζ are called the dynamic and second viscosity, respectively, and can be approximated by $\eta \approx 10^{-3}$ Pa s and $\zeta \approx \frac{4}{3} \times 10^{-3}$ Pa s [1].

As mentioned thermal effects will not be considered in this report, however, we will need a single result from thermodanamics. It can easely be derived, e.g. from the ideal gas law, that the pressure depends on the density, thus

$$p = p(\rho) \tag{2.3}$$

2.2   The Reynolds number

When characterizing a given fluidic problem it is important to show whether the flow is laminar or turbulent. For this purpose the Reynolds number can be calculated for the given system. Laminar flow occurs at low Reynolds numbers, where viscous forces are dominant, and is characterized by smooth, constant fluid motion. Turbulent flow, on the other hand, occurs at high Reynolds numbers and is dominated by inertial forces which tend to produce random vortices and other flow fluctuations [3]. In this section we want to identify in which flow regime the given microfluidic problem is.

The Reynolds number is given as the ratio of inertial forces $\left(\frac{V_0}{\rho}\right)$ to viscous forces $\left(\frac{\eta}{L_0}\right)$ [1, eq. (2.39)]

$$\mathrm{Re} \equiv \frac{\rho V_0 L_0}{\eta} \approx \frac{10^3 \mathrm{kg/m}^3 \cdot 10^{-5}\mathrm{m/s} \cdot 10^{-3}\mathrm{m}}{10^{-3}\mathrm{Pa\,s}} \approx 10^{-2} \tag{2.4}$$

The used parameters are for a system consisting of a waterfilled square silicon microchamper and an ultrasound frequency of order 1 MHz [1, p. 266].

It is seen that the calculated Reynolds number is low, i.e. $\mathrm{Re} \ll 1$, thus the flow is expected to be in the laminar regime.[kilde Bruus bog side 26]

2.3   General perturbation theory

The derived governing equations for microfluidic problems are seen to be a set of coupled, partial differential equations. The problem here is the non-linearity of the Navier–Stokes equation. Because of this the system of equations can only be solved analytical in a few idealized cases. The solution can, however, for most cases be approximated analytically using perturbation theory.

Perturbation theory in generel comprises mathematical methods that are used to find an approximate solution to a problem which cannot be solved excatly. This is done by starting from the exact solution of a related problem. The theory is applicable when the non-linear equation can be formulated by adding a small term to the equation of an exactly solvable problem.

By making the non-linear Navier–Stokes equation dimensionless the relative size of the non-linear term can be found by comparing it to the linear terms. The relative size of the non-linear term is called the perturbation parameter. Thus it describes how far the non-linear equation deviates from the simpler linear equation. When the perturbation parameter is sufficiently small we can assume that the solution of the non-linear equation can be expressed as a power series in the perturbation parameter α. Thus in general we have

$$u = u_0 + \alpha u_1 + \alpha^2 u_2 + ..., \tag{2.5}$$

The first term u_0 is the solution to the unperturbed equation. Here we observe that the perturbation parameter α should be smaller than one , or else the power series will diverge.

The non-linear equation can be formulated in terms of some partial differential operator D acting on $u(\mathbf{r}, t)$

$$\mathrm{D}u(\mathbf{r}, t) = 0 \tag{2.6}$$

Now assume that the differential operator can be written as a series expansion

$$\mathrm{D} = \mathrm{D}_0 + \alpha \mathrm{D}_1 + \alpha^2 \mathrm{D}_2 + ..., \tag{2.7}$$

Inserting the perturbation series for D and u in (2.6) we get

$$
\begin{aligned}
\mathrm{D}u &= (\mathrm{D}_0 + \alpha\mathrm{D}_1 + \alpha^2\mathrm{D}_2 + ...)(u_0 + \alpha u_1 + \alpha^2 u_2 + ...) && \text{(2.8a)} \\
&= \mathrm{D}_0 u_0 + \alpha(\mathrm{D}_1 u_0 + \mathrm{D}_0 u_1) + \alpha^2(\mathrm{D}_2 u_0 + \mathrm{D}_1 u_1 + \mathrm{D}_0 u_2) + ... && \text{(2.8b)} \\
&= 0 && \text{(2.8c)}
\end{aligned}
$$

For this to hold for any value of α each term must be zero, as they are linear independent. Therefore we get the following infinite system of equations to solve

$$
\begin{aligned}
\mathrm{D}_0 u_0 &= 0 && \text{(2.9a)} \\
\mathrm{D}_1 u_1 &= -\mathrm{D}_1 u_0 && \text{(2.9b)} \\
\mathrm{D}_0 u_2 &= -\mathrm{D}_2 u_0 - \mathrm{D}_1 u_1 && \text{(2.9c)} \\
&\quad... && \text{(2.9d)}
\end{aligned}
$$

This perturbation procedure should also be applied to the given boundary condition. The zero order equation should be solved first by using the zeroth order boundary conditions. The found solution should then be inserted into the first order equation which now can be solved by using the first order boundary conditions and so forth. The difference between the correct solution and the approximated decrease as more terms are taken into account in the power series. In most cases, however, it is only worthwhile to calculate up to the second order contribution.

2.4 Perturbation of the governing equations

In order to pertubate the given system of coupled partial differential equations we expand the velocity and density in power series in some small perturbation parameter α. We will calculate up to the second order contribution. The pressure is additionally taylor expanded to second order around the stationary value of the density ρ_0. The unperturbed (stationary) state is taken to be a homogeneous liquid at rest in thermal equilibrium. Thus the zero order terms take constant values, and the initial velocity is zero. The governing equations was found in section 2.1 to be

$$
\begin{aligned}
p &= p(\rho) && \text{(2.10a)} \\
\partial_t \rho(\mathbf{r}, t) &= -\boldsymbol{\nabla} \cdot (\rho\mathbf{v}) && \text{(2.10b)} \\
\rho[\partial_t \mathbf{v} + (\mathbf{v} \cdot \boldsymbol{\nabla})\mathbf{v}] &= -\boldsymbol{\nabla}p + \eta\nabla^2\mathbf{v} + \left(\zeta + \frac{\eta}{3}\right)\boldsymbol{\nabla}(\boldsymbol{\nabla} \cdot \mathbf{v}) && \text{(2.10c)}
\end{aligned}
$$

The expanded velocity, density and pressure is given by

$$
\begin{aligned}
\mathbf{v} &= 0 + \alpha\mathbf{v}_1 + \alpha^2\mathbf{v}_2 + ... && \text{(2.11a)} \\
\rho &= \rho_0 + \alpha\rho_1 + \alpha^2\rho_2 + ... && \text{(2.11b)} \\
p(\rho) &= p_0 + (\partial_\rho p)_0(\rho - \rho_0) + \frac{1}{2}(\partial_\rho^2 p)_0(\rho - \rho_0)^2 + ... && \text{(2.11c)}
\end{aligned}
$$

We have set $\mathbf{v}_0 = \mathbf{0}$ as we assume our initial system to be a steady state system with zero initial velocity. The zero order terms p_0 and ρ_0 are constant initial values.

By using (2.11) and the termodynamical result $(\partial_\rho p)_0 = c_a^2$, where c_a is the speed of sound as shown in appendix B, we get

$$
\begin{aligned}
p(\rho) &= p_0 + c_a^2(\rho_0 + \alpha\rho_1 + \alpha^2\rho_2 - \rho_0) + \frac{1}{2}(\partial_\rho c_a^2)_0(\rho_0 + \alpha\rho_1 + \alpha^2\rho_2 - \rho_0)^2 && \text{(2.12a)} \\
&= p_0 + c_a^2(\alpha\rho_1 + \alpha^2\rho_2) + \frac{1}{2}(\partial_\rho c_a^2)_0\alpha^2\rho_1^2 && \text{(2.12b)} \\
&= p_0 + \alpha c_a^2\rho_1 + \alpha^2(c_a^2\rho_2 + \frac{1}{2}(\partial_\rho c_a^2)_0\rho_1^2) && \text{(2.12c)}
\end{aligned}
$$

Notice that we only calculate up to the second order contribution, thus all terms including α^3 or higher orders are excluded.

The expansions in (2.11) are now inserted into the continuity equation (2.10b)

$$\partial_t(\rho_0 + \alpha\rho_1 + \alpha^2\rho_2) = -\boldsymbol{\nabla} \cdot ((\rho_0 + \alpha\rho_1 + \alpha^2\rho_2)(\alpha\mathbf{v}_1 + \alpha^2\mathbf{v}_2)) \Rightarrow \tag{2.13a}$$

$$\partial_t\rho_0 + \alpha\partial_t\rho_1 + \alpha^2\partial_t\rho_2 = -\alpha\boldsymbol{\nabla} \cdot (\mathbf{v}_1\rho_0) - \alpha^2\boldsymbol{\nabla} \cdot (\mathbf{v}_1\rho_1 + \mathbf{v}_2\rho_0) \tag{2.13b}$$

The expansions in (2.11) are now inserted into the left hand side (LHS) and next into the right hand side (RHS) of the Navier–Stokes equation (2.10c) and thus

$$\text{LHS} = (\rho_0 + \alpha\rho_1 + \alpha^2\rho_2)[\partial_t(\alpha\mathbf{v}_1 + \alpha^2\mathbf{v}_2) + ((\alpha\mathbf{v}_1 + \alpha^2\mathbf{v}_2) \cdot \boldsymbol{\nabla})(\alpha\mathbf{v}_1 + \alpha^2\mathbf{v}_2)] \tag{2.14a}$$

$$= \rho_0\partial_t(\alpha\mathbf{v}_1 + \alpha^2\mathbf{v}_2) + \alpha^2\rho_1\partial_t\mathbf{v}_1 + \alpha^2\rho_0(\mathbf{v}_1 \cdot \boldsymbol{\nabla})\mathbf{v}_1 \tag{2.14b}$$

$$= \alpha\rho_0\partial_t\mathbf{v}_1 + \alpha^2(\rho_0\partial_t\mathbf{v}_2 + \rho_1\partial_t\mathbf{v}_1 + \rho_0(\mathbf{v}_1 \cdot \boldsymbol{\nabla})\mathbf{v}_1) \tag{2.14c}$$

$$\text{RHS} = -\boldsymbol{\nabla}(p_0 + \alpha p_1 + \alpha^2 p_2) + \eta\nabla^2(\alpha\mathbf{v}_1 + \alpha^2\mathbf{v}_2) + (\zeta + \frac{\eta}{3})\boldsymbol{\nabla}(\boldsymbol{\nabla} \cdot (\alpha\mathbf{v}_1 + \alpha^2\mathbf{v}_2)) \tag{2.15a}$$

$$= -\boldsymbol{\nabla}p_0 + \alpha(\eta\nabla^2\mathbf{v}_1 + (\zeta + \frac{\eta}{3})\boldsymbol{\nabla}(\boldsymbol{\nabla} \cdot \mathbf{v}_1) - \boldsymbol{\nabla}p_1) + \alpha^2(\eta\nabla^2\mathbf{v}_2 + (\zeta + \frac{\eta}{3})\boldsymbol{\nabla}(\boldsymbol{\nabla} \cdot \mathbf{v}_2) - \boldsymbol{\nabla}p_2)$$

By remembering α^0, α^1, and α^2 as linear independent from each other, we get the following system of coupled equations

$$\alpha^0 : \qquad \partial_t\rho_0 = 0 \tag{2.16a}$$

$$\nabla p_0 = 0 \tag{2.16b}$$

$$\alpha^1 : \qquad p_1 = c_a^2\rho_1 \tag{2.17a}$$

$$\partial_t\rho_1 = -\rho_0\nabla \cdot \mathbf{v}_1 \tag{2.17b}$$

$$\rho_0\partial_t\mathbf{v}_1 = \eta\nabla^2\mathbf{v}_1 + (\zeta + \frac{\eta}{3})\nabla(\nabla \cdot \mathbf{v}_1) - \nabla p_1 \tag{2.17c}$$

$$\alpha^2 : \qquad p_2 = c_a^2\rho_2 + \frac{1}{2}(\partial_\rho c_a^2)_0\rho_1^2 \tag{2.18a}$$

$$\partial_t\rho_2 = -\nabla \cdot (\mathbf{v}_1\rho_1 + \mathbf{v}_2\rho_0) \tag{2.18b}$$

$$\rho_0\partial_t\mathbf{v}_2 = \eta\nabla^2\mathbf{v}_2 + (\zeta + \frac{\eta}{3})\nabla(\nabla \cdot \mathbf{v}_2) - \nabla p_2 - \rho_1\partial_t\mathbf{v}_1 - \rho_0(\mathbf{v}_1 \cdot \nabla)\mathbf{v}_1 \tag{2.18c}$$

It can also be seen that constants are solutions to the unperturbed governing equations as they should be.

2.5 Acoustic Streaming

As mentioned in the introduction we want to investigate the acoustic streaming phenomen in microscale systems. As the streaming is recorded by a series of discrete measurements done by PIV the observed velocity field is actually an average over time. Thus the further treatment of the governing equations will only concern the time-averaged equations and results.

As we are considering frequencies in the MHz range the period of one oscillation will be much smaller than the time between two successive measurements done by PIV. As all the first order field has the same time dependence as the oscillations the time average of these can be considered to be zero. However, the second order fields given by (2.18) are seen to contain products of two time harmonic first order fields. The time-average of two such fields are given by [1, eq. (10.49]

$$\langle A(t)B(t)\rangle = \frac{1}{2}\text{Re}\,[A_0 B_0^*] \tag{2.19}$$

Here the asterix denotes the complex conjugate, and A_0, B_0 are complex amplitudes. Thus the time-average of the product of two first order fields is different from zero. By intuition this makes good sense as a time-average of a product of two first order harmonic factors, i.e. $\langle \cos^2(\omega t) \rangle$, is $\frac{1}{2}$.

The time-average of the second order pertubation of the continuity equation is given by

$$\langle \partial_t \rho_2 \rangle \;=\; -\langle \nabla \cdot (\mathbf{v}_1 \rho_1 + \mathbf{v}_2 \rho_0) \rangle \Rightarrow \tag{2.20a}$$

$$0 \;=\; -\nabla \cdot (\langle \mathbf{v}_1 \rho_1 \rangle + \rho_0 \langle \mathbf{v}_2 \rangle) \Rightarrow \tag{2.20b}$$

$$\nabla \cdot \langle \mathbf{v}_2 \rangle \;=\; -\frac{1}{\rho_0} \nabla \cdot \langle \mathbf{v}_1 \rho_1 \rangle \tag{2.20c}$$

We have used that in steady state with a harmonic driving force, the second order fields must be periodic in the fundamental period, and thus they can be decomposed in Fourier series which may contain a constant terms. After taking the time derivative the constants are eliminated, and by time averaging all the remaining (higher) harmonics are also eliminated, yielding $\langle \partial_t \rho_2 \rangle = 0$ and $\langle \partial_t \mathbf{v}_2 \rangle = \mathbf{0}$.

The second order perturbation of the Navier–Stokes' equation will now be time averaged. From above we saw that $\langle \partial_t \mathbf{v}_2 \rangle = 0$ and thus a time average of equation (2.18c) will yield

$$\nabla \langle p_2 \rangle \;=\; \eta \nabla^2 \langle \mathbf{v}_2 \rangle + (\zeta + \frac{\eta}{3}) \nabla (\nabla \cdot \langle \mathbf{v}_2 \rangle) - \langle \rho_1 \partial_t \mathbf{v}_1 \rangle - \rho_0 \langle (\mathbf{v}_1 \cdot \nabla) \mathbf{v}_1 \rangle \tag{2.21}$$

The divergence is hereafter taken on both sides, and (2.20c) is inserted, thus

$$\nabla^2 \langle p_2 \rangle \;=\; \eta \nabla^2 \nabla \cdot \langle \mathbf{v}_2 \rangle + (\zeta + \frac{\eta}{3}) \nabla^2 (\nabla \cdot \langle \mathbf{v}_2 \rangle) - \nabla \cdot \langle \rho_1 \partial_t \mathbf{v}_1 \rangle - \rho_0 \nabla \cdot \langle (\mathbf{v}_1 \cdot \nabla) \mathbf{v}_1 \rangle \tag{2.22a}$$

$$=\; (\zeta + \frac{4\eta}{3}) \nabla^2 \nabla \cdot \langle \mathbf{v}_2 \rangle + i\omega \nabla \cdot \langle \rho_1 \mathbf{v}_1 \rangle - \rho_0 \nabla \cdot \langle (\mathbf{v}_1 \cdot \nabla) \mathbf{v}_1 \rangle \tag{2.22b}$$

$$=\; -\frac{\zeta + \frac{4\eta}{3}}{\rho_0} \nabla^2 \nabla \cdot \langle \mathbf{v}_1 \rho_1 \rangle + i\omega \nabla \cdot \langle \rho_1 \mathbf{v}_1 \rangle - \rho_0 \nabla \cdot \langle (\mathbf{v}_1 \cdot \nabla) \mathbf{v}_1 \rangle \tag{2.22c}$$

$$=\; -\left(\frac{\zeta + \frac{4\eta}{3}}{\rho_0} \nabla^2 - i\omega \right) \nabla \cdot \langle \mathbf{v}_1 \rho_1 \rangle - \rho_0 \nabla \cdot \langle (\mathbf{v}_1 \cdot \nabla) \mathbf{v}_1 \rangle \tag{2.22d}$$

Now by inserting (2.18a) we get

$$\nabla^2 \langle \rho_2 \rangle \;=\; -\left(\frac{\zeta + \frac{4\eta}{3}}{\rho_0 c_a^2} \nabla^2 - i\frac{\omega}{c_a^2} \right) \nabla \cdot \langle \mathbf{v}_1 \rho_1 \rangle - \frac{\rho_0}{c_a^2} \nabla \cdot \langle (\mathbf{v}_1 \cdot \nabla) \mathbf{v}_1 \rangle - \frac{1}{2 c_a^2} (\partial_\rho c_a^2)_0 \nabla^2 \langle \rho_1^2 \rangle \tag{2.23}$$

This is the time-averaged second order pertubed Navier–Stokes equation.

A possible solution to (2.20c) is seen to be

$$\langle \mathbf{v}_2 \rangle = -\frac{1}{\rho_0} \langle \rho_1 \mathbf{v}_1 \rangle + \langle \mathbf{v}_{2\mathrm{inc}} \rangle \tag{2.24}$$

where $\langle \mathbf{v}_{2\mathrm{inc}} \rangle$ must fulfill the incompressible continuity equation

$$\nabla \cdot \langle \mathbf{v}_{2\mathrm{inc}} \rangle = 0 \tag{2.25}$$

However, it should be noted that this expression is not guaranteed to be a solution to a given boundary value problem.

In order to find $\langle \mathbf{v}_{2\mathrm{inc}} \rangle$ it is necessary to reformulate the impermeable boundary conditions given in section 2.8. In addition it is required to solve the time-averaged second order perturbed Navier–Stokes equation for $\langle \mathbf{v}_{2\mathrm{inc}} \rangle$. Because of time concern there has not been time for such an analysis during this thesis, but it would definitely be interesting to investigate further as it is an important part of the next step in understanding the streaming phenomenon.

It is seen that the trivial solution, $\langle \mathbf{v}_{2\mathrm{inc}} \rangle = 0$, is a valid solution for equation (2.25). This is hardly the right solution, but as we have not fully solved the time-averaged second order equations we are not able to determine $\langle \mathbf{v}_{2\mathrm{inc}} \rangle$. Thus we are forced only to consider the term $-\frac{1}{\rho_0} \langle \rho_1 \mathbf{v}_1 \rangle$ which we are able to calculate. Well knowing that this expression is only coupled to the full solution we will throughout the rest of this thesis refer to this term as the streaming velocity and thus assume

$$\langle \mathbf{v}_2 \rangle = -\frac{1}{\rho_0} \langle \rho_1 \mathbf{v}_1 \rangle \tag{2.26}$$

Even though this is not excactly correct it is reasonable to asssume that (2.26) will provide a indication of the form of the real solution. In other words, if (2.26) turns out to generate a streaming pattern it would would be likely that also the real solution would give a similar streaming pattern.

It should be noted that the streaming velocity given by (2.26) consists of a product of two first order fields, and thus it is seen by equation (2.19) that the oscillating acoustic field will impart a time-independent (DC) component to the velocity of the fluid.

Last we find the combination of equation (2.19) and (2.26) to yield

$$\langle \mathbf{v}_2 \rangle \quad = \quad -\frac{1}{2\rho_0} \mathrm{Re} \left[\mathbf{v}_{01} \rho_{01}^* \right] \tag{2.27}$$

2.6   Deriving the wave equation

When the viscosity is neglected the first order perturbations of the continuity and the Navier–Stokes equation in (2.17) are reduced to

$$\partial_t \rho_1 \quad = \quad -\rho_0 \boldsymbol{\nabla} \cdot \mathbf{v}_1 \tag{2.28a}$$
$$\rho_0 \partial_t \mathbf{v}_1 \quad = \quad -\boldsymbol{\nabla} p_1 \tag{2.28b}$$

Now by using that $p_1 = c_a^2 \rho_1$ and differentiating with respect to t on both sides of equation (2.28a) and finally taking the divergence on both sides of equation (2.28b) we get the following two equations

$$c_a^{-2} \partial_t^2 p_1 \quad = \quad -\rho_0 \partial_t (\boldsymbol{\nabla} \cdot \mathbf{v}_1) \tag{2.29a}$$
$$\rho_0 \partial_t (\boldsymbol{\nabla} \cdot \mathbf{v}_1) \quad = \quad -\nabla^2 p_1 \tag{2.29b}$$

Notice that we have used $\partial_i \partial_t v_i = \partial_t \partial_i v_i$ as $\mathbf{v}$ is assumed to be a sufficiently smooth function. Combining these two equations we get

$$\frac{1}{c_a^2} \partial_t^2 p_1 \quad = \quad \nabla^2 p_1 \tag{2.30}$$

This equation is recognized as a standard wave equation. Comparing to the general form of a wave equation $\nabla^2 \psi = \frac{1}{v^2} \partial_t^2 \psi$, where v is the speed of the wave, we can, again, see that c_a must be the speed of sound as equation (2.30) describes a pressure wave which is a sound wave by definition.

The solution to the wave equation depends on the boundary and initial conditions. However, for any double differentiable function f it is easely found by direct substituting that $p_1(x,t) = f(x \pm c_a t)$ is a solution to the one-dimensional form of equation (2.30).

A simple special case of a solution to equation (2.30) is the planar wave with amplitude ρ_{10} propagating along the wavevector $\mathbf{k} = k\,\mathbf{e}_k$ with the angular frequency $\omega = c_a k$

$$p_1 = p_{10}\, e^{i(\mathbf{k} \cdot \mathbf{r} - \omega t)} \tag{2.31}$$

In relation to the frequency f and the wavelength λ we have

$$\omega \quad = \quad 2\pi f \tag{2.32}$$
$$k \quad = \quad \frac{2\pi}{\lambda} \tag{2.33}$$

Another class of simple solutions to the wave equation (2.30) is the standing waves

$$p_1(\mathbf{r}, t) = p_1(\mathbf{r}) e^{-\mathrm{i}\omega t} \tag{2.34}$$

Inserting this into the wave equation we get

$$\nabla^2 (p_1(\mathbf{r}) e^{-\mathrm{i}\omega t}) = \frac{1}{c_a^2} \partial_t^2 (p(\mathbf{r}) e^{-\mathrm{i}\omega t}) \tag{2.35a}$$

$$\Leftrightarrow$$

$$\nabla^2 p_1(\mathbf{r}) = \frac{\omega^2}{c_a^2} p_1(\mathbf{r}) = k^2 p_1(\mathbf{r}) \tag{2.35b}$$

This is a Helmholtz equation which can be solved for given boundary conditions and which do not depend on time. This equation only have solutions for certain, discrete values of the wavenumber k. These solutions is the so-called eigenmodes for the system.

In this section we have assumed that the viscosity is neglectable. This assumption was made to make the situation more simple to analyze for the time being. In the next section we will include the viscosity and estimate the characteristic damping lenght for sound waves in a acoustofludic system.

2.7 Viscous damping in first order fields

In this section we are going to investegate what happens when the viscous damping is not neglected in the first order pertubation. The first order pertubation of the viscous Navier–Stokes equation reads

$$\rho_0 \partial_t \mathbf{v}_1 = -c_a^2 \boldsymbol{\nabla} \rho_1 + \eta \nabla^2 \mathbf{v}_1 + (\zeta + \frac{\eta}{3}) \boldsymbol{\nabla} (\boldsymbol{\nabla} \cdot \mathbf{v}_1) \tag{2.36}$$

By taking the divergence of this equation and interchanging the order of differentiation in various terms, we obtain

$$\rho_0 \partial_t (\boldsymbol{\nabla} \cdot \mathbf{v}_1) = -\nabla^2 p_1 + (\zeta + \frac{4\eta}{3}) \nabla^2 (\boldsymbol{\nabla} \cdot \mathbf{v}_1) \tag{2.37}$$

In order to derive a equation for p_1 we insert the first order continuity equation (2.17b) in the equation above

$$-c_a^{-2} \partial_t^2 p_1 = -\nabla^2 p_1 - c_a^{-2} \frac{\zeta + \frac{4\eta}{3}}{\rho_0} \nabla^2 (\partial_t p_1) \tag{2.38a}$$

$$\Leftrightarrow$$

$$\partial_t^2 p_1 = c_a^2 \nabla^2 p_1 + \frac{\zeta + \frac{4\eta}{3}}{\rho_0} \nabla^2 (\partial_t p_1) \tag{2.38b}$$

In the case where the boundary conditions consist of harmonic oscillations in time we seek solutions with an harmonic time dependence, thus

$$p_1(\mathbf{r}, t) = p_1(\mathbf{r}) e^{-\mathrm{i}\omega t} \tag{2.39}$$

Inserting this solution into equation (2.38) we arrive at a wave equation for the first-order pressure field p_1,

$$\partial_t^2 p_1(\mathbf{r}) e^{-\mathrm{i}\omega t} = c_a^2 \nabla^2 p_1(\mathbf{r}) e^{-\mathrm{i}\omega t} + \frac{\zeta + \frac{4\eta}{3}}{\rho_0} \nabla^2 (\partial_t p_1(\mathbf{r}) e^{-\mathrm{i}\omega t}) \tag{2.40a}$$

$$\Leftrightarrow$$

$$-\omega^2 p_1(\mathbf{r}) e^{-\mathrm{i}\omega t} = c_a^2 \left[1 - \mathrm{i} \frac{(\zeta + \frac{4\eta}{3})\omega}{\rho_0 c_a^2} \right] \nabla^2 p_1(\mathbf{r}) e^{-\mathrm{i}\omega t} \tag{2.40b}$$

$$\Leftrightarrow$$

$$\omega^2 p_1 = -c_a^2 [1 - \mathrm{i}2\gamma] \nabla^2 p_1 \tag{2.40c}$$

Where we have defined γ as

$$\gamma(\omega) \quad \equiv \quad \frac{(\zeta + \frac{4\eta}{3})\omega}{2\rho_0 c_a^2} \tag{2.41}$$

The value of γ is quite small for ultrasound waves used in acoustofluidics with $\omega \approx 10^7 \mathrm{s}^{-1}$ in water

$$\gamma \quad \approx \quad \frac{\frac{8}{3} \cdot 10^{-3}\,\mathrm{Pa \cdot s}\,10^7\,\mathrm{s}^{-1}}{2 \cdot 10^3\,\frac{\mathrm{kg}}{\mathrm{m}^3} \cdot (1.5 \cdot 10^3\,\frac{\mathrm{m}}{\mathrm{s}})^2} \tag{2.42a}$$

$$\approx \quad 0.6 \cdot 10^{-5} \ll 1. \tag{2.42b}$$

The small value of γ implies that we can make the approximation $[1 - \mathrm{i}2\gamma] = [1 + \mathrm{i}\gamma]^{-2}$. The next step is to isolate $\nabla^2 p_1$ in (2.40) and thus obtain the final version of the wave equation for ρ_1

$$\nabla^2 p_1 = -\left[\frac{\omega}{c_a}(1 + \mathrm{i}\gamma)\right]^2 p_1 = -[k_0(1 + \mathrm{i}\gamma)]^2 p_1 = -k^2 p_1 \tag{2.43}$$

This equation is seen to be a Helmholtz equation for damped waves, with a complexed-valued wave number $k = k_0(1 + \mathrm{i}\gamma)$, and a real-valued wave number $k_0 = \frac{\omega}{c_a}$. A solution to this equation is given by

$$p_1 = A\,e^{\mathrm{i}(\mathbf{k}\cdot\mathbf{r} - \omega t)} \tag{2.44}$$

where A is a constant. In one dimension it can be written as

$$p_1 = e^{\mathrm{i}kx}e^{-\mathrm{i}\omega t} = e^{\mathrm{i}k_0(1+\mathrm{i}\gamma)x}e^{-\mathrm{i}\omega t} = e^{-\gamma k_0 x}e^{\mathrm{i}(k_0 x - \omega t)} \tag{2.45}$$

Here we observe a exponential decay in the amplitude due to the damping term $k_0\gamma$. Thus γ can be regarded as an acoustic damping factor. The characteristic damping lenght x_c can now be expressed as

$$x_c = \frac{1}{\gamma k_0} \approx \frac{1}{1.5 \cdot 10^{-6} \cdot 4.2 \cdot 10^3\,\mathrm{m}^{-1}} = 149\,\mathrm{m} \tag{2.46}$$

The found value for the characteristic damping lenght is for ultrasound waves in aqueous acoustofluidics [1, p. 260]. The damping lenght is rather high, so compared to the micrometer scale we operate with this damping is quite small.

2.8   Boundary layer theory

In this section we will investigate the so-called boundary layer where the viscosity becomes an importent factor. The no-slip boundary condition will be introduced and the boundary layer's effect on the first order fields and the acoustic streaming will be commented.

At fluid solid interfaces, it can be observed in the continuum regime that the fluid stick to the solid boundary, so that we can safely take the fluid and solid velocities to be identical at the interface. This is called the no-slip condition. The microscopic origin of this condition is the assumption of complete momentum relaxtion between the molecules of the wall and the outmost molecules of the fluid that collide with the wall. The no-slip condition does thus state that

$$\mathbf{v}(\mathbf{r}) = \mathbf{v}_{\mathrm{wall}} \tag{2.47}$$

Where $\mathbf{v}(\mathbf{r})$ is the fluid velocity within one intermolecular distance to the solid wall and $\mathbf{v}_{\mathrm{wall}}$ is the velocity of the solid wall.
This equation can be decomposed into an equation for the parallel and perdicular (to the wall) component, respectively. So for a bounding wall having the normal vector $\mathbf{n}$, this leads to the following conditions [4]

    1) The wall is impermeable: $\mathbf{v} \cdot \mathbf{n} = \mathbf{U} \cdot \mathbf{n}$.

2) The fluid does not slip relative to the wall: $\mathbf{v} \times \mathbf{n} = \mathbf{U} \times \mathbf{n}$.

The first condition states that the fluid cannot penetrate through the wall which is reasonable enough. This condition does implie that if the walls is vibrating, i.e. the velocity of the wall is harmonic in time, then the fluid will also begin to vibrate. These vibrations will for certain frequencies result in resonance in the champer. This is shown analytically in section 3.1, 3.2 and 3.3.

The second condition is that the fluid does not slip relative to the wall and is not as obvious as the first. The underlying explanation is that the fluid interacts with the wall in the same way as with other fluids. Thus there cannot exist any discontinuity in velocity, if so, an infinite viscous stress would arise. This condition will be investegated in the following.

In the bulk fluid, inertial forces dominates the flow and the flow is close to be unaffected by viscosity. But at any solid surface there exists a thin boundary layer in which viscous forces are important. Over this layer the fluid velocity decreases significantly from its bulk flow value to zero (relative to the boundary) at the solid surface, according to the second no-slip condition. The situation is sketched in figure 2.1.
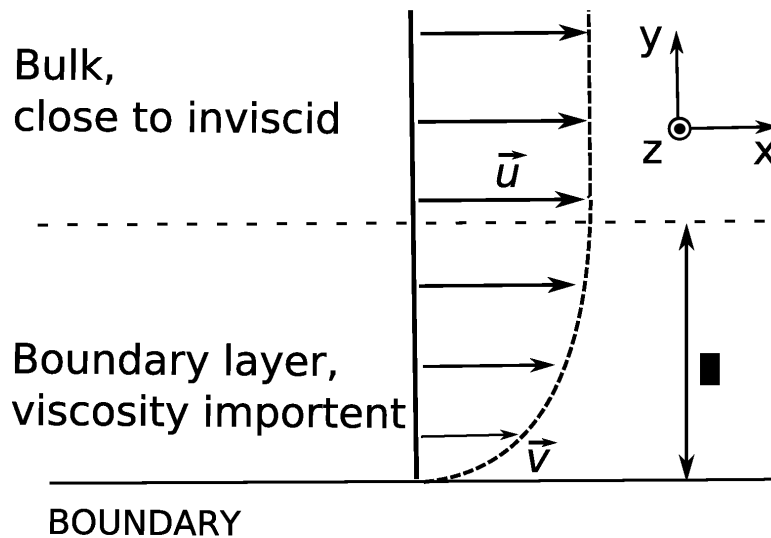
Figure 2.1: The sketch illustrates the so-called boundary layer. The thickness of the layer is indicated by δ, the velocity in the bulk is here $\mathbf{u}$, while the velocity near the boundary is $\mathbf{v}$. It is seen that the velocity decreases significantly from its bulk flow value to zero (relative to the boundary) at the solid surface. It should be noticed that our micro system is oscillating such that the velocity changes direction in time.

In the following we will try to estimate the boundary layers impact on the first-order fields. In order to do so we will find the thickness of the boundary layer at a fixed rigid wall and compare it with the length scale in the experimental setup.

The boundary layer is chosen to end when the viscous forces is of the same order of magnitude as the inertial forces. In this region close to the surface we expect that the length scale in the direction parallel to the boundary will be long in relation to the length scale perpendicular to the surface. We also expect the velocity scale in the direction parallel to the surface will be comparable to the free stream velocity outside the boundary layer.

The length scale in the direction parallel to the surface, the x direction, is assumed to be ℓ. Here ℓ is the amplitude of the oscillating actuation wall. The length scale in the direction perperdicular to the surface, the y direction, is δ. This length scale δ is taken to be the distance from the wall to where the inertial and viscous forces are comparable and can thus be used as a measure of the layer thickness.

For a 2D incompressible flow, the Navier–Stokes equation for the velocity in the x-direction and the continuity equation is given by (C.6) and (D.20)

$$\rho \left[\partial_t u_x + u_x \partial_x u_x + u_y \partial_y u_x \right] = -\partial_x p + \eta \left[\partial_{xx} u_x + \partial_{yy} u_x \right] \tag{2.48a}$$

$$\partial_x u_x + \partial_y u_y = 0 \tag{2.48b}$$

Note that we are only interested in an order of magnitude analysis, so the flow is taken to be incompressible. The order of magnitude of the terms in the continuity equation, and the viscous and inertial terms in the Navier–Stokes equation for the velocity in the x-direction are given by

$$|\partial_x u_x| = |\partial_y u_y| \Rightarrow \tag{2.49a}$$

$$\frac{U_x}{\ell} \approx \frac{U_y}{\delta} \Leftrightarrow \tag{2.49b}$$

$$U_y \approx \frac{\delta U_x}{\ell} \tag{2.49c}$$

$$|F_{inertia}| = |\rho \left[u_x \partial_x u_x + u_y \partial_y u_x \right]| \tag{2.50a}$$

$$\approx \frac{\rho U_x^2}{\ell} + \frac{\rho U_y U_x}{\delta} \tag{2.50b}$$

$$= \frac{\rho U_x^2}{\ell} + \frac{\rho \delta U_x^2}{\ell \delta} \tag{2.50c}$$

$$\approx \frac{\rho U_x^2}{\ell} \tag{2.50d}$$

$$|F_{visc}| = |\eta \left[\partial_{xx} u_x + \partial_{yy} u_x \right]| \tag{2.51a}$$

$$\approx \frac{\eta U_x}{\ell^2} + \frac{\eta U_x}{\delta^2} \tag{2.51b}$$

$$= \frac{\eta U_x}{\delta^2} \left(1 + \frac{\delta^2}{\ell^2} \right) \approx \frac{\eta U_x}{\delta^2} \tag{2.51c}$$

Where U_x and U_y are the magnitude of the x and y components of the velocity, respectively. We have used that $\ell \gg \delta$. Anticipating the result that the boundary layer thickness δ is small, we see from (2.49) that the characteristic velocity perpedicular to the wall U_y is also small, as we would expect intuitively.

The viscous and inertial forces per volume are then comparable when

$$\frac{\rho U_x^2}{\ell} \approx \frac{\eta U_x}{\delta^2} \Rightarrow \tag{2.52a}$$

$$\delta \approx \sqrt{\frac{\nu \ell}{U_x}} \tag{2.52b}$$

Here we have introduced the kinematic viscosity, $\nu \equiv \frac{\eta}{\rho}$.

The given problem can also be regarded as a diffusion process, and the deduced relation for δ can in this way be identified as the momentum diffusion length.

The fluid velocity is given by

$$U_x \approx \omega \cdot \ell \tag{2.53}$$

Now the thickness of the boundary layer, δ, can be estimated as the following in water at frequencies in the low MHz range

$$\delta \approx \sqrt{\frac{\nu}{\omega}} \approx \sqrt{\frac{10^{-6}\text{m}^2/\text{s}}{10^6/\text{s}}} = 1\mu\text{m} \ll \lambda \approx 1.5\text{mm} \tag{2.54}$$

It is seen that the thickness of the boundary layer is neglectable in our system and will thus only result in a insignificant correction to the overall first-order fields. Thus we can discard the no-slip condition in the treatment of the first order fields. This means that we in the further treatment of first-order bulk dynamics can apply a less restrictive slip condition and determine the x- and y-velocities v_{1x} and v_{1y} solely from the impermeable boundary condition.

If we do have a boundary layer in the first order fields the same must be the case for the second order fields. The boundary layer can by comprehensive analysis be found to entails the existence of a a time-independent boundary layer flow with vorticity [9]. The boundary layer can thereby introduce vorticity into an otherwise irrotational flow field. The boundary layer will thus result in some level of acostic streaming in microsystems. This resulting streaming has, however, been shown [2] that it could not account for the experimentally observed streaming patterns. In other words we must seek an alternative explanation for the observed acoustic streaming. Note that the phenomonon though can result from a combination of various contributions, including the boundary layer. But the boundary layer cannot, as mentioned, account for the observed streaming alone. In the next sections will we investergate if the viscous forces in the bulk can be involved.

In conclusion, the boundary layer can be neglected when treating the first order fields. The boundary layer has, however, been shown to give rise to a time-independent boundary layer flow with vorticity, which could not account for the experimentally observed streaming patterns.

Chapter 3

Analytical analysis

3.1 Acoustic resonances in 1D problem with viscosity

In this section we will show the phenomenon of acoustic resonance in a simple one dimensional viscos system, and estimate the size of the perturbation parameter for this system. This will give us a indication whether perturbation is a acceptable mathematically approach in this type of problems.

As a simple example of acoustic actuation, we consider the one dimensional setup skeched in figure 3.1.

$$v_1 = -\omega\ell\, e^{-\mathrm{i}\omega t} \qquad\qquad v_1 = \omega\ell\, e^{-\mathrm{i}\omega t}$$

-L   L   X
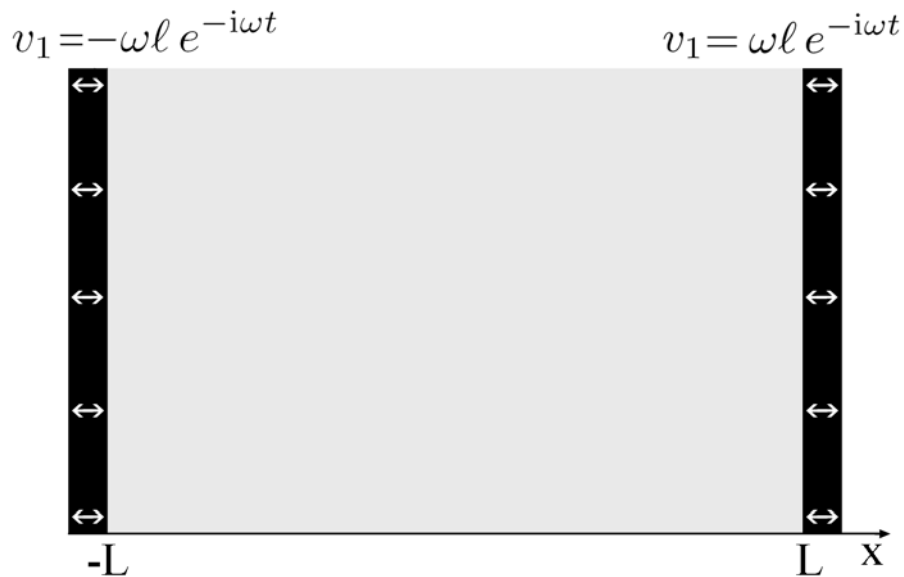
Figure 3.1: A sketch of a one-dimensional system. Two planar walls are placed at $x = -L$ and $x = L$, respectivily, and they are set to oscillate in antiphase.

    In this setup, two planar walls are placed at $x = -L$ and $x = L$ and are set to oscillate in antiphase. The tiny displacement of the walls due to the oscillation is assume to be much smaller than the dimensions of the system, and the oscillating walls can therefore be considered to have a fixed position. The oscillating walls are assumed to be perfect oscillators, meaning that they will retain the same amplitude and frequency no matter the pressure field next to them. Furthermore, the oscillating walls will be assume to be perfectly reflecting, i.e. no energy will leave the system through the walls. These assumptions will be applied to every oscillating wall throughout this report. Of course these assumptions are not exactly physical correct, and therefore we could happen to get unrealistic strong fields in resonance which could not be obtained in reality.

The oscillating walls are harmonically oscillating in time, and as the first order perturbations of the governing equations is linear, all fields derived from the first order equations will have the same harmonic time dependence as the oscillating walls. This will apply for all first order fields considered throughout this report.

The oscillations is modeled by the following velocity boundary conditions

$$v_1(-L, t) = -\omega\ell\, e^{-\mathrm{i}\omega t} \tag{3.1a}$$

$$v_1(L, t) = \omega\ell\, e^{-\mathrm{i}\omega t} \tag{3.1b}$$

In order to fulfill the wave equation derived in section 2.30 and the boundary conditions we try a solution consisting of the superposition of two counter-propagating plane waves, thus

$$p_1(x, t) = \left(A\, e^{\mathrm{i}kx} + B\, e^{-\mathrm{i}kx}\right) e^{-\mathrm{i}\omega t} \tag{3.2}$$

Notice that coefficients A and B in (3.2) are arbitrary constants.

In order to find the coefficients A and B in (3.2) we must find a expression that relates the first order pressure to the first order velocity. This can be done by combining the continuity and Navier–Stokes equation. The first order continuity and Navier–Stokes equation is respectivly given in (2.17). In one dimension these equations reads

$$\partial_t \rho_1 = -\rho_0\, \partial_x v_1 \tag{3.3a}$$

$$\rho_0 \partial_t v_1 = -\partial_x p_1 + (\zeta + \frac{4}{3}\eta)\partial_x^2 v_1 \tag{3.3b}$$

The continuity equation (3.3a) can now be derived with respect to x on both sides and inserted into the Navier–Stokes equation (3.3b). This leads to the following expression

$$\rho_0 \partial_t v_1 = -(1 + \frac{\zeta + \frac{4}{3}\eta}{c_a^2 \rho_0}\partial_t)\partial_x p_1 \tag{3.4}$$

Because of the harmonic boundary conditions we also expect a harmonic time depence in v_1. Therefore we have that $\partial_t v_1 = -\mathrm{i}\omega v_1$. Now by using this and inserting the solution (3.2) into equation (3.4) we get

$$-\mathrm{i}\omega\rho_0 v_1 = -\left(1 - \mathrm{i}\frac{(\zeta + \frac{4}{3}\eta)\omega}{c_a^2 \rho_0}\right)\mathrm{i}k\left(A\, e^{\mathrm{i}kx} - B\, e^{-\mathrm{i}kx}\right)e^{-\mathrm{i}\omega t} \tag{3.5a}$$

$$\Leftrightarrow$$

$$-\mathrm{i}\omega\rho_0 v_1 = -(1 - \mathrm{i}2\gamma)\,\mathrm{i}k\left(A\, e^{\mathrm{i}kx} - B\, e^{-\mathrm{i}kx}\right)e^{-\mathrm{i}\omega t} \tag{3.5b}$$

$$\Leftrightarrow$$

$$v_1 = \frac{k}{\omega\rho_0}(1 - \mathrm{i}2\gamma)\left(A\, e^{\mathrm{i}kx} - B\, e^{-\mathrm{i}kx}\right)e^{-\mathrm{i}\omega t} \tag{3.5c}$$

As previous we have that $(1 - \mathrm{i}2\gamma) \approx (1 + \mathrm{i}\gamma)^{-2}$ as γ is very small and so

$$\frac{k}{\omega\rho_0}(1 - \mathrm{i}2\gamma) = \frac{\omega k}{c_a^2 \rho_0 k_0^2 (1 - \mathrm{i}\gamma)^2} = \frac{\omega}{c_a^2 k \rho_0} \tag{3.6}$$

Thus

$$v_1 = \frac{\omega}{c_a^2 k \rho_0}\left(A\, e^{\mathrm{i}kx} - B\, e^{-\mathrm{i}kx}\right)e^{-\mathrm{i}\omega t} \tag{3.7}$$

Using the boundary condition (3.1a) we get

$$v_1(-L, t) = \frac{\omega}{c_a^2 k \rho_0}\left(A\, e^{-\mathrm{i}kL} - B\, e^{\mathrm{i}kL}\right)e^{-\mathrm{i}\omega t} = -\omega\ell\, e^{-\mathrm{i}\omega t} \tag{3.8a}$$

$$\Leftrightarrow$$

$$A\, e^{-\mathrm{i}kL} - B\, e^{\mathrm{i}kL} = -c_a^2 \ell k \rho_0 \tag{3.8b}$$

Using boundary condition (3.1b) we get

$$v_1(L,t) = \frac{\omega}{c_a^2 k \rho_0} \left(A\,e^{ikL} - B\,e^{-ikL} \right) e^{-i\omega t} = \omega \ell\, e^{-i\omega t} \tag{3.9a}$$

$$\Leftrightarrow$$

$$A\,e^{ikL} - B\,e^{-ikL} = c_a^2 \ell k \rho_0 \tag{3.9b}$$

Combining equation (3.8) og (3.9) we get

$$A\,e^{-ikL} - B\,e^{ikL} = -A\,e^{ikL} + B\,e^{-ikL} \tag{3.10a}$$

$$\Leftrightarrow$$

$$A\left(e^{-ikL} + e^{ikL}\right) = B\left(e^{-ikL} + e^{ikL}\right) \tag{3.10b}$$

$$\Leftrightarrow$$

$$A = B \tag{3.10c}$$

Substituting this result into equation (3.8) we get

$$A\,e^{-ikL} - A\,e^{ikL} = -c_a^2 \ell k \rho_0 \tag{3.11a}$$

$$\Leftrightarrow$$

$$A = \frac{c_a^2 \ell k \rho_0}{e^{ikL} - e^{-ikL}} = -\frac{ic_a^2 \ell k \rho_0}{2\sin(kL)} \tag{3.11b}$$

In conclusion these boundary conditions implies that

$$A = B = -\frac{ic_a^2 \ell k \rho_0}{2\sin(kL)} \tag{3.12}$$

The first order pressure and velocity are given by (3.2), (3.7). By inserting the found coefficients we get the following solutions

$$
\begin{aligned}
v_1(x,t) &= \omega\ell \frac{\sin(kx)}{\sin(kL)} e^{-i\omega t} = \omega\ell \frac{\sin(k_0 x + i\gamma k_0 x)}{\sin(k_0 L + i\gamma k_0 L)} e^{-i\omega t} \\
p_1(x,t) &= -i\rho_0 k c_a^2 \ell \frac{\cos(kx)}{\sin(kL)} e^{-i\omega t} = -i\rho_0 k_0 (1+i\gamma) c_a^2 \ell \frac{\cos(k_0 x + i\gamma k_0 x)}{\sin(k_0 L + i\gamma k_0 L)} e^{-i\omega t}
\end{aligned}
$$

Notice that these solutions is standing waves, as we would have expected for a closed system.

As γ is small, it makes sense to make a Taylor expansion around $\gamma = 0$. Making a first order Taylor expansion of the sine and cosines and using that $\omega = k_0 c_a$ we get

$$v_1(x,t) \approx \omega\ell \frac{\sin(k_0 x) + i\gamma k_0 x \cos(k_0 x)}{\sin(k_0 L) + i\gamma k_0 L \cos(k_0 L)} e^{i\omega t} \tag{3.13}$$

$$p_1(x,t) \approx -\rho_0 c_a^2 k_0 (1+i\gamma)\ell \frac{\cos(k_0 x) - i\gamma k_0 x \sin(k_0 x)}{\sin(k_0 L) + i\gamma k_0 L \cos(k_0 L)} e^{i\omega t} \tag{3.14a}$$

$$\approx -\rho_0 c_a^2 k_0 \ell \frac{\cos(k_0 x) - i\gamma k_0 x \sin(k_0 x)}{\sin(k_0 L) + i\gamma k_0 L \cos(k_0 L)} e^{i\omega t} \tag{3.14b}$$

The last approximations has been made as $k \approx k_0$.

In general the imaginary terms in the numerator and denominator can be neglected when $k_0 L \neq \pi n$, where n is an integer, as $\gamma k_0 L << 1$. This corresponds to the off-resonance mode, and the order of magnitude of the density field, found using equation (2.17a), and the velocity field becomes

$$|v_1(x,t)| \approx \omega\ell = \frac{\omega\ell}{c_a} c_a \tag{3.15}$$

$$|\rho_1(x,t)| \approx \rho_0 k_0 \ell = \frac{\omega\ell}{c_a} \rho_0 \tag{3.16}$$

This shows that our pertubation parameter is in fact $\frac{\omega \ell}{c_a}$. As mentioned previously we have $\omega \approx 10^{-6}$ rad/s, $\ell \approx 1$ nm and $c_a \approx 10^3$ m/s and thus the pertubation parameter α becomes

$$\alpha \equiv \frac{\omega \ell}{c_a} \approx 10^{-6} \tag{3.17}$$

So at offresonance the pertubation parameter is much smaller than unity, and it is thus justified that we have used pertubation theory to solve this problem at this condition. However, in the resonance mode were $k_0 = \frac{n\pi}{L}, n = 1, 2, ...$ equation (3.14) yields

$$v_1(x,t) \approx \omega \ell \frac{\sin\left(\frac{n\pi}{L}x\right) + \mathrm{i}\gamma\frac{n\pi}{L}x\cos\left(\frac{n\pi}{L}x\right)}{\sin(n\pi) + \mathrm{i}\gamma n\pi \cos(n\pi)} e^{\mathrm{i}\omega t} \tag{3.18a}$$

$$= \omega \ell (-1)^n \left(\frac{-\mathrm{i}}{n\pi\gamma} \sin\left(\frac{n\pi}{L}x\right) + \frac{x}{L}\cos\left(\frac{n\pi}{L}x\right) \right) e^{\mathrm{i}\omega t} \tag{3.18b}$$

$$\rho_1(x,t) \approx -\rho_0 \frac{n\pi}{L}\ell \frac{\cos\left(\frac{n\pi}{L}x\right) - \mathrm{i}\gamma\frac{n\pi}{L}x\sin\left(\frac{n\pi}{L}x\right)}{\sin(n\pi) + \mathrm{i}\gamma n\pi \cos(n\pi)} e^{\mathrm{i}\omega t} \tag{3.19a}$$

$$= \rho_0 (-1)^n \frac{n\pi}{L}\ell \left(\frac{\mathrm{i}}{n\pi\gamma} \cos\left(\frac{n\pi}{L}x\right) - \frac{x}{L}\sin\left(\frac{n\pi}{L}x\right) \right) e^{\mathrm{i}\omega t} \tag{3.19b}$$

As $\frac{1}{n\pi\gamma} >> \frac{x}{L}$ we have that

$$|v_1(x,t)| \approx \frac{1}{n\pi\gamma} \frac{\omega \ell}{c_a} c_a \tag{3.20}$$

$$|\rho_1(x,t)| \approx \frac{1}{n\pi\gamma} \frac{\omega \ell}{c_a} \rho_0 \tag{3.21}$$

Thus the pertubation parameter at resonancee has the following value for $n = 1$:

$$\alpha_{\text{resonance}} \equiv \frac{1}{n\pi\gamma} \frac{\omega \ell}{c_a} \approx \frac{10^{-6}}{3 \cdot 10^{-5}} \approx 3 \cdot 10^{-2} \tag{3.22}$$

We can now see that the pertubation factor at resonance is still smaller than unity, but is so large that this is close to invalidate the whole pertubation approach.

In figure 3.2 the velocity field has been plottet at off-resonance and on-resonance, i.e. $\omega = \frac{3\pi c_a}{2L}$ and $\omega = \frac{2\pi c_a}{L}$, respectivily. The parameters used are $\ell = 10^{-9}$ m, $c_a = 1483$ m/s, $L = 0.001$ m and $\rho_0 = 1000$ kg/m^3.

We notice that the magnitude of the fields at off- and on-resonance is corresponding to the approximations in equation (3.20) and (3.21) which predicted $|v_1| \approx \omega \ell = 0.007$ m/s and $|v_1| \approx \frac{1}{n\pi\gamma}\omega \ell = 111$ m/s for off- and on-resonance, respectively.

3.2   Streaming in closde, viscous, two-dimensional problem

We now turn to a simpel 2D problem. We have a square box, consisting of a fluid, with oscillating walls at $x = -L$, $x = L$, $y = -L$ and $y = L$. The walls parallel to each other will be oscillating in anti-phase, and the amplitude of the walls parallel to the x-axis will have a amplitude three times greater than the other two. The system is sketched in figure 3.3.

First the first order pressure will be found in order to compare the pressure field with experimental results. Next the streaming velocity field will be found and discussed.

We assume to vibrate the whole system with the same frequency and so all components have the same time dependence $e^{-\mathrm{i}\omega t}$.
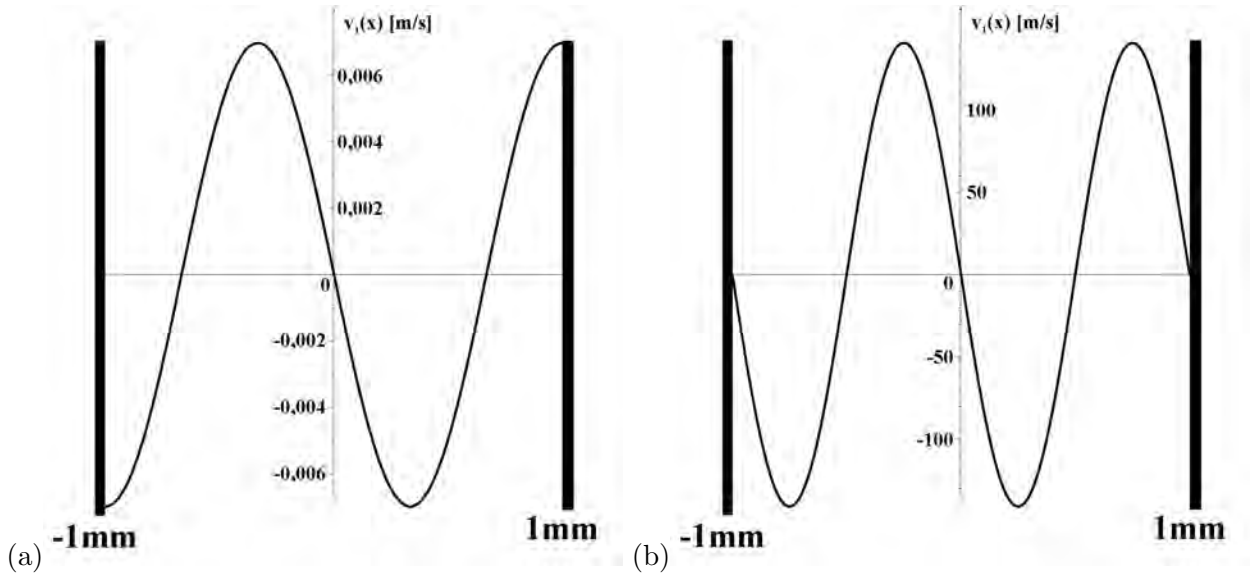
Figure 3.2: The velocity field distribution in 1D, viscid system with two oscillating walls. (a) is at off-resonance, i.e. $\omega = \frac{3\pi c_a}{2L}$, and (b) is at on-resonance, i.e. $\omega = \frac{2\pi c_a}{L}$. Notice that the velocity field is significantly greater in resonance.
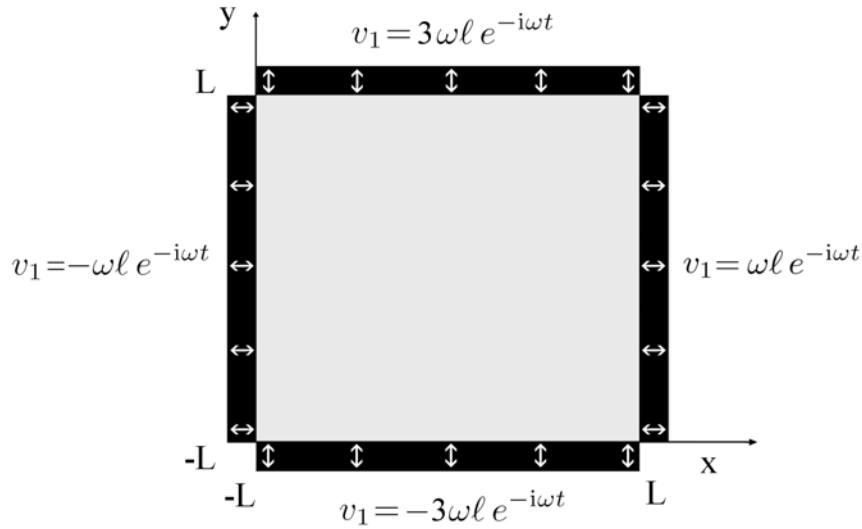
Figure 3.3: A sketch of a two-dimensional system. Four planar, oscillating walls are placed at $x = -L$, $x = L$, $y = -L$ and $y = L$, respectivily.

The boundary conditions are given by

$$
\begin{aligned}
v_x(-L, y, t) &= -\omega\ell\, e^{-i\omega t} & \text{(3.23a)} \\
v_x(L, y, t) &= \omega\ell\, e^{-i\omega t} & \text{(3.23b)} \\
v_y(x, -L, t) &= -3\omega\ell\, e^{-i\omega t} & \text{(3.23c)} \\
v_y(x, L, t) &= 3\omega\ell\, e^{-i\omega t} & \text{(3.23d)}
\end{aligned}
$$

Note that this is the first order pertubated boundary conditions as $\mathbf{v}_0 = \mathbf{0}$ is the initial value.

From section 2.4 we have the pertubation equations. The zeroth order pertubations ρ_0 and p_0 is steady-state values and thus taken to be constants. The first order pertubations is found in section 2.4 as

$$
\begin{align}
p_1 &= c_a^2 \rho_1 \tag{3.24a}\\
\partial_t \rho_1 &= -\rho_0 \boldsymbol{\nabla} \cdot \mathbf{v}_1 \tag{3.24b}\\
\rho_0 \partial_t \mathbf{v}_1 &= \eta \nabla^2 \mathbf{v}_1 + \left(\zeta + \frac{\eta}{3}\right) \boldsymbol{\nabla}\left(\boldsymbol{\nabla} \cdot \mathbf{v}_1\right) - \boldsymbol{\nabla} p_1 \tag{3.24c}
\end{align}
$$

In 2D with the fields depending on x and y and the velocity vector given by $\mathbf{v}_1 = \begin{pmatrix} v_x \\ v_y \end{pmatrix}$ and we have

$$
\begin{align}
p_1 &= c_a^2 \rho_1 \tag{3.25a}\\
\partial_t \rho_1 &= -\rho_0 \partial_x v_x - \rho_0 \partial_y v_y \tag{3.25b}\\
\rho_0 \partial_t v_x &= \eta \partial_x^2 v_x + \eta \partial_y^2 v_x + \left(\zeta + \frac{\eta}{3}\right)\left(\partial_x^2 v_x + \partial_x \partial_y v_y\right) - \partial_x p_1 \tag{3.25c}\\
\rho_0 \partial_t v_y &= \eta \partial_x^2 v_y + \eta \partial_y^2 v_y + \left(\zeta + \frac{\eta}{3}\right)\left(\partial_x \partial_y v_x + \partial_y^2 v_y\right) - \partial_y p_1 \tag{3.25d}
\end{align}
$$

Substituting equation (3.25a) into (3.25c) and (3.25d) and differentiating with respect to t on both sides of both equations we get

$$
\begin{align}
\rho_0 \partial_t^2 v_x &= \eta \partial_t \partial_x^2 v_x + \eta \partial_t \partial_y^2 v_x + \partial_t \left(\zeta + \frac{\eta}{3}\right)\left(\partial_x^2 v_x + \partial_x \partial_y v_y\right) - c_a^2 \partial_x \partial_t \rho_1 \tag{3.26a}\\
\rho_0 \partial_t^2 v_y &= \eta \partial_t \partial_x^2 v_y + \eta \partial_t \partial_y^2 v_y + \partial_t \left(\zeta + \frac{\eta}{3}\right)\left(\partial_x \partial_y v_x + \partial_y^2 v_y\right) - c_a^2 \partial_y \partial_t \rho_1 \tag{3.26b}
\end{align}
$$

We have here assume that $\partial_t \partial_x = \partial_x \partial_t$. Now substituting equation (3.25b) into both equations we get

$$
\begin{align}
\rho_0 \partial_t^2 v_x &= \eta \partial_t \partial_x^2 v_x + \eta \partial_t \partial_y^2 v_x + \partial_t \left(\zeta + \frac{\eta}{3}\right)\left(\partial_x^2 v_x + \partial_x \partial_y v_y\right) + c_a^2 \partial_x \left(\rho_0 \partial_x v_x + \rho_0 \partial_y v_y\right) \tag{3.27a}\\
\rho_0 \partial_t^2 v_y &= \eta \partial_t \partial_x^2 v_y + \eta \partial_t \partial_y^2 v_y + \partial_t \left(\zeta + \frac{\eta}{3}\right)\left(\partial_x \partial_y v_x + \partial_y^2 v_y\right) + c_a^2 \partial_y \left(\rho_0 \partial_x v_x + \rho_0 \partial_y v_y\right) \tag{3.27b}
\end{align}
$$

As the boundary conditions are time dependent and the equations are linear it would be make sense if the functions v_x and v_y had the same time dependence as the boundary conditions. Further we assume that v_x only depend on x and t as the boundary conditions in x are independent of y. Likewise v_y only depend on y and t. Thus we guess at solutions on the following form

$$
\begin{align}
v_x(x, y, t) &= v_{x0}(x)\, e^{-\mathrm{i}\omega t} \tag{3.28a}\\
v_y(x, y, t) &= v_{y0}(y)\, e^{-\mathrm{i}\omega t} \tag{3.28b}
\end{align}
$$

By substituting this into the equations in (3.27) we get

$$
-\rho_0 \omega^2 v_{x0} = -\mathrm{i}\omega\eta \partial_x^2 v_{x0} - \mathrm{i}\omega\left(\zeta + \frac{\eta}{3}\right)\partial_x^2 v_{x0} + c_a^2 \rho_0 \partial_x^2 v_{x0} \tag{3.29a}
$$
$$
\Leftrightarrow
$$
$$
\partial_x^2 v_{x0} \frac{c_a^2}{\omega^2}\left(1 - \mathrm{i}2\gamma\right) + v_{x0} = 0 \tag{3.29b}
$$

and

$$
-\rho_0 \omega^2 v_{y0} = -\mathrm{i}\omega\eta \partial_y^2 v_{y0} - \mathrm{i}\omega\left(\zeta + \frac{\eta}{3}\right)\partial_y^2 v_{y0} + c_a^2 \rho_0 \partial_y^2 v_{y0} \tag{3.30a}
$$
$$
\Leftrightarrow
$$
$$
\partial_y^2 v_{y0} \frac{c_a^2}{\omega^2}\left(1 - \mathrm{i}2\gamma\right) + v_{y0} = 0 \tag{3.30b}
$$

We have here used definition (2.41) of γ. As shown previously γ is very small i acoustofluidics and so we can make the approximation $(1 - \text{i}2\gamma) \approx (1 + \text{i}\gamma)^{-2}$. This leads to the equations

$$\partial_x^2 v_{x0} + k^2 v_{x0} = 0 \tag{3.31a}$$
$$\partial_y^2 v_{y0} + k^2 v_{y0} = 0 \tag{3.31b}$$

where $k = k_0(1 + \text{i}\gamma)$ and $k_0 = \frac{\omega}{c_a}$. The obvious solution to these two equations are a linear combination of counterpropergating waves

$$v_{x0} = A\,e^{\text{i}kx} + B\,e^{-\text{i}kx} \tag{3.32a}$$
$$v_{y0} = C\,e^{\text{i}ky} + D\,e^{-\text{i}ky} \tag{3.32b}$$

where A, B, C and D are arbitrary constant.

Now using the boundary conditions in (3.23) we get

$$v_x(-L, y, t) = \left(A\,e^{-\text{i}kL} + B\,e^{\text{i}kL}\right) e^{-\text{i}\omega t} = -\omega\ell\,e^{-\text{i}\omega t} \tag{3.33a}$$
$$v_x(L, y, t) = \left(A\,e^{\text{i}kL} + B\,e^{-\text{i}kL}\right) e^{-\text{i}\omega t} = \omega\ell\,e^{-\text{i}\omega t} \tag{3.33b}$$
$$v_y(x, -L, t) = \left(C\,e^{-\text{i}kL} + D\,e^{\text{i}kL}\right) e^{-\text{i}\omega t} = -3\omega\ell\,e^{-\text{i}\omega t} \tag{3.33c}$$
$$v_y(x, L, t) = \left(C\,e^{\text{i}kL} + D\,e^{-\text{i}kL}\right) e^{-\text{i}\omega t} = 3\omega\ell\,e^{-\text{i}\omega t} \tag{3.33d}$$

Reducing these four equations leads to

$$A\,e^{-\text{i}kL} + B\,e^{\text{i}kL} = -\omega\ell \tag{3.34a}$$
$$A\,e^{\text{i}kL} + B\,e^{-\text{i}kL} = \omega\ell \tag{3.34b}$$
$$C\,e^{-\text{i}kL} + D\,e^{\text{i}kL} = -3\omega\ell \tag{3.34c}$$
$$C\,e^{\text{i}kL} + D\,e^{-\text{i}kL} = 3\omega\ell \tag{3.34d}$$

Solving this leads to

$$A = -B = \frac{\omega\ell}{2\text{i}\sin(kL)} \tag{3.35a}$$

$$C = -D = \frac{3\omega\ell}{2\text{i}\sin(kL)} \tag{3.35b}$$

Substituting this into (3.32) and using (3.28) leads to

$$v_x = \frac{\omega\ell}{2\text{i}\sin(kL)}\left(e^{\text{i}kx} - e^{-\text{i}kx}\right) e^{-\text{i}\omega t} = \omega\ell\frac{\sin(kx)}{\sin(kL)}e^{-\text{i}\omega t} \tag{3.36a}$$

$$v_y = \frac{3\omega\ell}{2\text{i}\sin(kL)}\left(e^{\text{i}ky} - e^{-\text{i}ky}\right) e^{-\text{i}\omega t} = 3\omega\ell\frac{\sin(ky)}{\sin(kL)}e^{-\text{i}\omega t} \tag{3.36b}$$

Now from equation (3.25a) and (3.25b) we get

$$\rho_1 = -\frac{\text{i}\rho_0\ell k}{\sin(kL)}\left[\cos(kx) + 3\cos(ky)\right] e^{-\text{i}\omega t} \tag{3.37}$$

$$p_1 = -\frac{\text{i}c_a^2\rho_0\ell k}{\sin(kL)}\left[\cos(kx) + 3\cos(ky)\right] e^{-\text{i}\omega t} \tag{3.38}$$

The pressure field is seen to be at resonance when

$$\sin(k_0 L) \approx 0 \tag{3.39a}$$
$$\Leftrightarrow$$
$$\omega_R \approx \frac{\pi c_a}{L}n \tag{3.39b}$$

where n is a arbitrary positive integer.

The pressure field at resonance is plottet in figure 3.4 (a). The plot shows that the pressure at this frequency displays a characteristic resonance pattern in the chamber. This resonance pressure pattern is seen to be similar to the experimentially found pattern shown in figure 1.2 [!!!henvisning til figuren i introduktion med hagsætters trykmønster]. This simpel model and the first order approximation does thus seem sufficient when one want to describe the pressure field seen in a liquid filled micro system. By variating the time it can be observed that the pressure waves is actually propagating. But as the attenuation, due to viscous loss, of the pressure waves is small, the waves is be close to be standing waves.

By using equation (2.27) the streaming velocity in the x- and y-direction can now be found as

$$\langle v_{2x} \rangle = -\frac{1}{\rho_0} \langle \rho_1 v^*_{1x} \rangle = \frac{1}{2} Re \left[i\ell^2 \omega k \frac{[\cos(kx) + 3\cos(ky)]\sin(k^*x)}{\sin(kL)\sin(k^*L)} \right] \tag{3.40a}$$

$$\langle v_{2y} \rangle = -\frac{1}{\rho_0} \langle \rho_1 v^*_{1y} \rangle = \frac{1}{2} Re \left[i3\ell^2 \omega k \frac{[\cos(kx) + 3\cos(ky)]\sin(k^*y)}{\sin(kL)\sin(k^*L)} \right] \tag{3.40b}$$

where $k = k_0(1 + i\gamma)$. From these equations it is seen that for zero damping there does not excist any streaming velocity. So the streaming is zero for a closed inviscid system. In figure 3.4(b) a fieldplot of the streaming velocity is shown. The plot shows that viscosity actually implies a non-zero streaming velocity in the system. However, the streaming caused by viscosity can not explain the observed streaming in the experiments [Henvsing til Peders afhandling!!!] .

(a)   (a)
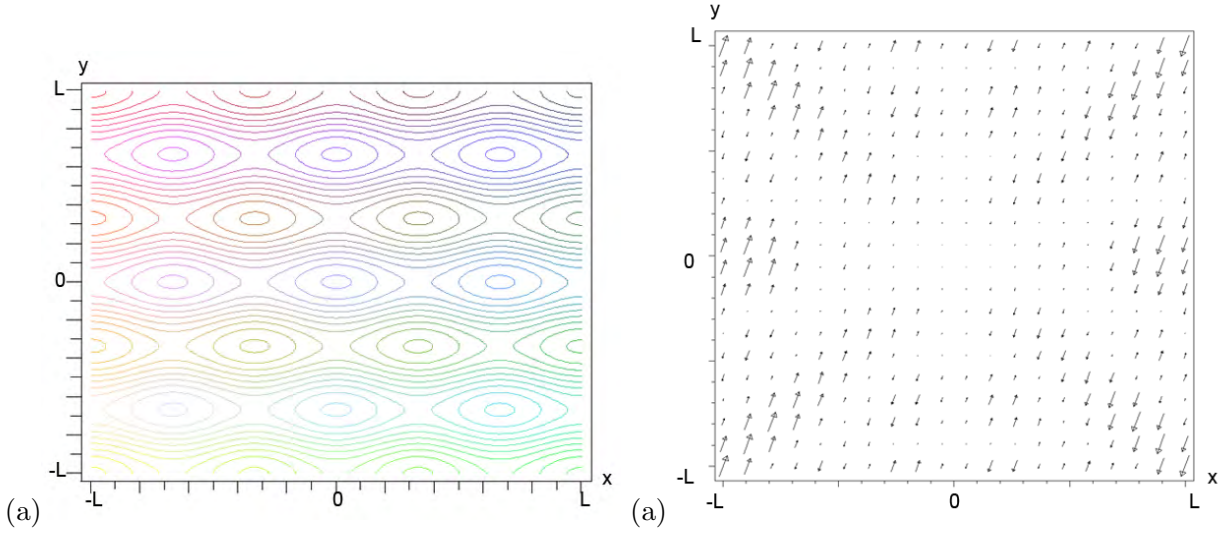
Figure 3.4: (a) Contour plot of the pressure field in a closed 2D system excited at its resonance frequency $\omega = \frac{3\pi c_a}{L}$. The fluid is taken to be water, and the length/ width of the chamber is set to L = 1mm. The plot shows that the pressure at this frequency displays a characteristic resonance pattern in the chamber. (b) Fieldplot of the streaming velocity in the same system. The plot shows that viscosity actually implies a non-zero streaming velocity in the system.

3.3   Traveling waves in multilayer systems

In this section we will investigate how travelling sound waves propagates through one or more transitions from one material to another. At first in section 3.3.1 we will investigate how a wave will propagate from one material to another, introduce the acoustic impedance Z and consider the reflection of a wave at a material transition. Second in section 3.3.2 we will consider the case of a three layer system consisting of water, silicon and air,

respectively, oscillated by a single oscillating wall. In this three layer system we will investigate how the pressure and streaming velocity depend on the frequency at which the system is oscillated. We will also investigate how the pressure and streaming velocity is affected if the outer layer is not considered to be air but another material.

The calculations are only made in 1D to make the calculations manageable. However they will provide valuable intuition and results which can later be used, when we move on to more complex calculations in 2D.

3.3.1 Transition, reflectance and transmittance

In this section we will investigate how a sound wave propagates through a transition between two diffenrent materials. This is done by considering the first-order pressure field in a 1D system with no viscousity.

A normalized sound wave is coming in from minus infinity traveling in a material a. At $x = 0$ we have a transition from material a to material b. The material b will continue untill infinity. The system is sketched in figure 3.5.
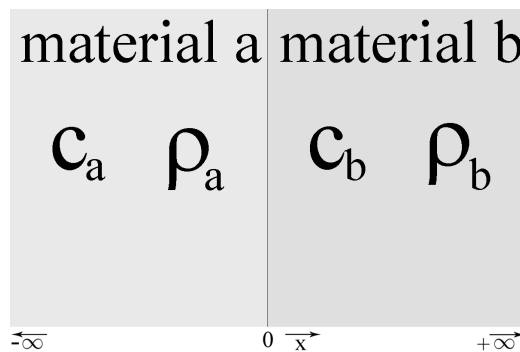

Figure 3.5: A transition from material a to material b. The two materials have different physical parameters which will affect a sound wave sent into the transition between the two materials.

We are considering a normalized incoming sound wave. At the transition from material a and material b a part of the wave will be reflected and some will be transmitted. The reflected wave will travel to the left and the transmitted wave will travel to the right. Thus the solution will be on the form

$$p_1(x,t) = \begin{cases} e^{i(k_a x - \omega t)} + B_a\, e^{i(-k_a x - \omega t)} & , x < 0 \\ A_b\, e^{i(k_b x - \omega t)} & , 0 < x \end{cases} \tag{3.41}$$

In this section the index "a" is refering to the material a and the index "b" is refering to the material b.

We now have two unknown amplitudes which have to be determined. This will require two boundary conditions. The two boundary conditions are continuity in the pressure field and velocity field at the material transition, at $x = 0$. Mathematical speaking the two boundery conditions are

BC 1) $p(0^-) = p(0^+)$

BC 2) $v(0^-) = v(0^+)$

where $v(0^-)$ means the limit of v as $x \to 0$ from the left. Similar $v(0^+)$ means the limit of v as $x \to 0$ from the right.

The first boundary condition gives us

$$1 + B_a = A_b \tag{3.42}$$

Now using the first order, non-viscous Navier–Stokes equation $\rho_0 \partial_t v_1 = -\partial_x p_1$ and the solution guess, we derive the following for an arbitrary material j as the timedependens of the velocity field is the same as the pressure

field.

$$-\mathrm{i}\omega\rho_j v_j \quad = \quad -\mathrm{i}k_j \left(A_j\, e^{\mathrm{i}(k_j x - \omega t)} - B_j\, e^{\mathrm{i}(-k_j x - \omega t)} \right) \tag{3.43a}$$

$$\Leftrightarrow$$

$$v_j \quad = \quad \frac{k_j}{\omega \rho_j} \left(A_j\, e^{\mathrm{i}(k_j x - \omega t)} - B_j\, e^{\mathrm{i}(-k_j x - \omega t)} \right) \tag{3.43b}$$

Using (3.43b) the second boundary condition leads to

$$\frac{k_a}{\omega \rho_a} \left(e^{-\mathrm{i}\omega t} - B_a\, e^{-\mathrm{i}\omega t} \right) \quad = \quad \frac{1}{\omega \rho_b} A_b k_b\, e^{-\mathrm{i}\omega t} \tag{3.44a}$$

$$\Leftrightarrow$$

$$1 - B_a \quad = \quad \frac{\rho_a k_b}{\rho_b k_a} A_b \tag{3.44b}$$

We now introduce the acoustic impedance Z and the acoustic impedance ratio z_{ab} defined by

$$Z_j \quad \equiv \quad \rho_j c_j \tag{3.45}$$

$$z_{ab} \quad \equiv \quad \frac{Z_a}{Z_b} = \frac{\rho_a c_a}{\rho_b c_b} \tag{3.46}$$

As $k = \omega/c$ equation (3.44b) gives us

$$1 - B_a \quad = \quad z_{ab} A_b \tag{3.47}$$

Now solving equation (3.42) and (3.47) gives us the two amplitudes

$$B_a \quad = \quad \frac{1 - z_{ab}}{1 + z_{ab}} \tag{3.48a}$$

$$A_b \quad = \quad \frac{2}{1 + z_{ab}} \tag{3.48b}$$

It is now obviously to define these to amplitudes to be the reflection coefficient r and the transmission coefficient t, respectively. Thus

$$r \quad \equiv \quad B_a = \frac{1 - z_{ab}}{1 + z_{ab}} \tag{3.49}$$

$$t \quad \equiv \quad A_b = \frac{2}{1 + z_{ab}} \tag{3.50}$$

We notice that the reflected wave will suffer a phase shift by π if the impedance ratio is greater than one. In figure 3.6 is a plot of a sound wave going from silicon to water. We notice that both the pressure field and velocity field is continues at the transition which was the two boundary conditions. Further we also notice that the reflected wave obtaines a phase shift of π compared to the incoming wave as the impedance ration z_{ab} is greater than one.

To see how the energy of the acoustic wave is reflected and transmitted at the transition, we now introduce the acoustic intensity which is the acoustic energy current density [1, eq. (15.29)] and for a material j given by

$$I_{ac} = \langle v_j p_j \rangle = \left\langle \frac{1}{\mathrm{i}\omega \rho_j} p_1 \partial_x p_1 \right\rangle \tag{3.51}$$

We have here again used the first order, non-viscous Navier-Stokes equation $\rho_0 \partial_t v_1 = -\partial_x p_1$. Thus for the incoming wave, the reflected wave and the transmitted wave, respectively, we have

$$I_{ac,i} \quad = \quad \frac{k_a}{\omega \rho_a} \tag{3.52a}$$

$$I_{ac,r} \quad = \quad \frac{k_a}{\omega \rho_a} B_a^2 \tag{3.52b}$$

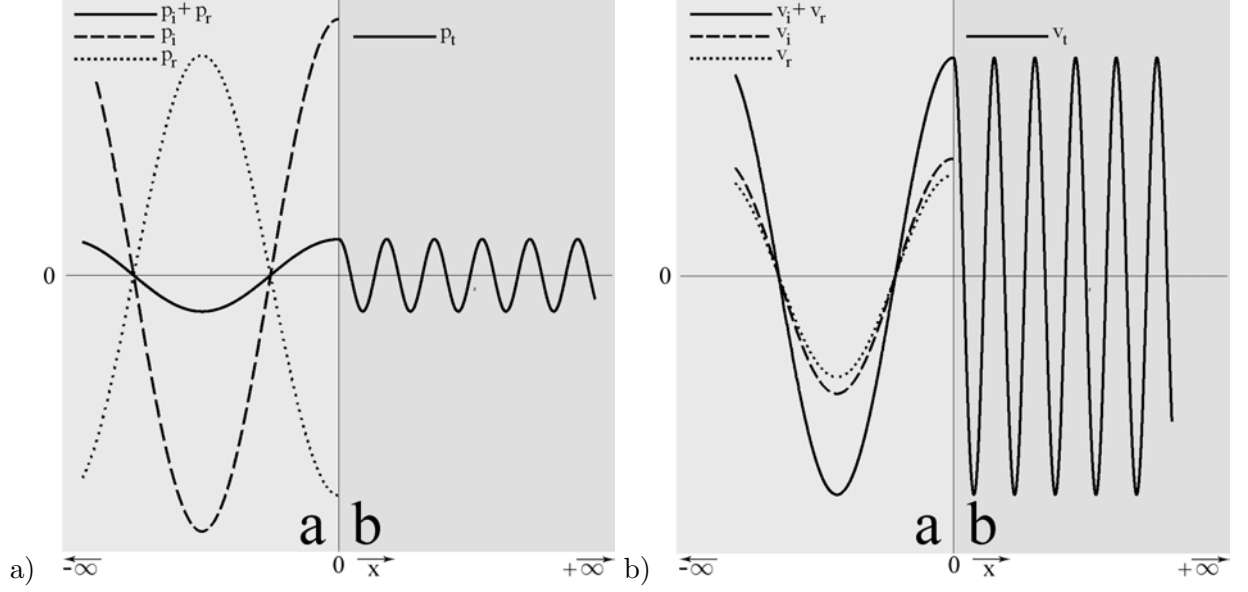$$I_{ac,t} \quad = \quad \frac{k_b}{\omega \rho_b} A_b^2 \tag{3.52c}$$

Figure 3.6: The pressure field (a) and the velocity field (b) distribution in a system where a traveling sound wave is sent from material a through a transition to material b. The incoming waves p_i and v_i are dashed, the reflected waves p_r and v_r are dotted and the resulting waves is solid. In material b the resulting wave is the transmitted wave. In this specific case the material a is silicon and material b is water. We notice that both the pressure field and velocity field is continuous at the transition and that the reflected pressure wave obtaines a phase shift of π compared to the incoming pressure wave.

Now we can define the reflection and transmittance as

$$R \equiv \frac{I_{ac,r}}{I_{ac,i}} = B_a^2 = r^2 = \left(\frac{1-z_{ab}}{1+z_{ab}}\right)^2 \tag{3.53}$$

$$T \equiv \frac{I_{ac,t}}{I_{ac,i}} = \frac{\rho_a k_b}{\rho_b k_a} A_b^2 = z_{ab} t^2 = \frac{4z_{ab}}{(1+z_{ab})^2} \tag{3.54}$$

As the energy of the wave should be conserved we need the sum of the reflected and transmitted intensity to be one. This is clearly fulfilled as

$$R + T = \left(\frac{1-z_{ab}}{1+z_{ab}}\right)^2 + \frac{4z_{ab}}{(1+z_{ab})^2} = \frac{1-2z_{ab}+z_{ab}^2+4z_{ab}}{(1+z_{ab})^2} = \frac{1+2z_{ab}+z_{ab}^2}{1+2z_{ab}+z_{ab}^2} = 1 \tag{3.55}$$

We notice that when the impedance ratio is one then the reflectance is zero and the transmission is one and thus the whole wave is transmitted through the transition without reflection. Two other important special cases are $z_{ab} \to 0$ and $z_{ab} \to \infty$. In both cases the transmittance is zero and the reflection is one. In figure 3.7 the reflectance and transmittance has been plottet as a function of the impedance ratio z_{ab}.

We also notice that the reflectance, R, is unchanged by the substitution $z \to \frac{1}{z}$. This can be shown with the simple rewritting

$$R(1/z) = \left(\frac{1-\frac{1}{z}}{1+\frac{1}{z}}\right)^2 = \left(\frac{z-1}{z+1}\right)^2 = \left(\frac{1-z}{1+z}\right)^2 = R(z) \tag{3.56}$$

This means that the reflection, and thus the transmission, is the same from material a to material b as from material b to material a. This will turn out to be an important point which we will benefit from in the later analysis of a more complex systems.
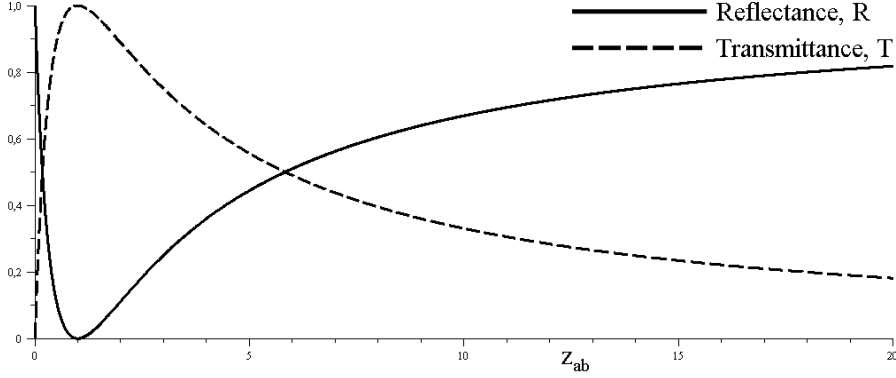
Figure 3.7: The reflection and transmission of a sound wave going through a transition between two materials, a and b respectively, with a impedance ratio of $z_{ab} = \frac{\rho_a c_a}{\rho_b c_b}$.

As we later will introduce problems which contains transitions from water to silicon and from silicon to air, we will now calculate the reflectance in these cases.

$$R_{\text{water,silicon}} = \left(\frac{1 - \frac{\rho_w c_w}{\rho_s c_s}}{1 + \frac{\rho_w c_w}{\rho_s c_s}}\right)^2 = \left(\frac{1 - \frac{1000 \cdot 1483}{2300 \cdot 8500}}{1 + \frac{1000 \cdot 1483}{2300 \cdot 8500}}\right)^2 = 0.7379 \tag{3.57a}$$

$$R_{\text{silicon,air}} = \left(\frac{1 - \frac{\rho_a c_a}{\rho_s c_s}}{1 + \frac{\rho_a c_a}{\rho_s c_s}}\right)^2 = \left(\frac{1 - \frac{1.2 \cdot 343}{2300 \cdot 8500}}{1 + \frac{1.2 \cdot 343}{2300 \cdot 8500}}\right)^2 = 0.9999 \tag{3.57b}$$

It is worth noticing that the transition from water to silicon, which we earlier considered to be reflecting everything, in fact only reflects about 74% of the energy in a sound wave. On the other the transition from silicon to air seems to be reflecting almost everything. However, we will later discover that even this very little transmission of 0.0001 % of the energy can be very a important feature of a system when one wants to see streaming phenomenons.

3.3.2 Resonance and streaming in an open, three layer system

In this section we are investigating resonance and streaming in a water chamber surrounded by silicon. We will restrict ourselves to investigate a non-viscous, one-dimensional multilayer system as we in section 3.2 saw that we ought to be looking for streaming which is not caused by the viscousity of the liquid.

The system consists of a water-filled layer enclosed by a layer of silicon and a layer of air. The system is actuated by an oscillating wall, placed at the beginning of the water layer (layer 1) at $x = 0$. The silicon layer (layer 2) starts at $x = x_1$ and end at $x = x_2$. The air layer (layer 3) starts at $x = x_2$ and is assumed to be infinite long. In figure 3.8 the situation is sketched. This system is an attempt to make a 1D model which is qualitivily similar to the experimental setup described in section 1.3. To make the calculations more general, we will look at a case with three layers of material a, b and c, respectively.

The velocity of the oscillating wall is given by

$$v_{\text{wall}} = \ell\omega\, e^{-i\omega t} \tag{3.58}$$

We assume the first order velocity field in each region to be a sum of two counter-propagating waves with a time dependens equal to the oscillating wall. However in layer 3 no waves will be going to the left as this layer continues to infinity. Thus the pressure field is given by

$$p_1(x,t) = \begin{cases} \left(A_1 e^{ik_a x} + B_1 e^{-ik_a x}\right) e^{-i\omega t} & , 0 < x < x_1 \\ \left(A_2 e^{ik_b x} + B_2 e^{-ik_b x}\right) e^{-i\omega t} & , x_1 < x < x_2 \\ A_3 e^{ik_c x}\, e^{-i\omega t} & , x > x_2 \end{cases} \tag{3.59}$$
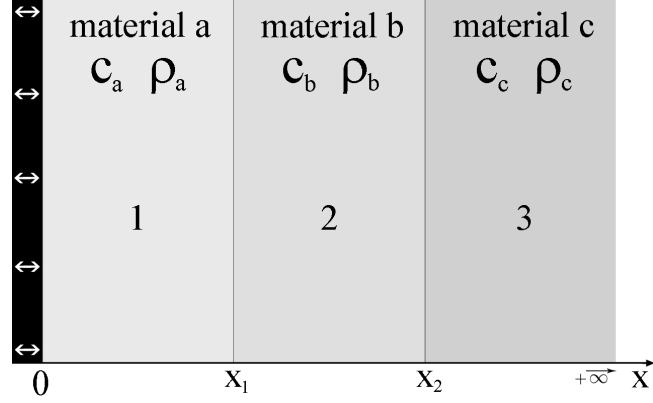
Figure 3.8: A three layer system. The black area to the right is a oscillating wall. The lightest area are material a with the density ρ_a and in which the speed of sound is c_a. The second lightest area is material b with the physical parameters ρ_b and c_b. The darkest grey area is material c with the physical parameters ρ_c and c_c. The three material transitions are placed at $x = 0$, $x = x_1$ and $x = x_2$, respectively. The oscillating wall will generate sound waves that will propagate through the system. How the sound wave will respond to the two transitions between the materials will depend on the physical parameters of the materials.

We now have five unknown amplitudes which have to be determined which requires five boundary conditions. The first boundary condition is that the velocity field will follow the oscillating wall and thus has the same amplitude as the oscillating wall at $x = 0$. The last four boundery conditions are that we have to have continuity in the pressure field and velocity field at $x = x_1$ and $x = x_2$ where the material is changing. Mathematical speaking the five boundery conditions are

BC 1 $v(0) = v_{\text{wall}}$

BC 2 $v(x_1^-) = v(x_1^+)$

BC 3 $p(x_1^-) = p(x_1^+)$

BC 4 $v(x_2^-) = v(x_2^+)$

BC 5 $p(x_2^-) = p(x_2^+)$

where $v(x_1^-)$ means the limit of v as $x \to x_1$ from the left. Similar $v(x_1^+)$ means the limit of v as $x \to x_1$ from the right.

First we use the third boundery condition to get

$$A_1 e^{ik_a x_1} + B_1 e^{-ik_a x_1} = A_2 e^{ik_b x_1} + B_2 e^{-ik_b x_1} \tag{3.60}$$

Now using the first order, non-viscous Navier–Stokes equation $\rho_0 \partial_t v_1 = -\partial_x p_1$ and the solution guess, we derive the following for a material j as the time dependens of the velocity field is the same as the pressure field.

$$-i\omega \rho_j v = -ik_j \left(A\, e^{i(k_j x - \omega t)} - B\, e^{i(-k_j x - \omega t)} \right) \tag{3.61a}$$

$$\Leftrightarrow$$

$$v = \frac{k_j}{\omega \rho_j} \left(A\, e^{i(k_j x - \omega t)} - B\, e^{i(-k_j x - \omega t)} \right) \tag{3.61b}$$

Using (3.61b) the second boundary condition leads to

$$\frac{k_a}{\omega \rho_a} \left(A_1\, e^{ik_a x_1} - B_1\, e^{-ik_a x_1} \right) = \frac{k_b}{\omega \rho_b} \left(A_2\, e^{ik_b x_1} - B_2\, e^{-ik_b x_1} \right) \tag{3.62}$$

The results from boundary condition two and three can now be written in matrix notation

$$
\begin{pmatrix}
e^{ik_a x_1} & e^{-ik_a x_1} \\
\frac{k_a}{\omega\rho_a} e^{ik_a x_1} & -\frac{k_a}{\omega\rho_a} e^{-ik_a x_1}
\end{pmatrix}
\begin{pmatrix} A_1 \\ B_1 \end{pmatrix}
=
\begin{pmatrix}
e^{ik_b x_1} & e^{-ik_b x_1} \\
\frac{k_b}{\omega\rho_b} e^{ik_b x_1} & -\frac{k_b}{\omega\rho_b} e^{-ik_b x_1}
\end{pmatrix}
\begin{pmatrix} A_2 \\ B_2 \end{pmatrix}
\tag{3.63}
$$

Rearranging we get

$$
\begin{pmatrix} A_2 \\ B_2 \end{pmatrix} = \mathbf{T}_{b,a} \begin{pmatrix} A_1 \\ B_1 \end{pmatrix}
\tag{3.64}
$$

where

$$
\mathbf{T}_{b,a} =
\begin{pmatrix}
\frac{1}{2}\left(1+\frac{1}{z_{ab}}\right) e^{i(k_a-k_b)x_1} & \frac{1}{2}\left(1-\frac{1}{z_{ab}}\right) e^{-i(k_a+k_b)x_1} \\
\frac{1}{2}\left(1-\frac{1}{z_{ab}}\right) e^{i(k_a+k_b)x_1} & \frac{1}{2}\left(1+\frac{1}{z_{ab}}\right) e^{-i(k_a-k_b)x_1}
\end{pmatrix}
\tag{3.65}
$$

We have here used the impedance ratio defined by (3.46).

Similar boundary conditions four and five leads to

$$
\begin{pmatrix} A_3 \\ 0 \end{pmatrix} = \mathbf{T}_{a,b} \begin{pmatrix} A_2 \\ B_2 \end{pmatrix}
\tag{3.66}
$$

where

$$
\mathbf{T}_{c,b} = \frac{1}{2}
\begin{pmatrix}
\frac{1}{2}\left(1+\frac{1}{z_{bc}}\right) e^{i(k_b-k_c)x_2} & \frac{1}{2}\left(1-\frac{1}{z_{bc}}\right) e^{-i(k_b+k_c)x_2} \\
\frac{1}{2}\left(1-\frac{1}{z_{bc}}\right) e^{i(k_b+k_c)x_2} & \frac{1}{2}\left(1+\frac{1}{z_{bc}}\right) e^{-i(k_b-k_c)x_2}
\end{pmatrix}
\tag{3.67}
$$

Now using boundary condition one and equation (3.61b) we get

$$
\frac{k_a}{\omega\rho_a}\left(A_1 e^{-i\omega t} - B_1 e^{-i-\omega t}\right) = \ell\omega e^{-i\omega t}
\tag{3.68a}
$$
$$
\Leftrightarrow
$$
$$
A_1 = \frac{\ell\omega^2\rho_a}{k_a} + B_1
\tag{3.68b}
$$

We now have the final relations from which all five amplitudes can be found

$$
A_1 = \frac{\ell\omega^2\rho_a}{k_a} + B_1
\tag{3.69}
$$
$$
\begin{pmatrix} A_3 \\ 0 \end{pmatrix} = \mathbf{T}_{c,b}\mathbf{T}_{b,a} \begin{pmatrix} A_1 \\ B_1 \end{pmatrix}
\tag{3.70}
$$
$$
\begin{pmatrix} A_2 \\ B_2 \end{pmatrix} = \mathbf{T}_{b,a} \begin{pmatrix} A_1 \\ B_1 \end{pmatrix}
\tag{3.71}
$$

Investigation of pressure resonance in the water layer

We now consider the basic case where material a is water, material b is silicon, material c is air, $\ell = 1$nm, $x_1 = 2$mm and $x_2 = 9$mm. These will be the standard parameters which is used throughout this chapter if nothing else is mentioned.

In 1D in section 3.1 we found that the eigenmodes in a closed, one-layer system of length $2L$ was seen when $k = \frac{n\pi}{L}$. This wavenumber corresponds to the layer supporting an integer of wavelengths. However, if a similar analysis was done for a 1D, inviscid system with one oscillating wall and one non-oscillating hard wall, one would find that the layer supported an integer of half wavelengths. The latter resembles the situation in our three layer system, and thus we would expect the resonance frequencies in the water layer to be close to those who corresponds to an integer of half wavelengths in the layer, i.e. $\omega = \frac{\pi c_a}{x_1}n$ where n is an integer.

In figure 3.9 the solution has been plottet for $\left(\omega = 4.5\frac{\pi c_a}{x_1}\right)$ which is a off-resonancee frequency in a similar 1D problem and $\left(= 4\frac{\pi c_a}{x_1}\right)$ which is a on-resonance frequecy in a similar 1D problem. The solution is depended of time and we have chosen to show the solutions at times where the pressure field in the water layer is at its maximum.
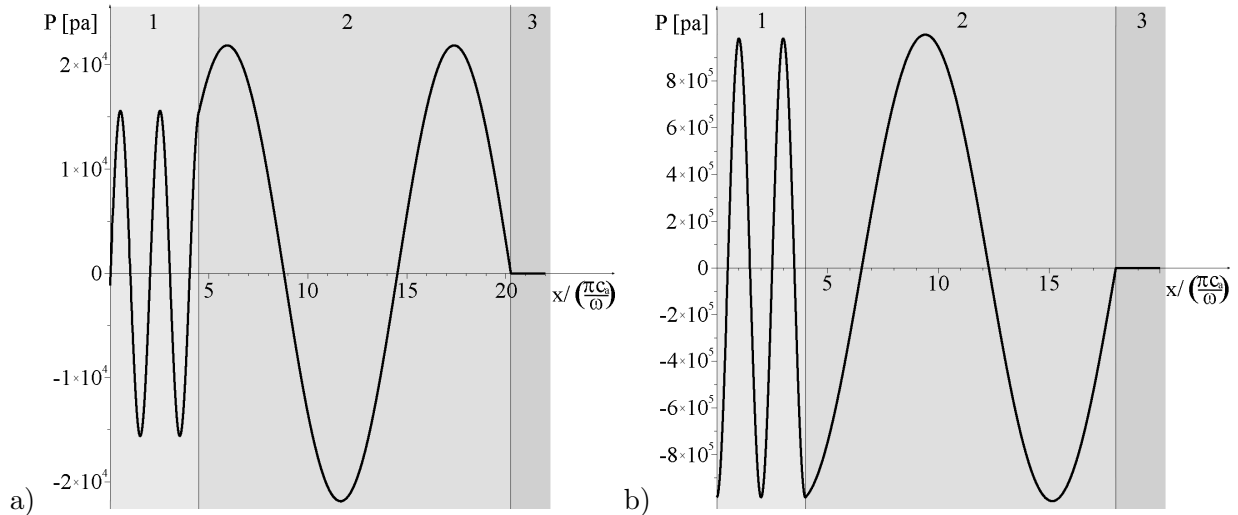

Figure 3.9: (a) and (b) is the pressure field distribution for $\omega = 4.5\frac{\pi c_a}{x_1}$ and $\omega = 4\frac{\pi c_a}{x_1}$, respectively. We have a system where sound waves is generated by an oscillating wall at $x = 0$ and distributed in a three layer system. Material a, b and c is water, silicon and air respectively. The pressure field is in both cases plottet at a time where the pressure in the water layer is at it's maximum. Notice the continuity in the pressure field which was one of the boundary conditions. Also notice that the pressure field generated in the water layer is much greater when $\omega = 4\frac{\pi c_a}{x_1}$ which is a eigenmode in a similar, closed, one-layer, 1D problem.

The first thing to notice in figure 3.9 is that the third and fifth boundary condition is fulfilled. Second we observe that a much greater pressure field is build up in the water layer as the frequecy is set to the resonance frequency found in the closed 1D problem. This indicates that even in a system with energy loss, it is possible to build up a considerable pressure field. The energy loss in the system is caused by the pressure field going into layer three and thus leaving the system. As can been seen in figure 3.9 not much of the sound is leaving the system which is a consequence of the high reflectance at a transition between silicon and air. This reflection was calculated in equation (3.57b) to be $R = 0.9999$.

To get a more quantitative description of this resonance phenomenon in our multilayer system one can find the maximum pressure in the water layer as a function of the angular frequency, ω. This is done by differentiating the Euclidean ℓ^2-norm $||p_1||_2$ of $p_1 \in \mathbb{C}$ with respect to x and then determine the maximum of $||p_1||_2$ which is in fact the maximum of p_1. The maximum of p_1 in the water layer is plottet in figure 3.10 (a) as a function of the angular frequency.

In figure 3.10 (a) we notice that there are very sharp peaks close to the eigenfrequencies for a similar, closed, one-layer, 1D problem. Just as important is to notice that even though the peaks are close to the eigenfrequecies from the 1D problem they are not placed exactly at the same frequencies. Due to the energy loss the pressure field is travelling waves which causes the resonance frequencies to be different from the eigenfrequencies from the 1D problem in which standing waves is generated. Also the fact that we have a multilayer system will cause a change in the resonance frequencis. We have seen that a resonance is possible in the water layer at special frequencies, but also the silicon layer has particular favourable frequencies which causes resonance in the silicon

(a)   (b)
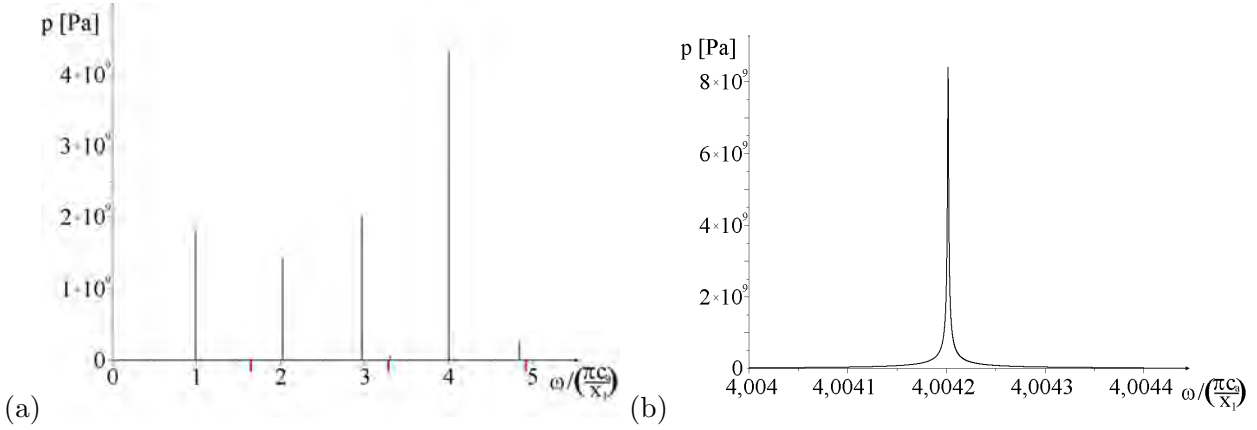
Figure 3.10: Plot of the maximum pressure in the water layer of the three layer system in figure 3.8. (a) is a plot containing five resonance frequencies and (b) is only containing one resonance frequency. The x-axis is scaled such that one unit is the eigenfrequency for a similar, closed, one-layer, 1D problem, i.e. $\omega = \frac{\pi c_a}{x_1} n$ where n is an integer. The red marks at the x-axis is the frequencies which corresponds to a integer of half wavelengths in the silicon layer, i.e. $\omega = \frac{\pi c_b}{x_2 - x_1} n$, where n is an interger. Notice the very sharp peaks close to, but not exactly placed at, the eigenfrequencies from the 1D problem.

layer. A high pressure field in the silicon layer will affect the pressure field in the water layer and such the maximum pressure in the water layer will also depend on the geometry of the silicon layer. This is also seen in figure 3.10 (a) where there are small peaks close to the frequencies which support waves in the silicon layer.

In figure 3.10 (b) the focus is set on the fourth peak from figure 3.10 (a). As seen the peak is very narrow, which indicates that the energy loss of the system is very small. Also notice that the peak in figure 3.10 (b) is higher than it is in figure 3.10 (a). This is caused by limited resolution in the plot, but is not important as we only want to see there the is a resonance. The actually amplitude does not matter in our analysis at this point. However, the fact that our computer evaluates functions at discrete points will always be a problem and therefor we ought to be aware that the height of such sharp peaks may not be 100 % correct [1]. In principle we can not know what happens in between those diskrete points, but that is a problem we have to accept.

Investigation of streaming

In section 2.5 we found that the acustic streaming, i.e. the time-averaged second order pertubation of the velocity, could be approximated by equation 2.26. Thus we need to find the first order density and first order velocity. ρ_1 is given by

$$\rho_1(x,t) = \frac{1}{c_a^2} p_1 = \frac{1}{c_a^2} \begin{cases} \left(A_1 e^{ik_a x} + B_1 e^{-ik_a x} \right) e^{-i\omega t} & , 0 < x < x_1 \\ \left(A_2 e^{ik_b x} + B_2 e^{-ik_b x} \right) e^{-i\omega t} & , x_1 < x < x_2 \\ A_3 e^{ik_c x} e^{-i\omega t} & , x > x_2 \end{cases} \tag{3.72}$$

The velocity is given by equation (3.61b)

$$v_1(x,t) = \begin{cases} \frac{k_a}{\omega \rho_a} \left(A_1 e^{ik_a x} - B_1 e^{-ik_a x} \right) e^{-i\omega t} & , 0 < x < x_1 \\ \frac{k_b}{\omega \rho_b} \left(A_2 e^{ik_b x} - B_2 e^{-ik_b x} \right) e^{-i\omega t} & , x_1 < x < x_2 \\ \frac{k_c}{\omega \rho_c} A_3 e^{ik_c x} e^{-i\omega t} & , x > x_2 \end{cases} \tag{3.73}$$

---

[1] Of course we have been plotting with as high resolution as our computer capacity would allow.

Now by using equation 2.26 the streaming in the water layer can be approxímated as

$$\langle v_2 \rangle = -\frac{1}{rho_a}\langle \rho_1 v_1 \rangle = -\frac{1}{2}\frac{1}{c_a^2}\frac{k_a}{\omega\rho_a^2}Re\left[\left(A_1 e^{ik_a x} + B_1 e^{-ik_a x}\right)\cdot\left(A_1^* e^{-ik_a x} - B_1^* e^{ik_a x}\right)\right] \qquad (3.74a)$$

$$= -\frac{k_a}{2c_a^2\omega\rho_a^2}Re\left[|A_1|^2 - |B_1|^2 + A_1^* B_1 e^{-i2k_a x} - A_1 B_1^* e^{i2k_a x}\right] \qquad (3.74b)$$

From this expression we see that the absolute average of the streaming velocity $\langle v_2 \rangle$ can be approximated by

$$\langle v_2 \rangle_{\text{avr}} \approx \frac{k_a}{2c_a^2\omega\rho_a^2}\left(|A_1|^2 - |B_1|^2\right) \qquad (3.75)$$

This is a very important result. In section 3.2 where a closed 2D system was threated we saw that the streamning velocity purely depended on the viscousity. We now see that if we allow energy to leave the system we get a streaming velocity that does not depend on the viscousity.
To see if the streaming velocity is greater at some special resonance frequencies, like the pressure, the average streaming from equation (3.75) has been plottet as a function of the angular frequency ω.
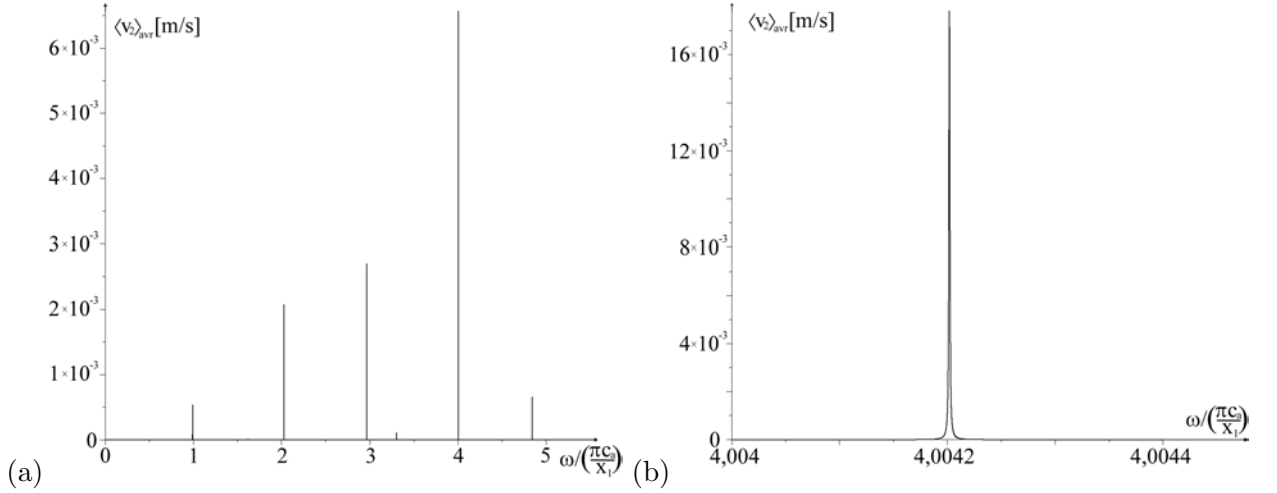

Figure 3.11: Plot of the average streaming velocity in the water layer of the three layer system in figure 3.8. (a) is a plot containing five resonance frequencies and (b) is only containing one resonance frequency. The x-axis is scaled such that one unit is the eigenfrequency for a similar, closed, one-layer, 1D problem, i.e. $\omega = \frac{\pi c_a}{x_1}n$ where n is an integer. The red marks at the x-axis is the frequencies which corresponds to a integer of half wavelength in the silicon layer, i.e. $\omega = \frac{\pi c_b}{x_2 - x_1}n$ where n is an interger. Notice the very sharp peaks close to, but not exactly placed at, the eigenfrequencies for a similar, closed, one-layer, 1D problem. Also notice that the peaks occurs at exactly the same frequencies as in figure 3.10 where we plottet the maximum pressure.

In figure 3.11 (a) we see the exact same pattern as before. At some special angular frequencies, close to the eigenfrequencies for a similar, closed, one-layer, 1D problem, the streaming velocity is significantly enhanced. The peaks are placed at the same frequencies as the peaks seen in figure 3.10. However, a new peak has occured at $\omega \approx \frac{3.3\pi c_a}{x_1}$ which is a wavelength supported by the silicon layer. As mentioned the height of these peaks ought not to be taken into consideration as the resolution of the plot can make a difference. In figure 3.11 (b) we see a plot focused on the peak close to $\omega = \frac{4\pi c_a}{x_1}$. We here notice that the peak in the streaming velocity is narrower than the peak in the pressure which was plottet in figure 3.10 (b).

Impedance variation

In our multilayer, 1D system we have now seen that there exist certain resonance frequencies. At these resonance frequencies both the pressure, the energy and the streaming velocity will be significantly enhanced compared to other frequencies. We now want to investigate how this resonance phenomonon depends on energy loss in the system. The energy loss is in other words the sound wave that escapes the silicon layer, i.e. is transmitted into the air layer. As we saw in section 3.3.1 the loss depends on the impedanse ration between silicon and air. Let us now consider a case where the air layer is replaced by some other material with an impedance Z_c such that the impedanse ratio between silicon and the outer layer becomes $z_{bc} = \frac{c_s \rho_s}{Z_c}$. We will investigate the resonance frequency close to $\omega = \frac{4\pi c_a}{x_1}$ and see how the impedance ratio z_{bc} affects the pressure and streaming velocity in the water layer.

We first consider the pressure. As seen from equation (3.46) we can variate the impedance ratio z_{bc} by variating the density ρ_c and letting the speed of sound in layer c stay as the speed of sound in air. The maximum pressure has been plottet as a function of the impedance ratio z_{bc} and the angular frequency ω in figure 3.12. The are several interesting things to notice about figure 3.12. First we see that the center frequency of the peak is very well-defined for $z_{bc} << 1$ and $z_{bc} >> 1$, however, it is changing as z_{bc} is getting closer to 1 where the system has maximum energy loss. For $z_{bc} << 1$ the center frequency is about $\omega = 3.9255 \frac{\pi c_a}{x_1} = 9.1444 \cdot 10^6$ rad/s and for $z_{bc} >> 1$ the center frequency is about $\omega = 4.0042 \frac{\pi c_a}{x_1} = 9.3277 \cdot 10^6$ rad/s. That is a change of about $3 \cdot 10^5$ Hz. This change in center frequency is properly caused by the phaseshift of π which a incoming wave is getting when it is reflected at a transition where the impedance ratio is greater than one. When the outer layer of our system has an impedance greater than the one for silicon, then the impedance ratio will be smaller than one, and the wave which is reflected at the transition between silicon and the outer layer will not be given a phaseshift. When the outer layer of our system has an impedance smaller than the one for silicon, then the impedance ratio will be greater than one, and the wave which is reflected at the transition between silicon and the outer layer will be given a phaseshift of π. The phaseshift arises from analysis leading to equation 3.49. This phenomenon could be investigated further by plotting the left-going waves and right-going waves seperated in different systems. However, such an investigation is not in the interest of this report.

   Besides the phaseshift just mentioned, the plots in figure 3.12 looks pretty symmetric about the axis $z_{bc} = 1$. Actually this was also expected as the reflection in section 3.3.1 was shown to be unchanges be the substituation $z \rightarrow 1/z$, i.e. $R(z) = R(1/z)$.

   Second we notice that the maximum pressure build up in the water layer has a minimum at $z_{ab} \approx 1$. The minimum is not placed exactly at $z_{cb} = 1$, but when investigated further one will discover that the exact location on the z_{bc}-axis of this minimum depends both on the reasonans frequency and the geometry of the system. However, common for all cases is that the minimum is placed close the point where the impedance ratio is one. This makes good physical sense as it will be harder to build up energy in the system when much energy is leaving the system. A more quantitative description of the position of this minimum will not be investigated further in this report, however it could be an interesting subject for further studies. As we are more interested in strong pressure reasonans and streaming we will be contempt to conclude that, in general, the maximum will be smaller as the system is opened and more energy is allowed to leave.

Also worth to notice in figure 3.12 is the steady growing maximum pressure. Both when z_{bc} is going from the previously mentioned minimum towards zero and from the minimum towards infintity, the maximum pressure is rising steadily. In figure 3.12 (c) we can see that the graf is forming a straight line when ω is fixed at the resonance frequency and z_{bc} is varied. Since both the z_{bc}-axis and the pressure axis is plottet on a logarithmic scale, the maximum pressure must be a exponential function of z_{bc} when ω is fixed at the resonance frequency. Fixing ω at the center frequencies $\omega_1 = 9.150272 \cdot 10^6$ rad/s and $\omega_2 = 9.327752 \cdot 10^6$ rad/s, respectively, we find the following expression for the maximum pressure $max(p_1)$ as a function of z_{bc}

$$\begin{align}
max(p_1)(\omega = \omega_1, z_{bc}) &\approx 1.99 \cdot 10^4 \cdot z_{bc}^{-0.981} \quad , z_{ab} \lesssim 10^{-1} \tag{3.76a}\\
max(p_1)(\omega = \omega_2, z_{bc}) &\approx 1.95 \cdot 10^5 \cdot z_{bc}^{0.991} \quad , z_{ab} \gtrsim 10^0 \tag{3.76b}
\end{align}$$

Thus the maximum pressure will be almost inversely proportional to the impedance ration z_{bc} when the impedance ratio is changed from about 10^{-1} to 0 and directly proportional to the impedance ratio when the impedance ratio is changed from about 10^0 to infinity. Of course ω should be fixed at the resonance frequency for these relations to hold. We can thus conclude that if we want a strong pressure resonance the system shall
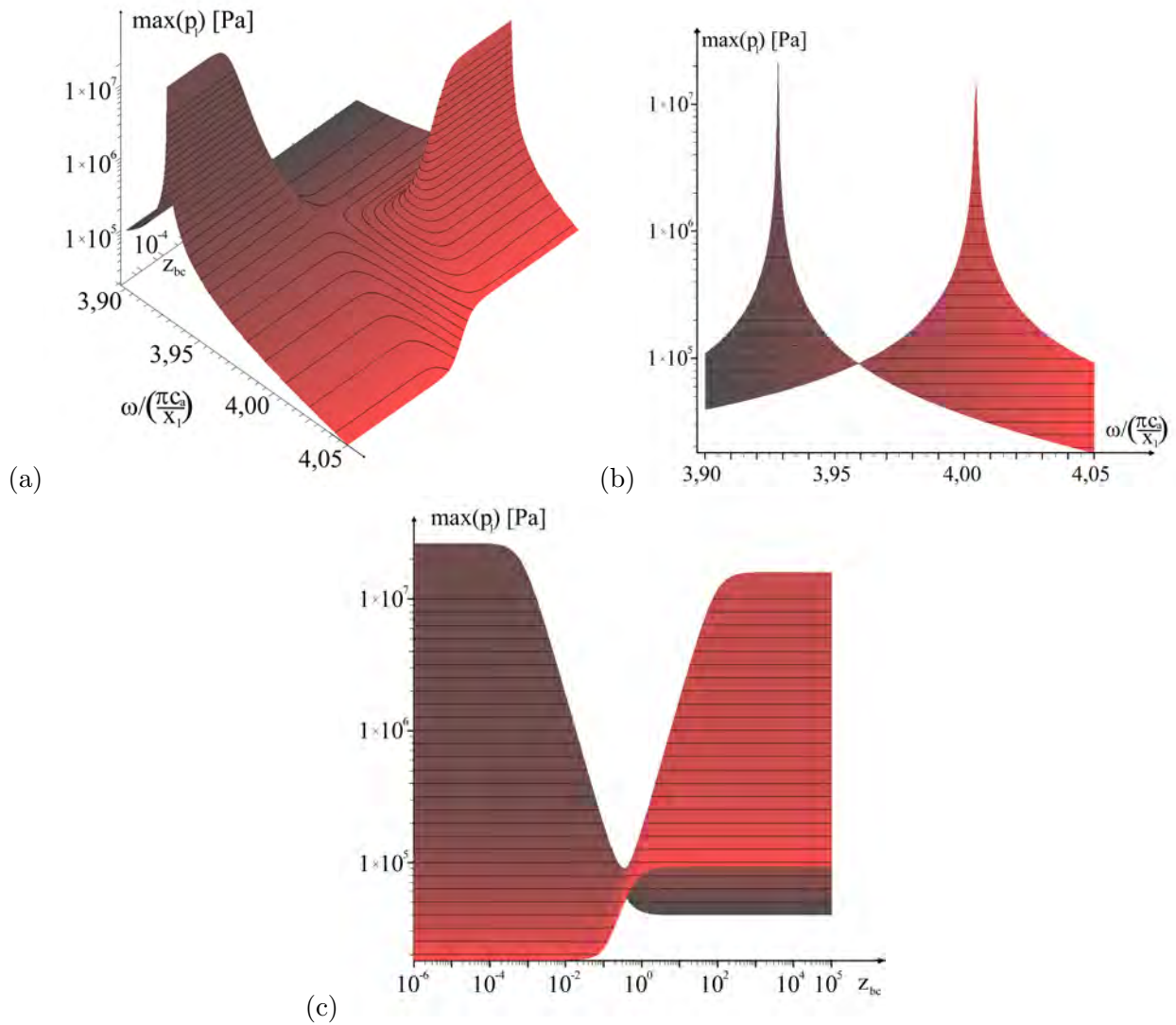
(a)

(b)

(c)

Figure 3.12: Plot of the of the maximum pressure in the water layer of the three layer system in figure 3.8. It is plottet as a function of the impedance ratio z_{bc} and the angular frequency ω. Both the maximum pressure and the impedance ratio have been plottet on a logarithmic scale. The ω-axis is scaled such that one unit is the eigenfrequency for a similar, closed, one-layer, 1D problem, i.e. $\omega = \frac{\pi c_a}{x_1} n$ where n is an integer. (a), (b) and (c) shows the three dimensional plot from three different angels. The contours are isobars. Notice that the center frequency of the peak changes somewhere close to $z_{bc} = 1$, where we also find the minimum of the maximum pressure. As the system is closed, i.e. $z_{bc} \to 0$ and $z_{bc} \to \infty$, the maximum pressure is rising as an power function untill a certain point where the maximum pressure seems to stay constant. However, these maxima occur due to lack of resolution and the pressure will in fact continue to rise as the system is closed.

be as closed as possible, i.e. the impdance ratio shall be very small or very big. This makes good sense as an impedance ratio far from one will not allow much energy to leave the system and thus more energy can be build up in the system. However, the fact that the maximum pressure is almost proportional to the impedance ratio is an interesting result.

Another interesting thing to notice in figure 3.12 is the apparent maxima of the maximum pressure. It looks

like the pressure will reach a maximum when the impedance ratio gets far away from one. In figure 3.12 it is seen to reach it's maximum about $z_{bc} = 10^{-4}$ and $z_{bc} = 10^3$. At this point one should get a little suspicious about this observation. When a non-viscous system is entirely closed and the oscillating wall keeps pumping energy into the system, the energy build up in the system would reach infinity. However, this also turnes out to be true. If one makes new plots zoomed in on the apparent maxima, one will discover that the pressure keeps rising but the peaks gets narrower as the system is closed. The maxima seen in figure 3.12 is showing because the resolution in the plot is not high enough. At some point the peaks are so narrow that they can be placed in between to evaluation points of the figure and thus is not seen. One interesting thing to note down, however, is that the top of a peak consists of a range of frequncies. This range gets narrower as the system is closed, and when a frequency is no longer within the range the maximum pressure will stay constant at this frequency, even if the system is further closed.

We now consider the average streamning velocity given by equation (3.75). Like the plot of the maximum pressure, the streaming velocity has been plottet as a function of the impedance ratio z_{bc} and the angular frequency ω in figure 3.13.

In figure 3.13 the general picture is that the streaming velocity is decreasing when the system is closed, and we see maximum streaming at $z_{bc} \approx 1$. However, at two reasonans frequencies, and a small range of frequencies around them, two peaks arises as the system is closed. The two resonance frequencies are the same as the resonance frequencies for the maximum pressure seen in figure 3.12. In figure 3.13 (c) we see that the streaming velocity at the two resonance frequencies is growing steadily as the system is closed. The graf is forming a straight line when ω is fixed at the center frequency and z_{bc} is varied. Since both the z_{bc}-axis and the velocity axis is plottet on a logarithmic scale, the streaming velocity must be a exponential function of z_{bc} when ω is fixed at the center frequency. Fixing ω at the center frequencies $\omega_1 = 9.150272 \cdot 10^6$ rad/s and $\omega_2 = 9.327752 \cdot 10^6$ rad/s, respectively, we find the following expression for the averaged streaming velocity v_{avr} as a function of z_{bc}

$$v_{\mathrm{avr}}(\omega = \omega_1, z_{bc}) \approx 3.84 \cdot 10^{-5} \cdot z_{bc}^{-1.000} \quad , z_{ab} \lesssim 10^{-1} \tag{3.77a}$$

$$v_{\mathrm{avr}}(\omega = \omega_2, z_{bc}) \approx 3.77 \cdot 10^{-4} \cdot z_{bc}^{1.001} \quad , z_{ab} \gtrsim 10^{0} \tag{3.77b}$$

Thus the streaming velocity will be almost inversely proportional to the impedance ration z_{bc} when the impedance ratio is changed from about 10^{-3} to 0 and directly proportional to the impedance ratio when the impedance ratio is changed from about 10^0 to infinity. This proportionality with respect to z_{bc} was also seen for the maximum pressure. Of course ω should be fixed at the center frequency for these relations to hold.

    What should also be noticed in figure 3.13 is the apparent maxima of the average streaming velocity. It looks like the streaming will reach a maximum at the resonance frequencies when the impedance ratio gets far away from one. However, this is not the case. The apparent maximum seen at $z_{bc} = 10^{-3}$ and $z_{bc} = 10^2$ in figure 3.13 (c) is not a maximum. Like we experienced analysing figure 3.12 it turns out that the peak at some point gets narrower than the resolution of the plot and thus is not detected. However, there is a difference when considering the streaming velocity. Considering the maximum pressure we noticed that the top of a peak consisted of a range of frequncies, and when a frequency was no longer within this range the maximum pressure would stay constant at this frequency if the system was further close. The peak of the streaming velocity also consists of a range of frequencies, but when the system is closing and a frequency no longer is within this range, then the streaming velocity will decrease as the system is further closed. In figure 3.13 we can see that when a frequency is not close enough to the peak then the streaming velocity will decrease about proportional to the impedance ratio z_{bc} as the system is further closed.

Summary of the result obtained through the analysis of 1D multilayer system

In section 3.3.1 we calculated the reflectance and the transmission of a sound wave meeting a material transition. We found that the reflectance given by equation 3.53 and the transmission given by equation 3.54 depended on the impedance ratio given by equation 3.46. Thus the impedance ratio will determine how much acoustic energy that will leave material a when a sound wave is going from material a and hits a transition to material b. We also found that the transmission of acoustic energy is the same going from material a to material b as going from material b to material a, i.e. T(1/z)=T(z).
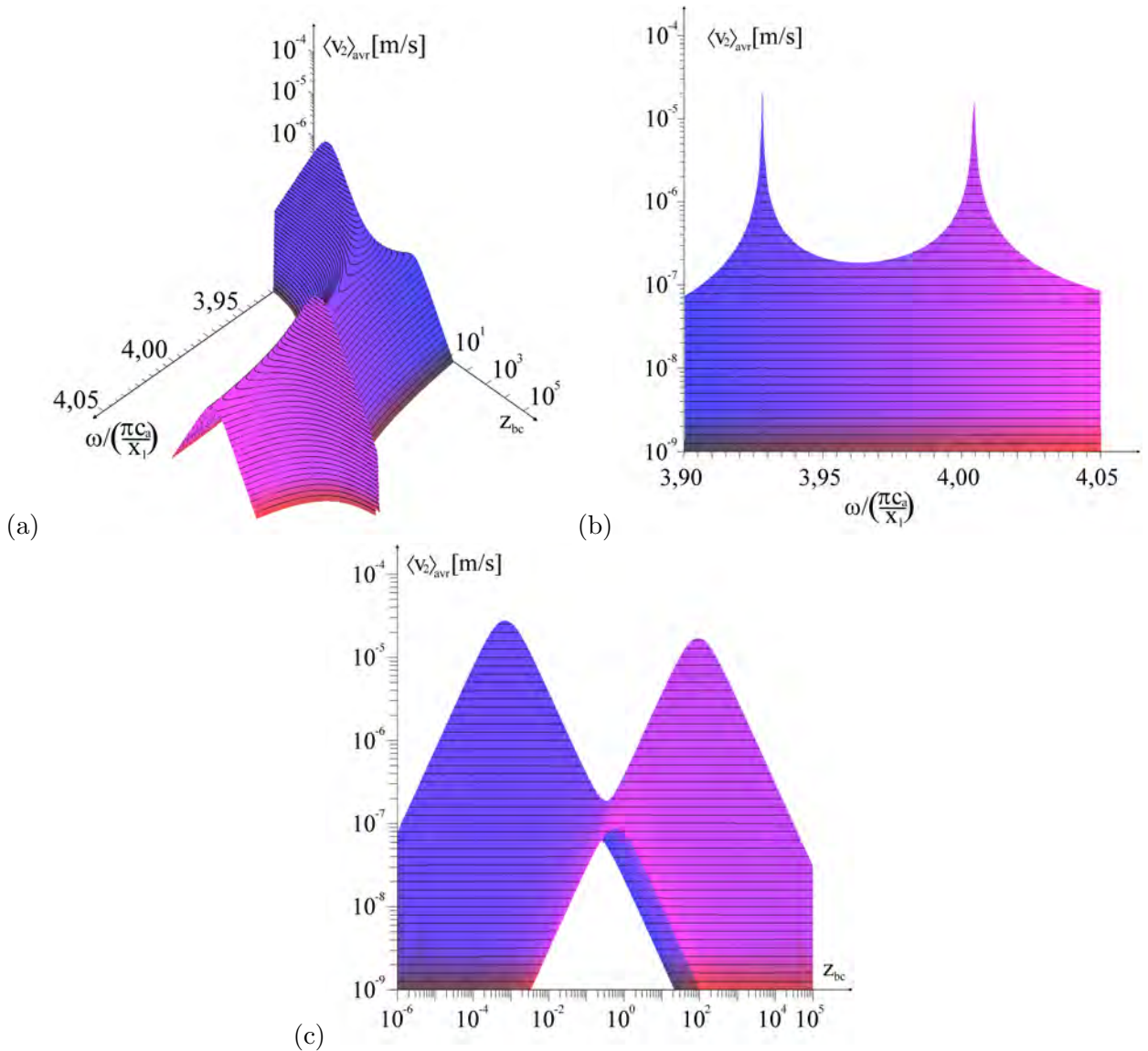
(a)

(b)

(c)

Figure 3.13: Plot of the average streaming velocity, given by equation 3.75, in the water layer of the three layer system in figure 3.8. It is plottet as a function of the impedance ratio z_{bc} and the angular frequency ω. Both the streaming velocity and the impedance ratio have been plottet on a logarithmic scale. The ω-axis is scaled such that one unit is the eigenfrequency for a similar, closed, one-layer, 1D problem, i.e. $\omega = \frac{\pi c_a}{x_1} n$ where n is an integer. (a), (b) and (c) shows the three dimensional plot from three different angles. The contours are isocontours. Notice that the center frequency of the peak changes somewhere close to $z_{bc} = 1$. As long as the frequency is at the center frequency of one of the peaks, the streaming velocity will increase as the system is closed, i.e. $z_{bc} \rightarrow 0$ and $z_{bc} \rightarrow \infty$. If the frequency is not at the centerfrequency or very close, the streaming velocity will decrease as the system is closed. The maxima occur due to lack of resolution and the rotation will in fact continue to rise as the system is closed.

In section 3.3.2 we calculated how the 1. order pressure field and velocity field was distributed in a three layer system with one oscillating wall. With the materials being water, silicon and air, respectively, we found

that the maximum pressure in the water layer became very large at certain resonance frequencies which was very close to the eigenfrequency for a similar, closed, one-layer, 1D problem. We also calculated the average streaming velocity and found that the it bacame very large at the same resonance frequencies as the maximum pressure.

In section 3.3.2 we considered an arbitrary material instead of air and tried to variate the impedance of this material. As the impedance ratio between silicon and the arbitrary material was varied from one towards zero or infinity the system is getting more and more closed, i.e. less energy will be allowed to leave the system. We found that at some impedance ratio far from one there would be a certain resonance frequency where both the pressure and the streaming velocity had a strong resonance. The pressure and streaming velocity at the resonance frequencies was found to be increasing proportional to the impedance ratio when the impedance ratio was far away from one and the system was further closed. In fact this would hold for a small range of frequencies around the resonance frequency. As the system was closed this range of frequencies would get smaller. This means that a certain frequency could be a part of the range of resonance frequencies at some impedance ratio close to one whereafter it would not be a part of the resonance frequencies as the system was closed to a certain point. When this happened the maximum pressure at this frequency would stay constant as the system was closed further and the streaming velocity at this frequency would decrease proportional to the impedance ratio as the system was closed further.

In short the pressure resonances and average streaming velocity resonance are found to become stronger as the system is closed. However, the range of frequencies at which the resonances are found will become smaller. It would be plausible to assume that the resonance of both pressure and streaming would go towards infinity as the system is totally closed, however, the ranges of frequencies at which this resonance was found would go towards zero.

Chapter 4

Basic COMSOL descriptions and simulations

4.1 Introduction to COMSOL

COMSOL is a numerical tool which is very convenient in our case. It is a numerical solver which is based on the Finite Element Method (FEM). For further information about FEM, see [1]. It allows one to solve an almost arbitrary partial differential equation in a one, two or three dimensional space. One can define an arbitrary geometry in which the differential equation should be solved. A broad variety of possible boundary conditions, which is sufficient in far the most cases, are available and one is able to control the precision of the numerical solution.

COMSOL is equiped with several different packages which target special kind of problems concerning e.g. heat, mechanics, elektromagnetism and acoustics. These packages have predefined differential equations, boundary conditions and solution forms which are typical for the given problem.

The versions used by us is COMSOL 3.3 and in our case the acoustic package within COMSOL Multiphysics is especially well-suited. In this package the Helmholtz equation in the pressure is solved, and this is exactly the equation we want to solve when we neglect the viscousity and want to find the first order pressure field. We have the option to choose some typical boundary conditions e.g. sound hard, sound soft, continuity and impedance. Further, we have different solution methods to our disposal, e.g. we can instruct COMSOL to search for eigenfrequencies and eigenmodes for a given closed system or find a stationary solution to a driven time harmonic open system. The defined problem can also be exported as a Matlab script in which one can do usual programming.

4.2 Reproducing the analytical result in COMSOL

In order to show that COMSOL are able to find correct solutions for the kind of problems we are going to solve, we have reproduce some of the analytically results found previously in chapter 3. The solution to the closed and open one-dimensional system treated in section 3.1 and 3.3, respectively, have been found numerically in COMSOL. The numerical solution was seen to be similar to the ones derived analytically. Also the two dimensional system considered in section 3.2 was solved numerically in COMSOL, and the solution is shown in figure 4.1. It is seen that this numerical solution is similar to the analytical solution in figure 3.4(a).

The two dimensional inviscid problem which was solved in section 3.2 included four oscillating walls with different amplitude. To solve this problem in COMSOL we simply draw a square with a side-length of 2 mm. The boundary conditions are set to normal acceleration with an arbitrary chosen amplitude of unity at $x = -L$ and $x = L$, and an arbitrary chosen amplitude of three times unity at $y = -L$ and $y = L$. In the subdomain settings the density is set to $\rho_1 = 1000\frac{\text{kg}}{\text{m}^3}$ and the sound velocity is set to $c_a = 1483\frac{\text{m}}{\text{s}}$. The excitation frequency is chosen to be $f = 4.45\,\text{MHz}$. Notice that even though COMSOL does not take viscousity into considerations
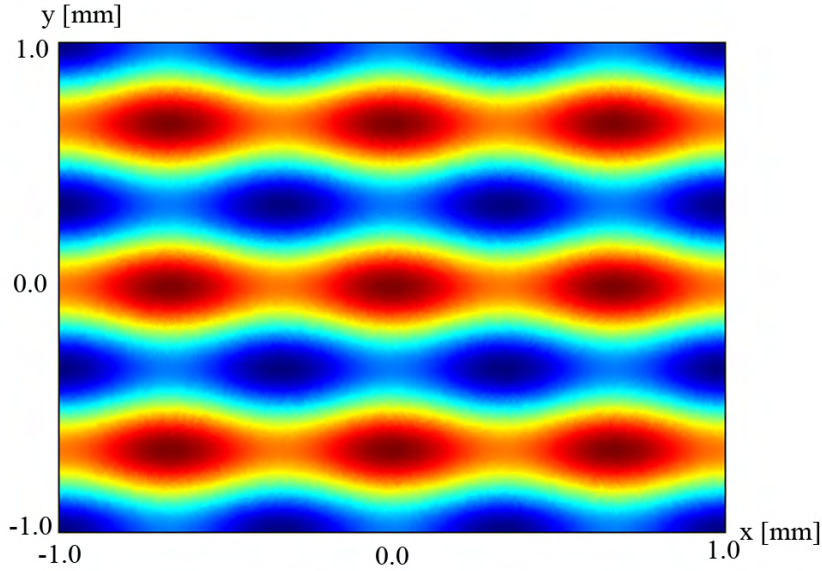
Figure 4.1: The numerical solution to the two dimensional problem introduced in section 3.2. The solution was obtained by using COMSOL.

the pressure fields is seen to be the same.

4.3   Modelling the experimential setup

In the following chapter we combine the theoretical work from the previous chapters with numerical implementations in COMSOL in order to simulate acoustic streaming in microsystems in resonance. But first we will introduce the used COMSOL model.

For the type of shallow resonating system used in the experimental setup it has by Jensen [7] been shown that 2D models are very well suited for describing the acoustic eigenmodes as long as the wavelength is more than twice the height of the resonating chamber. This condition is fulfilled for the system used in the experimental setup, referred to in the PhD. thesis by Hagsäter [8], when the actuation frequency is in the lower MHz range. Therefore we will restrict ourselves to a two dimensional analysis.

The given system involves a complex geometry and multiple material transitions. This type of problem is, as already mentioned, difficult to solve analytically, and is therefore chosen to be solved numerically. One of the best numerical PDE tools available to us is COMSOL MULTIPHYSICS which is based on the finite element method. COMSOL have in addition proven to give correct solutions to the problems already solved analytically. Thus we have chosen to use COMSOL as our primary modeling tool in our futher investegations.

4.3.1   Geometry

The geometry is set to consist of a small chamber with two thin channels on both sides. The chamber and channel is filled with water. Around the chamber and channels we have set a silicon rectangle. The boundary condition around the silicon rectangle is for the open system set to impedance conditions, and the impedance is as standard set to the impedance for air. This is approximately in accordance with the experimental model described in section 1.3. In the experimental arrangement the whole system is set to oscillate using a piezo actuator. This cannot be implemented in COMSOL, but to imitate the vibrations we will place a small actuator in the upper right corner of the silicon. Actually the actuator is constructed as a small hole in the silicon. The boundary is set to oscillate harmonically in time. A sketch of the geometry is shown in figure 4.2.
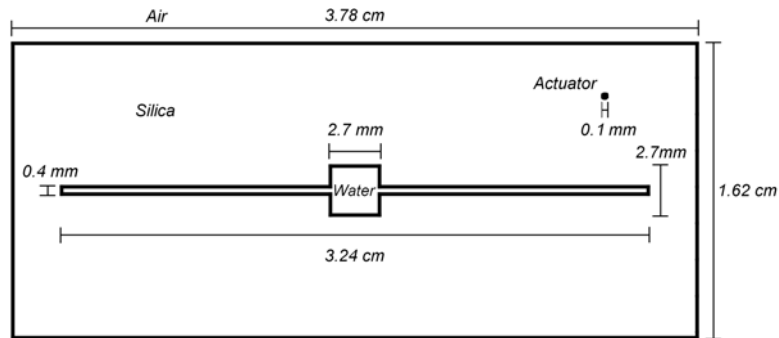
Figure 4.2: The geometry of the basic COMSOL model in 2D

4.3.2 Boundary conditions

We have three boundaries in this 2D model. First we have the boundary between the water filled chamber and channels and the surrounding silicon. As we will allow pressure waves to enter and leave the chamber the boundary condition here will be the so-called continuous boundary conditions. With this condition we require that the pressure and velocity field is continuous. Second we have the boundary between the silicon and the air. At this boundary we will use impedance conditions. This will allow part of the pressure waves to transmitted into the air. In fact this corresponds to the continuous boundary conditions where the air is treated as going to infinity where the pressure field is absorbed. In COMSOL this boundary condition is implemented by setting the input impedance to $\rho_{\text{air}} c_{a,\text{air}} = 1.25 \text{ kg/m}^3 \times 343 \text{ m/s} = 428.75 \text{ Pa} \cdot \text{s/m}$. The third and last boundary condition is our actuator. As mentioned the actuator is constructed as an hole in the silicon where the walls are allowed the vibrate. In COMSOL this is implemented by setting the boundary condition to normal acceleration with an arbitrary amplitude of unity. The wanted excitation frequency is thereafter set.

A sketch of the boundary conditions is shown in figure 4.3.
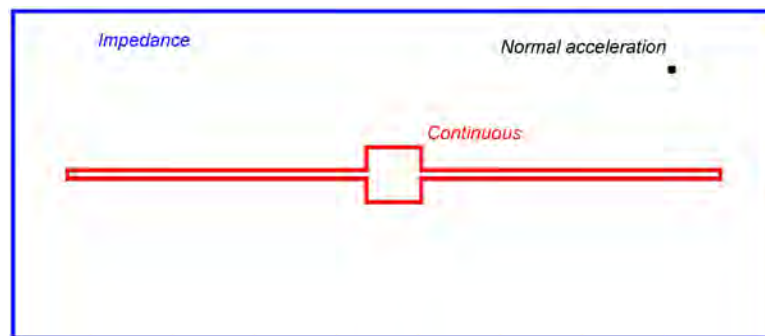

Figure 4.3: The boundary conditions of the basic COMSOL model in 2D

4.3.3 Subdomains settings

In the subdomains settings in COMSOL we have to specify that we want chamber and channel to be water and the surroundings to be silicon. This is done by specifying the density and speed of sound in each subdomain, chamber/channel and silicon, respectively. The used values are seen in table A.1.

4.3.4 Mesh

Before the PDE problem can be solved by COMSOL we have to create a finite element mesh. Finite Element Analysis uses a complex system of points called nodes which make a grid called a mesh. The mesh acts like a spider web in the sense that from each node a mesh element is extended to each of the adjacent nodes. Thus the mesh divides a given model domain into smaller subdomains. The smaller the subdomains, the more precise the solution and therefore a sufficiently fine mesh will have to be created in order to get the right solution. In the acoustic model user guide [6] it is recommended to have a mesh with a maximum size of $\frac{1}{5}$ of the wavelength. In a domain with silicon we then should have a maximum mesh size of

$$h_{max} \lesssim \frac{\lambda}{5} = \frac{c}{5f} = \frac{8500\text{m/s}}{5 \cdot 10^6 1/\text{s}} \approx 2 \cdot 10^{-3}\text{m} \tag{4.1}$$

as we operate with frequencies in the lower MHz range.
In water the maximum mesh size should be

$$h_{max} \lesssim \frac{\lambda}{5} = \frac{c}{5f} = \frac{1483\text{m/s}}{5 \cdot 10^6 1/\text{s}} \approx 3 \cdot 10^{-4}\text{m} \tag{4.2}$$

To be on the safe side we will set the maximum mesh size in silicon and water to be $h_{max} = 5 \cdot 10^{-4}$ and $h_{max} = 5 \cdot 10^{-5}$, respectively. The type of mesh COMSOL creates for our 2D model is illustrated in figure 4.4. Notice that the showed mesh is coarser then the mesh actually used in the simulations.
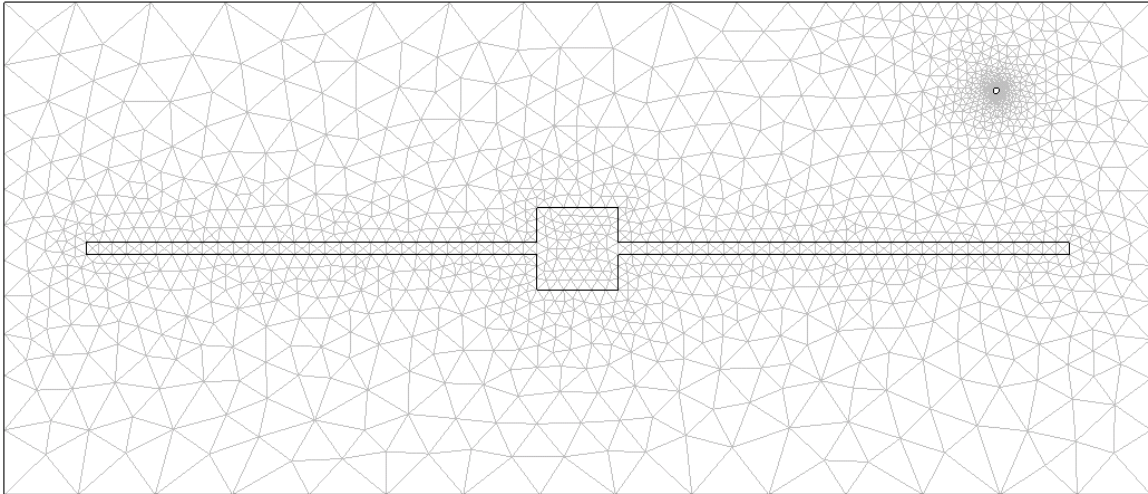
Figure 4.4: The figure shows the mesh COMSOL creates when the maximum mesh size in silicon and water to be $h_{max} = 5 \cdot 10^{-3}$ and $h_{max} = 5 \cdot 10^{-4}$, respectively. The mesh is thus seen to be finer inside the champer/channels. The mesh is in addition seen to be finer at the corners of the champer and around the actuator in the silicon. Notice that the showed mesh is coarser then the mesh actually used in the simulations.

Chapter 5

Full two-dimensional simulations

In the previous chapter did we introduce COMSOL and the 2D model we wish to investigate. In this chapter will we investigate the resonance in pressure and streaming velocity, as we did in 1D in section 3.3. First we will show the pressure and streaming in the system when driven to a resonance mode, and in this relation discuss how to determine the amount of streaming in the water chamber. Thereafter will we see how the placement of actuators affects the solution.

5.1   Simulation of the basic model

In section 3.3 we saw that there are certain resonance frequencies at which the pressure and streaming are significantly amplified in the one-dimensional system. In figure 5.1 it is shown that the same can be found to be the case for the two-dimensional COMSOL system. The figure shows a situation where the pressure waves in the chamber, at a given stationary time, is in resonance. There is also resonance in the silicon, but it is seen to be weaker than the resonance in the chamber. The system is driven at an excitation frequency of 1.46719 MHz. It is seen that the waves in the chamber have a wavelength which is approximately half the chamber width. In
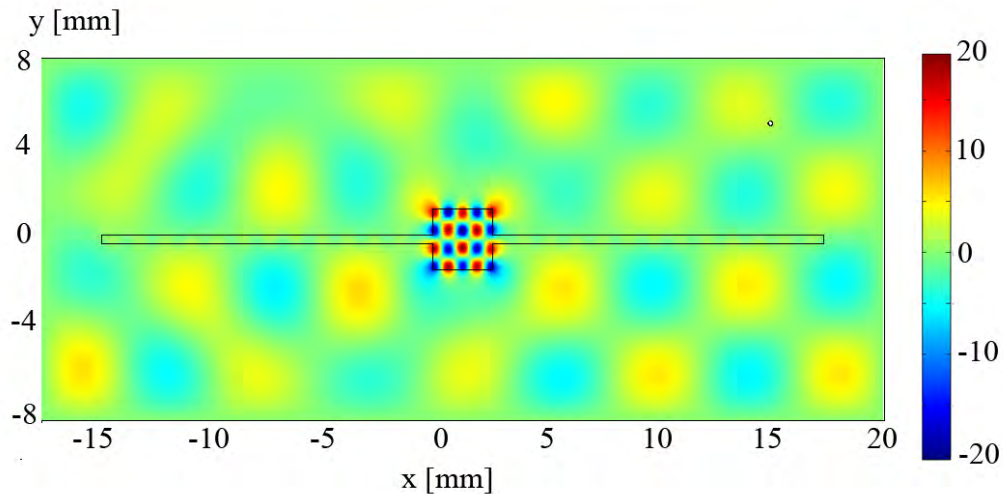
Figure 5.1: The figure shows a surface plot of the pressure in the system at a given time. The pressure waves are clearly seen to be in resonance inside the chamber. There is also resonance in the silicon, but it is seen to be weaker then the one in the chamber. The system is driven at an excitation frequency of 1.46719e6 Hz. The impedance is here set to the impedance for air, $Z_{air} = 1.25 \, \mathrm{kg/m^3} \cdot 343 \, \mathrm{m/s} = 428.75 \, \mathrm{Pa} \cdot \mathrm{s/m}$.

order to investigate if there is any acoustic streaming in the system, we have plottet the streaming velocity field in figure 5.2. The figure shows that there is a non-zero streaming velocity field present in the water chamber.
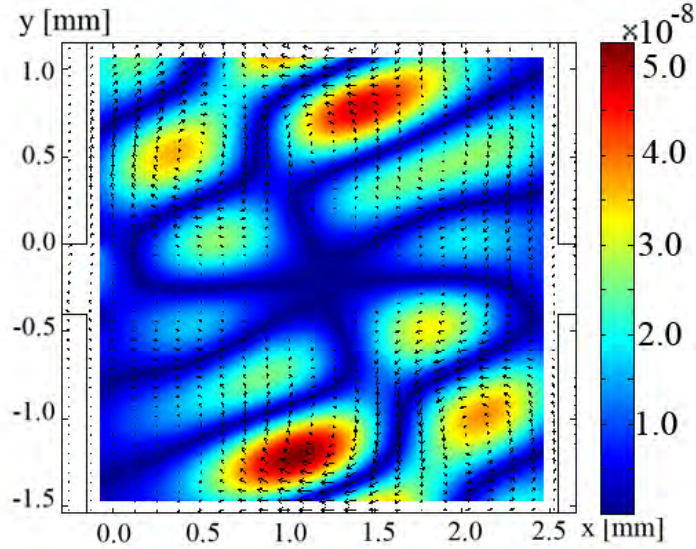
Figure 5.2: The figure illustrates two different ways of plotting the acoustic streaming. The vectors in the arrow plot indicate the size and direction of the local streaming velocity of fluid. The rotation of the streaming velocity is shown on the surface plot. The rotation does indicate how fast the velocity is rotating, and can thus be used as a measurement for the amount of streaming in our system.

The highest streaming velocity in the chamber is found to be $\langle v_2 \rangle_m$ $athrmmax \approx 4.2 \times 10^{-5} \mathrm{m\,s^{-1}}$. The order of magnitude of this velocity is reasonable compared to the one found experimentielly [8]. However, the arbitrary chosen amplitude of the actuator, along with the fact that the geometry and placement of the actuator, see section 5.2, have great influence on the calculated magnitude of the streaming velocity, implies that the actually magnitude of the streaming velocity should be evaluated with caution. The rotation [1] of the streaming velocity is shown as the surface plot in figure 5.2, and the applied acoustic field is seen to produce rotational and even vortical flow patterns in the water. The rotation field is seen to have a local maximum at every vortex and the greater the streaming velocity the greater the rotation will be. Thus we choose to measure of the amount of streaming in our system by the maximum value of the rotation.

Instead the rotation as a measure we could also use the magnitude of the streaming velocity. However, we are only interested in the streaming velocities which form the characteristic vortex patterns seen in figure 5.2, and thus we choose to use the the maximum rotation as a measure.

It is seen in figure 5.2 that the streaming velocity is not zero at the boundary of the chamber, and that some of the velocity continues out into the silicon. This shows that the found solution is not fully correct as the second order velocity ought to be zero at transition between water and silicon. The reason is that we did not calculate the $\mathbf{v}_{2\mathrm{inc}}$ term from equation (2.24), and so we did not find the full solution. Another comment which should be made about the plot regards the missing rotation field closed to the transition between water and silicon. This part of the rotation will not be taken into account as Matlab has some problems calculating the gradient close to the transition.

The flow profile wis seen not to be symmetric in the water chamber. In order to deal with this lack of symmetry we will try to place additional actuators in the model, symmetric aroundt the chamber, and see if this could effect the streaming pattern. This will be done in the next section.

The used Matlab script which genereted the shown plot in this section can be seen in appendix G.

---

[1]The mathematical expression for the rotation of the velocity field is given by $\partial_x \mathrm{v}_y - \partial_y \mathrm{v}_x$

5.2 Changing the placement and number of actuators

In the previous section we showed a example of chamber resonance and streaming in the used COMSOL model. In this section we will changes the position of the actuator and later add additional actuators. This will be done in order to observe how the found solution depend on the position and numbers of the actuator(s).

First we will try to change the position of the actuator and observe how the solution changes. The actuator is moved 3mm in the x-direction toward the chamber, and the problem is solved for the closest resonance frequency in the pressure. The solution for the pressure for both the old and new actuator position is shown in figure 5.3. The resonance frequency has changed 45 Hz, however, the overall pressure field is seen to be
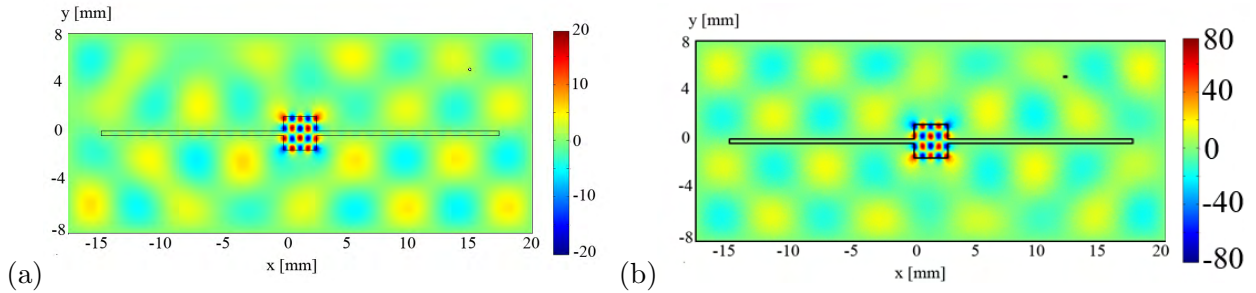
Figure 5.3: The figures shows surface plot of the pressure in the 2D system at a given time. (a) The pressure field before the actuator is moved at a frequency of 1.467190 MHz. (b) The pressure field after the actuator is moved 3mm in the x-direction toward the chamber at a frequency of 1.467235 MHz. The overall pressure field at resonance is seen to be nearly unaffected by the displacement.

unchanged.

The resulting velocity streaming for both actuator positions is displayed in figure 5.4. The velocity stream-

Figure 5.4: Surface plots of the rotation of the velocity streaming field together with arrowplots of the streaming velocity in the chamber. (a) The streaming before actuator is moved. (b) The streaming before actuator after the actuator is moved 3mm in the x-direction toward the chamber. The streaming pattern is seen to change significificantly.

ing pattern is on the contrary seen to change significificantly, and the magnitude of the rotation is enlarged by a factor of approximately 1000. Which means that our system is very sensitive to changes amoung others the position of the actuator. It does also mean that the absolute magnitude of the rotation should not be taken to

seriously, as previously mentioned.

In order to dealing with the lack of symmetry have we placed three additional actuators in the model, symmetric aroundt the chamber. It turned out that the resulting pressure field at the resonance frequency for the system with one actuactor changes dramatically, such that pressure field is mainely build up in the silicon. The streaming in the chamber is plottet in figure 5.5. The streaming pattern in the bottom half of the chamber is a mirror image of the upper half. So the placement and number of actuators greatly effect the found streaming velocityfield. The found resonance frequency is offcourse also sensitive for changes in the geometry, and the excact material parameters.

In conclusion does our numerical results depend on the placement and number of actuactor, the model geometry and the excact material parameters. This implies that a quantitativ comparation between the obtained numerical results and the experimental results should be performed with caution. Remember also that the here discussed streaming velocity is not the real streaming, but is only coupled to it.

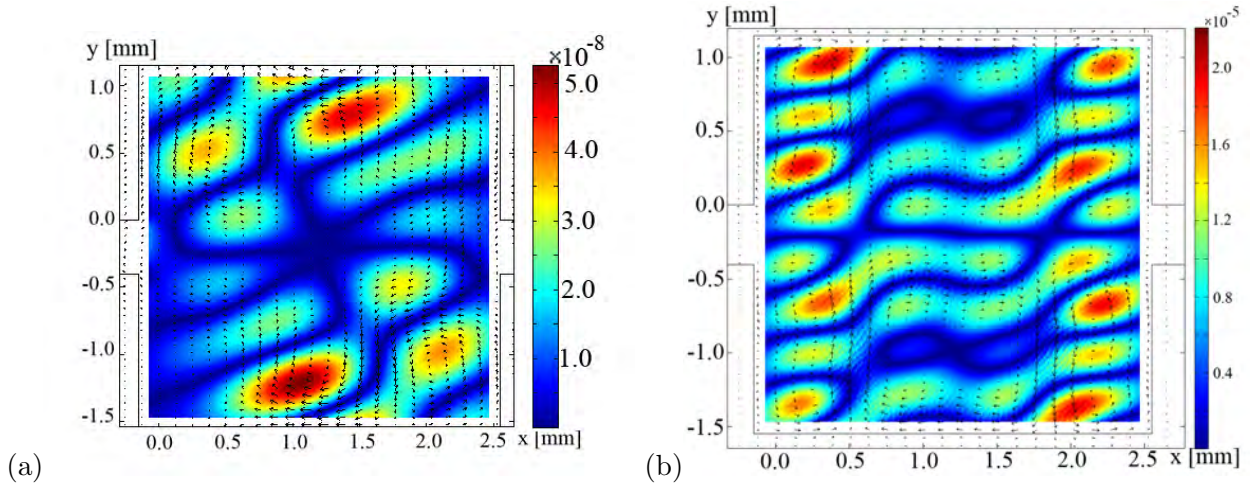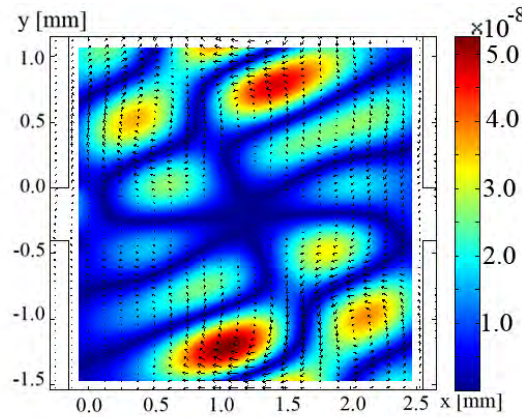Figure 5.5: Surface plot of the rotation of the velocity streaming field together with arrowplot of the streaming velocity in the chamber. This result is obtained with four actuators placed symmertically around the chamber. Notice the streaming pattern in the bottom half of the chamber is a mirror image of the upper half.

5.3   Impedance variation

As in section 3.3.2, where an analysis of a 1D, open, three layer system was considered, we want to variate the impedance of the outer layer which until now has been considered to be air. As we already know the impedance is the main factor that determines how much energy that will leave the system, i.e. how open the system are. As in the 1D system we want to investigate how the pressure resonancee and streaming velocity depend on the impedance of the outer layer.

On the basis of the 1D analysis in section 3.3 and the resonance found in section 5.1 it is natural to exspect that the maximum pressure and the streaming velocity, also in this 2D system, will have a maximum at certain resonance frequncies. To show that this in fact is the case we now consider a resonance pattern found with the outer layer having a impedance of $Z = 500 \, \mathrm{kg \, m^{-2} \, s^{-1}}$ and the frequency being $1.195957 \times 10^6 \, \mathrm{Hz}$. The pressure at this frequency and outer impedance has been plottet in figure 5.6.

As metioned we want to see how the pressure at resonance, like in figure 5.6, depend on the impedance in the outer layer. We also want to see how the streaming depend on the impedance in the outer layer. Therefore we have made three plots of the pressure and rotation as a function of the frequency at three different impedances of the outer layer, $Z = 500 \, \mathrm{kg \, m^{-2} \, s^{-1}}$, $Z = 1 \times 10^4 \, \mathrm{kg \, m^{-2} \, s^{-1}}$ and $Z = 1 \times 10^6 \, \mathrm{kg \, m^{-2} \, s^{-1}}$, respectively. The impedance ratio between the silicon and the outer layer is thus $z = 3,91 \times 10^4 \, \mathrm{kg \, m^{-2} \, s^{-1}}$, $z = 1.955 \times 10^3 \, \mathrm{kg \, m^{-2} \, s^{-1}}$ and $z = 19.55 \, \mathrm{kg \, m^{-2} \, s^{-1}}$, respectively. The three plots are shown in figure 5.7.
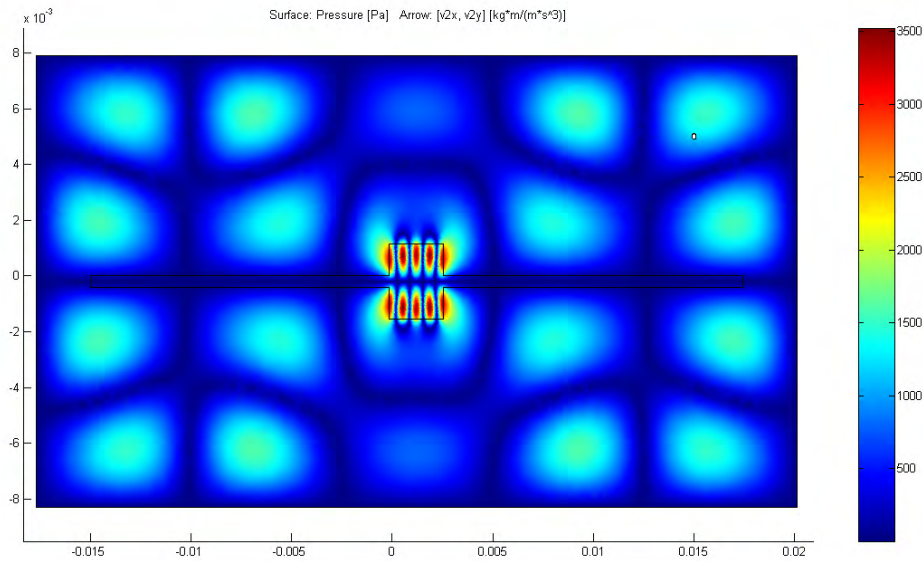
Figure 5.6: Plot of the pressure maximum in time. The inner chamber is water, the surrounding material is silicon and the outer layer has an impedance of $Z = 500\mathrm{kg\,m^{-2}\,s^{-1}}$. The system is excited by a frequency of 1.195957MHz. Notice the resonance in the water chamber and also a weak resonance in the silicon.

At the plots in figure 5.7 we see very sharp peaks at a certain resonance frequency for both pressure and rotation when the system is most closed, i.e. at figure 5.7 (c). Notice that the peaks are placed at the same frequency. However, as the system is opened up, i.e. the impedance ratio choosen closer to one, the resonance peaks will be flater and eventually almost disappear as seen in figure 5.7 (a). We should also notice that the weak maxima for pressure and rotation, that do occur in figure 5.7 (a), do not appear at the same frequency anymore.

Another thing to notice in figure 5.7 is that no matter if the peaks are sharp or not, the maxima being high or low, there are no other local maxima in the neighborhood of the resonance frequency. Making the plots in figure 5.7 a sweep of 500 Hz has been made and no other local maximum is to be seen. This observation will be quite important in the following analysis. As we are now working with COMSOL we can only calculate the maximum pressure and maximum rotation for a single value of the frequency and impedance at the time. In the 1D problem in section 3.3.2 we had an analytic expression for the pressure and streaming veloctity and could thus easely make a 3D plot, however, using COMSOL we have to have another approach. We will try to follow the maximum of these peaks as the impedance ratio is variated. In this way we should be able to describe how the resonance frequency and the maximum value of both pressure and rotation will depend on the impedance ratio.
Already now we would like to mention that the results, which are to be presented in the following part of report, is a product of calculations in COMSOL which are not easily done. The calculations are very time consuming and demands a high random access memory (RAM) capacity. We are fully aware of the fact that more calculations and a greater programming effort would have been to the advantage of this report. However, the programming which have been done, and the calculations which have followed, have taken several weeks to execute, and so our limited computer capacity have been a burden in this matter.

In order to make the following calculations in a systematical way, a small program in Matlab has been made. The basics of the program will now be explained. The program must be given a list of impedance of the outer

(a)

(b)

(c)
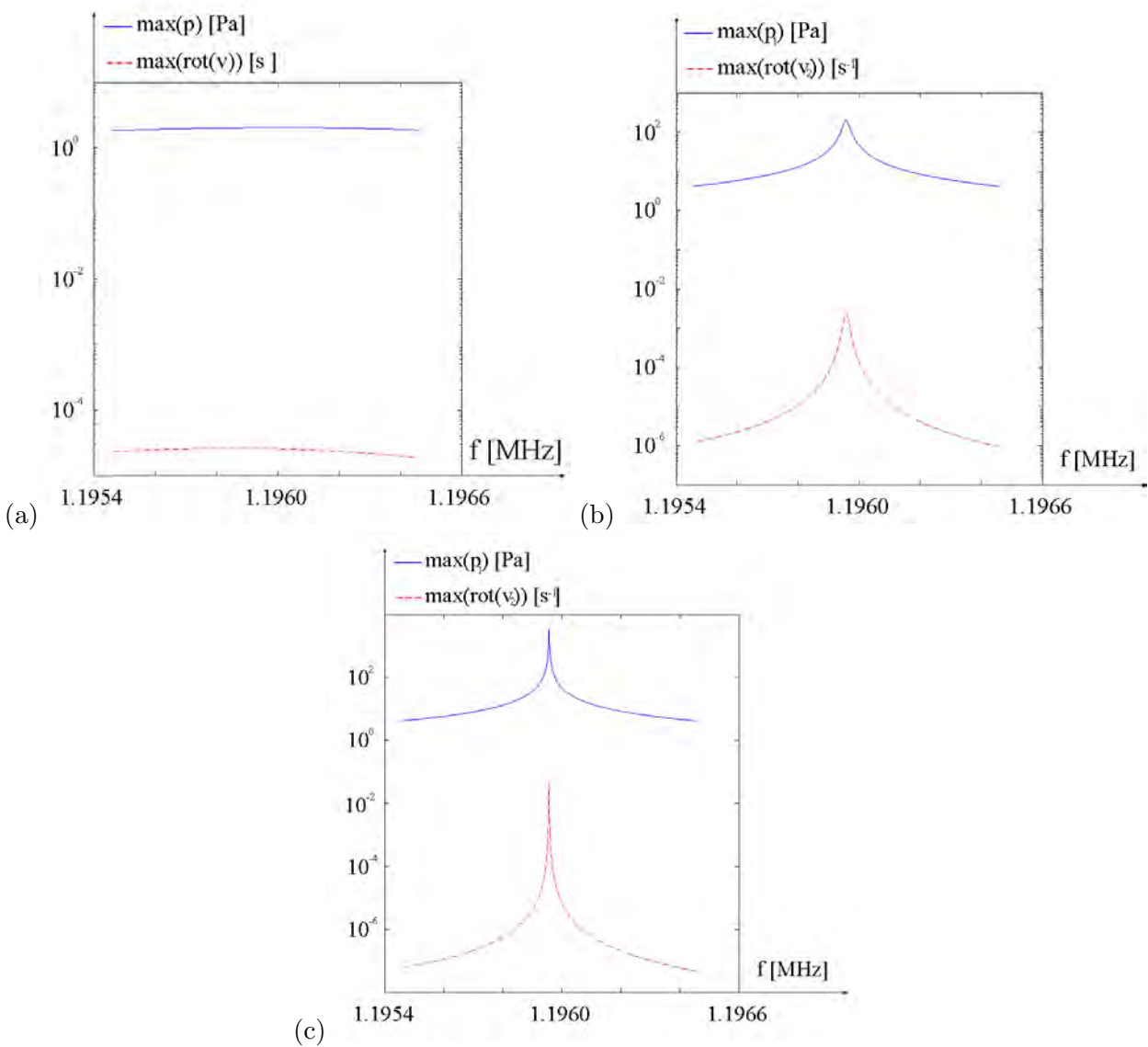
Figure 5.7: The pressure and rotation in the water champer as a function of the frequency at three different impedances ratios between the silicon and the outer layer. The impedance ratios are (a) $z = 19.55 \, \text{kg m}^{-2} \, \text{s}^{-1}$, (b) $z = 1.955 \times 10^3 \, \text{kg m}^{-2} \, \text{s}^{-1}$ and (c) $z = 3,91 \times 10^4 \, \text{kg m}^{-2} \, \text{s}^{-1}$, respectively. The resolution at the frequency axis is 1 Hz in general and 0.5 Hz at the peaks. Notice that both the pressure and rotation have a sharp peak at the same frequency when the system is most closed, i.e. at (c). When the system is more open and more energy is allowed to leave the system the resonance peaks for both pressure and rotation will be flater and have a lower maximum. Also notice that when the system gets opened up beyond a certain point, the pressure and rotation will not have resonance at the samme frequency which is seen at (a).

layer which one would like to investigate. Also a start frequency [2] must be given. The program will the scan

---

[2]A resonance frequency in the case of an impedance ratio much smaller than one can in COMSOL be found using the eigenfrequency solver. The eigenfrequency solver will solve the system considering the boundary between silicon and the outer layer to be inpermeabel (hard walls), i.e. no energy will leave the system. Thus the eigenfrequency solver can

a range of frequencies around the start frequency until a maximum is found. When a maximum is found the maximum value of the pressure or rotation is stored along with the resonance frequency and the impedance in the outer layer for which the problem was solved. The resonance frequency for the first impedance value will be used as the start guess for the second impedance to be solved for, and so the program continues until a resonance for all given impedances have been found. A surface plot of the calculated pressure or rotation as a function of the impedance and frequency will be shown. Also a plot of the solution like in figure 5.6 will be shown for each impedance at the resonance frequency. Given these plots the user can control that the nothing unexpected has occured during the process and that the program has found the right resonance pattern. As we have already seen the resonance is not as well-defined as the impedance ratio approach one, and also the resonance frequency will start to change, and so the plots can be very useful. The script with comments can be seen in appendix E, F H.

We have investigated the effect of an impedance variation in the neighborhood of three different resonance frequencies. In the following we will start by presenting the results obtained from the resonance seen in figure 5.6. After a full analysis of these results the results from the other two resonance frequencies will be shown and eventually turn out to show the qualitatively same results.

The maximum pressure and maximum rotation, and the resonance frequency for which both is found, in the water chamber are shown in figure 5.8 as a function of the impedance ratio between silicon and the outer layer.

We first consider figure 5.8 (b) which is a plot of the resonance frequency as a function of the impedance ration. We see that the resonance frequency for the pressure and the rotation is the samme when the impedance ratio is far away from one. As the impedance ratio is approaching one the resonance frequencies will suddenly start to change. The change in the resonance frequency for the pressure is most likely caused by the phaseshift of π which a wave hitting a transition will be getting if the impedance ratio is larger than one and will not be getting if the impedance ratio is smaller than one. The phaseshift arises from analysis leading to equation 3.49. Also the resonance frequency of the rotation is changing when the impedance ratio is approaching one. In this case the resonance frequency for the pressure and rotation, respectively, are moving away from each other, however, this should not undergo a greater analysis. In figure 5.7 (a) we saw that the resonance became very weak as the impedance ratio approached one, and knowing that the system is very sensitive to frequency and geometry, this is not neccesaraly the general case. In fact the analysis at other resonance frequencies we also later show that it is not the general case. Note that this drastic change in resonance frequency is making it harder for our Matlab/COMSOL program to find the resonance frequency as it has to sweep a much greater range of frequency. This is also the reason why we are missing points at very low rotation values, and one should be more cautious making conclusions based on calculations made with a impedance ratio close to one.

Now considering figure 5.8 (a) we see that the pressure has a minimum close to the impedance ratio being one. As mentioned before we should be cautious when considering the calculations done when the impedance ratio is close to one. It is also seen that the plot of the resonance frequency as a function of the impedance ratio does not seem to be continues at some impedance ratio close to one. This is also the reason why the rotation has not been calculated for a range around $z = 1$. However, the tendensy of both the pressure and rotation is quite clear; the minimum of both the pressure and rotation will be located for an impedance ratio close to one which was also the result from the 1D, multilayer analysis.

It is seen that when the impedance ratio is somewhat away from the minimun then both the pressure and rotation will increase as an exponential function as the slope of both grafs is forming a straight line in the plot were both axes are logarithmic. Fitting the obtained data we get the following expressions at resonance

$$\max(p_1)(z) \approx 3.03 \cdot 10^{-3} \cdot z_{bc}^{-0.986} \quad , z_{ab} \lesssim 10^{-2} \tag{5.1a}$$
$$\max(p_1)(z) \approx 1.08 \cdot 10^{-1} \cdot z_{bc}^{0.992} \quad , z_{ab} \gtrsim 10^{1} \tag{5.1b}$$
$$\max(rot(\langle v_2 \rangle))(z) \approx 6.41 \cdot 10^{-9} \cdot z_{bc}^{-0.999} \quad , z_{ab} \lesssim 10^{-2} \tag{5.1c}$$
$$\max(rot(\langle v_2 \rangle))(z) \approx 1.36 \cdot 10^{-6} \cdot z_{bc}^{0.991} \quad , z_{ab} \gtrsim 10^{1} \tag{5.1d}$$

We see that both the maximum pressure and the maximum rotation in resonance will be almost inversely proportional to the impedance ration z when the impedance ratio is changed from about 10^{-2} to 0 and directly proportional to the impedance ratio when the impedance ratio is changed from about 10^1 to infinity. We can

provide a good start guess, but one should be aware that the eigenfrequency solver might not find every eigenfrequency within the searching range.

(a)

(b)
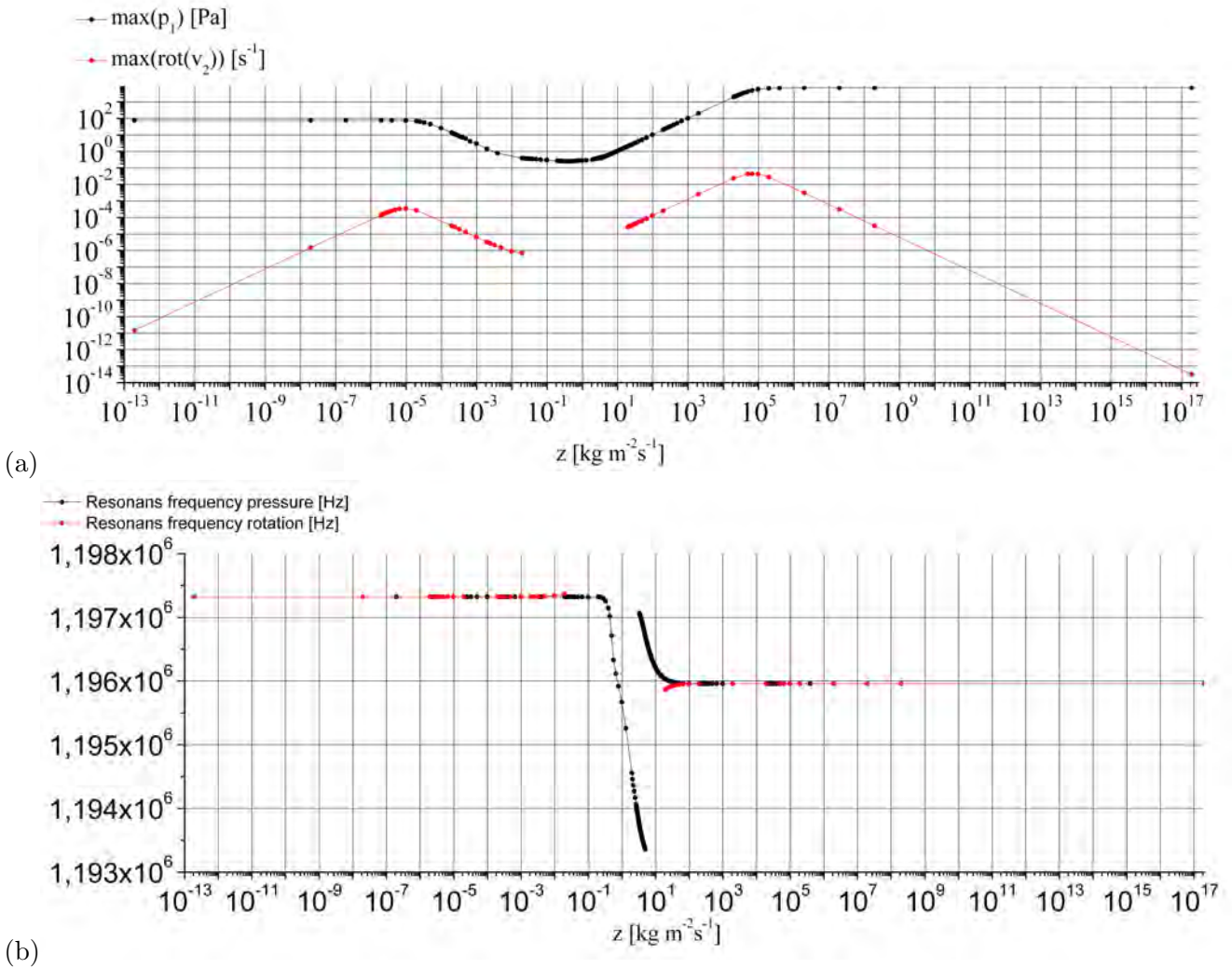
Figure 5.8: (a) is the maximum pressure (black) and maximum rotation (red) which was found in resonance as a function of the impedance ratio between the silicon and the outer layer in the 2D model used in COMSOL. (b) is the resonance frequency for the maximum pressure (black) and maximum rotation (red). Notice that the resonance frequencies are the same for both pressure and rotation for the impedance ratio far from one. As the impedance ratio approach one the resonance frequencies appart. Also notice that both pressure and rotation have a minimum when the impedance ratio is about one and will increase as the system is closed, i.e. the impedance going towards zero or infinity. Both the pressure and rotation seems to have a maximum at $z \approx 10^{-5}$ and $z \approx 10^{5}$, however, these maxima occur due to lack of resolution and both pressure and rotation will in fact continue to rise as the system is closed.

thus, like in the 1D analysis, conclude that if we want a strong pressure resonance and rotation the system shall be as closed as possible, i.e. the impdance ratio shall be very small or very big. As in the 1D analysis the pressure resonance was expected to increase as the system is closed. However, it is most interesting that also the rotation, and thus the streaming, is increasing proportional to the impedance ratio as the system is closed.

A last thing to be mentioned in figure 5.8 is the apparent maxima which both the pressure and rotation reach at $z \approx 10^{-5}$ and $z \approx 10^{5}$. However, in the 1D analysis we observed that the apparent maxima, which

seemed to be reach as the system was closed, were not maxima at all. The explanation was that the peaks became very narrow as the system was closed and thus could not be detected when the peak got narrower than the resolution. In the plots in figure 5.8 the resolution of the scan in the frequency domain is 1 Hz. To see if the maxima are real maxima or just a consequence of a finite resolution we have made some additional plot with different resolutions. The calculations are done under the same conditions as the plots in figure 5.8, but now we have plottet the interval $10^{-10} < Z_{\text{outer layer}} < 10^5$ with a resolution of 1 Hz, 0.1 Hz and 0.01 Hz, respectively. The plots are seen in figure 5.9.
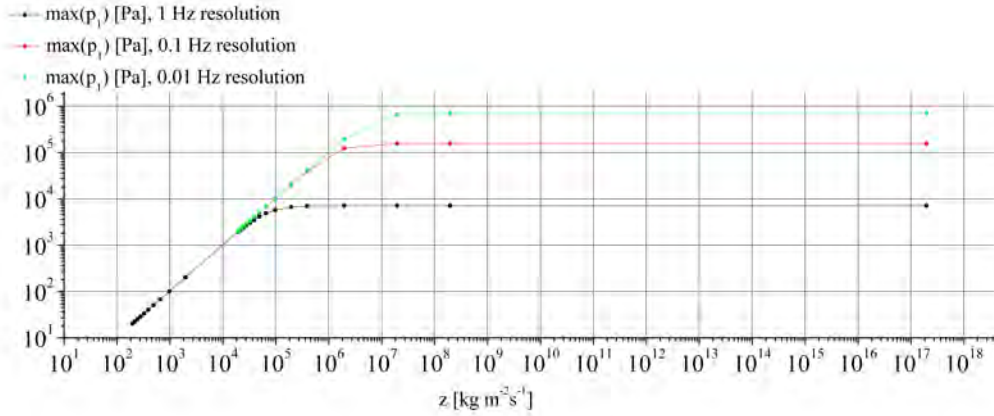
(a)
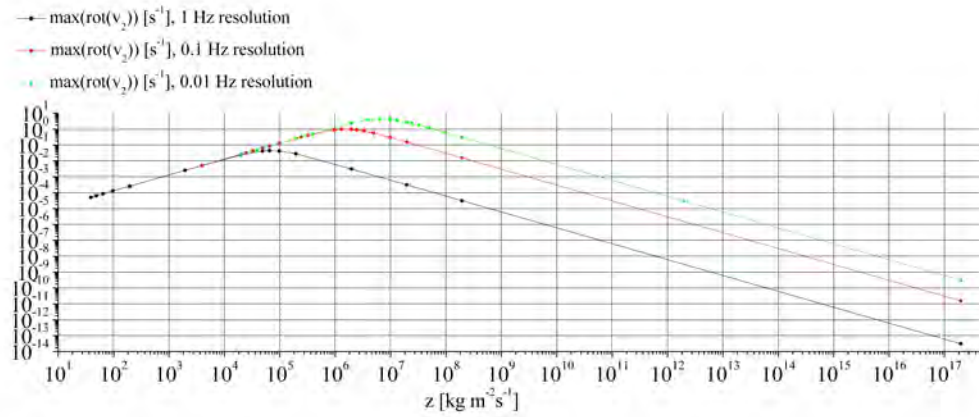
(b)

Figure 5.9: (a) is the maximum pressure found at resonance at three different resolutions in the frequency domain. (b) is the maximum rotation found at resonance at three different resolutions in the frequency domain. Both are plottet as a function of the impedance ratio between the silicon and the outer layer in the 2D model used in COMSOL. Notice that the maxima depend on the resolution.

The plots seems to confirm our suspicion. The maxima is not real maxima. Both the pressure and rotation will continue to increase as the system is closed, however, the range of resonance frequencies which support the increasing pressure and rotation will get narrower as the system is closed. As the resolution is increased the peak can be detected for systems which are more closed. We notice that when a frequency is not longer within the range of resonance frequencies then the pressure will stay constant at this frequency as the system is further closed. However, when a frequency is not longer within the range of resonance frequencies then the

rotation will start to decrease at a rate which is almost proportional to the impedance ratio at this frequency as the system is further closed.

As promised we will also have a look at the variation of the impedance ratio at two other resonances. In figure 5.10 the maximum pressure and rotation along with the center resonance frequencies has been plottet as a function of the impedance ratio. The plots are similar to those in figure 5.8, however, the resonance is now in the neighborhood of $\omega = 9.52 \times 10^5$ rad/s and $\omega = 1.47 \times 10^6$ rad/s.

As seen the plots in figure 5.10 are much alike the plots in figure 5.8. Both the resonance around $\omega = 9.52 \times 10^5$ rad/s and $\omega = 1.47 \times 10^6$ rad/s have a small change in resonance frequency as the impedance ratio goes from smaller than one to greaterthan one. Also both the maximum pressure and maximum rotation will have a minimum close to $z = 1$. As the system is closed the maximum pressure and maximum rotation will increase, and the width of the resonance peak will get narrower.

However, there is one thing that differs. When investegating the resonance around $\omega = 1.20 \times 10^6$ rad/s we found that maximum pressure and maximum rotation increased almost proportial to the impedance ratio as the system was closed. This is also the case in figure 5.10 (c), however, it is not in figure 5.10 (a). In this plot the maximum plot and rotation is, like the other two cases, increasing as a power function of the impedance ratio, but the absolute values of the powers is not very close to one, rather between 0.85 and 2.

5.4   Main results of the analysis in the full 2D COMSOL model

Overall a somewhat unambiguous picture has been forming. We have investigated three different resonance and qualitivily the analysis of the three cases are the same.

Both the pressure and streaming have resonance frequencies, or more precise a range of frequencies, which supports a significantly stronger pressure and streaming in the water champer. There are two main characteristics of the resonances: The range of frequencies which supports a resonance, i.e. the width in the frequency domain of the resonance peak, and the maximum value of the peak, i.e. the height of the resonance peak. In resonance both the pressure and the streaming was increasing proportional to the impedance ration z between the silicon layer and the outer layer as the system was close, i.e. as $z \to 0$ or $z \to \infty$. In all three investigated cases the pressure and the streaming seemed to be a power function of the impedance ratio in resonance. Furthermore, in two of the three case a almost clear proportionality between both the pressure and streaming, respectively, and the impedance ratio was seen, i.e. when the impedance ratio was decreasing from one towards zero we saw an inverse proportionality, and when the impedance ratio was increasing from one towards infinity we saw a directly proportionality. When not in resonance, i.e. considering a frequecy outside the range of resonance frequencies, the maximum pressure would stay constant as the system was closed further whereas the streaming would decrease proportional to the impedance ratio as the system was further closed. Both for pressure and streaming the range of resonance frequencies would get smaller as the system was closed, however, a precise dependences between the width of the resonance peak and impedance ratio have not been found but could be an interesting task for further studies. Our guess is that the peak eventually would go towards infinity in height and zero in width as the system is maximal closed. However, this still needs to be investigated further. The maximum of the resonance peak was in all three cases found to have a minimum in height and maximum in width at some impedance ratio close to one.
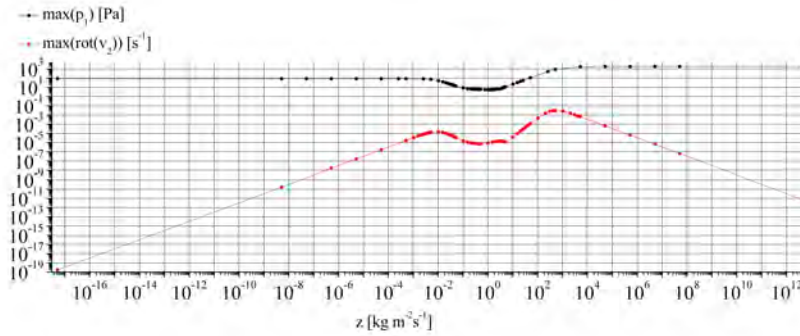
(a)
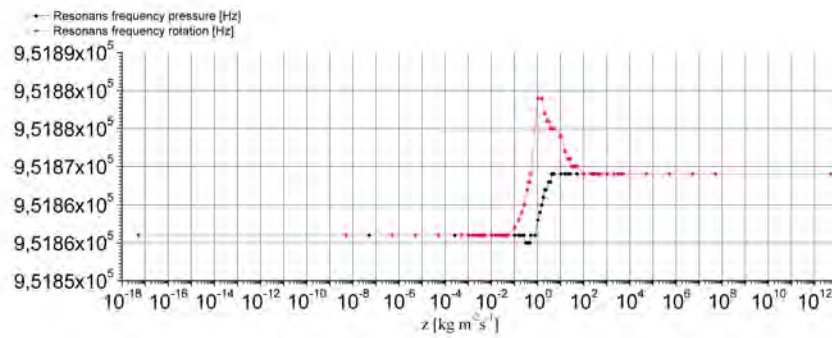
(b)
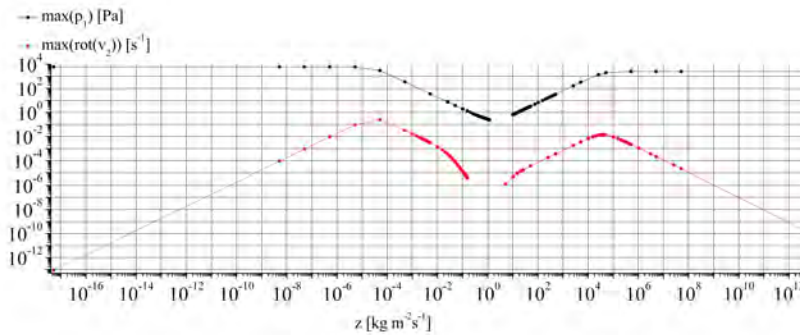
(c)
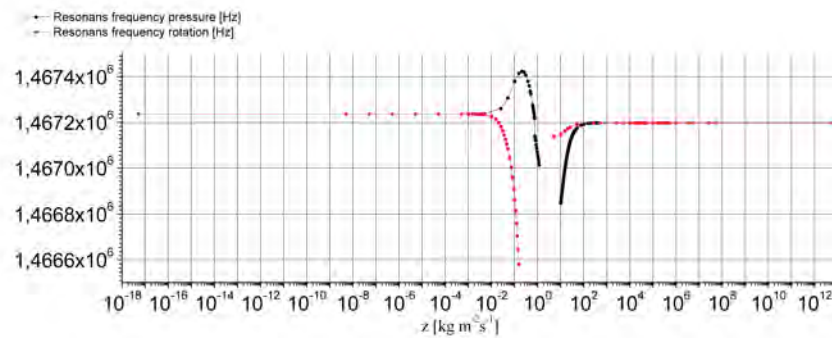
(d)

Figure 5.10: (a) and (c) is the maximum pressure (black) and maximum rotation (red) which was found in resonance as a function of the impedance ratio between the silicon and the outer layer in the 2D model used in COMSOL. (b) and (d) is the resonance frequency for the maximum pressure (black) and maximum rotation (red). The resonance showed in (a) has the resonance frequencies showed in (b), and the resonance showed in (c) has the resonance frequencies showed in (d).

Chapter 6

Conclusion

The governing equations used throughout this thesis are the continuity and the Navier–Stokes equations. Using pertubation theory we have been able to establish the first and second order continuity and Navier–Stokes equations. From these the more simple, time-averaged, second order equations was derived.

From the first order equations the Helmholtz equations was derived for viscous fluids, and a variety of simple problems was solved analytically. Solving a viscous, closed, one-dimensional problem resonance at certain frequencies was observed. Also the pertubation parameter for the one-dimensional system was estimated and found to be sufficiently small, both for the case of resonance and non-resonance.

The time-averaged, second order continuity equation was partially solved and a term contained in the solution, i.e. the time-average, second order velocity field, was found. This term was assumed to indicate the streaming velocity in a system and was hereafter taken as an expression for the streaming, eventhough it was only coupled to the real solution. A viscous, closed, two-dimensional system was considered, and the viscousity of the fluid was found to give rise to some amount of acoustic streaming. However, the streaming occuring due to the viscousity could not account for the experimental results.

Considering boundery layer theory we found that boundery layer could be neglected when the first order fields are calculated but not when calculating the second order fields. In fact the boundary layer can be found to be a second source to acoustic streaming, however, it cannot explain the streaming observed in experiments neither.

As the two mentioned sources of streaming was not able to account for the experimental results a third possible source of streaming was considered. Great efforts have been made in order to investigate how the energy dissipation to the surroundings of a system could give rise to acoustic streaming. Considering an one-dimensional system with an acoustic wave sent into a transition between two materials we found that the energy transmitted through the transition, i.e. the energy lost, depended on the acoustic impedance ratio of the two materials. This result was used to make a comprehensive analysis in a open, three layer, one-dimensional system with one oscillating wall. Both the first order pressure and the streaming was found analytically. Both quantities was plotted with respect to the frequency and the acoustic impedance ratio. A strong resonance was observed in a water layer for both the pressure and streaming at certain resonance frequencies. When the acoustic impedance ratio was much greater or smaller than one the resonance frequencies was well-defined and similar for pressure and streaming. However, when the impedance ratio was closed to one only a weak resonance was seen, and the resonance frequency would change. At resonance both the pressure and streaming was found to be increasing proportional to the impedance ratio when the impedance ratio was far away from one and the system was further closed, i.e. the impedance ratio was moved further away from one and so less energy was allowed to leave the system. When not at resonance the pressure would stay constant and the streaming would decrease as the system was further closed. The range of frequencies which supported a resonance would get smaller as the system was closed. The one-dimensional analysis provided many results, however, as always one should be cautious tranfering one-dimensional results to cases of higher dimensions. Thus the results in the one-dimensional analysis will only be considered to give a intuitive sense of the streaming phenomenon, rather than providing evidence.

In order to treat more complex systems COMSOL was introduced and shown to be able to reproduce the analytical results. In COMSOL a two-dimensional system, similar to the experimental setup, was made.

The system consisted of a small, squared water champer connected to a narrow channel and surrounded by silicon. The system was actuated by a small actuator. Others have shown that a two-dimensional system is well-suited for the analysis of a three-dimensional setup when one the spatial dimensions is small compared to the wavelength. I this COMSOL model the rotation of the streaming velocity was taken as a measure of the amount of streaming in the water champer. The streaming pattern in the water champer was seen to be very sensitive to changes in geometry, symmetry and actuator position and so there have been no efforts made to reproduce the actual streaming pattern found in experiments. However, like in the one-dimensional case, a comprehensive analysis of how the pressure and streaming was connected to the acoustic impedance ratio between the silcon and outer layer and the excitation frequency, respectively, have been made. Three different resonances was invesigated, and overall a somewhat unambiguous picture has been forming. Both the pressure and streaming have resonance frequencies, or more precise a range of frequencies, which supports a significantly stronger pressure and streaming in the water champer. There are two main characteristics of the resonances: The range of frequencies which supports a resonance, i.e. the width in the frequency domain of the resonance peak, and the maximum value of the peak, i.e. the height of the resonance peak. In resonance both the pressure and the streaming was increasing proportional to the acoustic impedance ration between the silicon layer and the outer layer as the system was close, i.e. as the impedance ratio was going from one towards zero or infinty. In all three investigated cases the pressure and streaming seemed to be a power function of the impedance ratio in resonance. Furthermore, in two of the three case a almost clear proportionality between both the pressure and the streaming, respectively, and the impedance ratio was seen, i.e. when the impedance ratio was decreasing from one towards zero we saw an inverse proportionality, and when the impedance ratio was increasing from one towards infinity we saw a directly proportionality. When not in resonance, i.e. considering a frequecy outside the range of resonance frequencies, the maximum pressure would stay constant as the system was closed further whereas the streaming would decrease proportional to the impedance ratio as the system was further closed. Both for pressure and streaming the range of resonance frequencies would get smaller as the system was closed, however, a precise dependences between the width of the resonance peak and impedance ratio have not been found. It is plausible to assume that the peak eventually would go towards infinity in height and zero in width as the system is maximal closed. The maximum of the resonance peak was in all three cases found to have a minimum in height and maximum in width at some impedance ratio close to one.

More data to support the two-dimensional analysis could be desired, however, the analysis was based on very time consuming and demanding computations in COMSOL. This set a natural limit to the amount of data which could be obtained within our time frame.

The main goal of this thesis was to investigate how the streaming phenomenon in resonant microfluic systems depended on the energy dissipation to the surroundings. We were only able to determine a part of the actual streaming velocity, however, analysis of this part strongly indicated that energy dissipation to the surroundings in fact is a source of acoustic streaming. Furthermore, numerical calculations indicated how the amount of streaming depended on the energy dissipation.

Chapter 7

Outlook

A natural extension to the work presented in this thesis, would be to carry out more simulation data to support the analysis of the streaming phenomenon. A few loose ends have been left for further studies. One interesting follow up could be the investigation of how the range of resonance frequencies depend on the acoustic impedance ratio, i.e. the amount of energy allowed leaving the system. Also a minimum of streaming was seen when the impedance ratio was close to unity. However the exact placement of this minimum could be investigated further.

Another interesting follow up could be the finding of the full solution to the second order equations. This would provide a fully correct expression for the streaming velocity, and one would the be able to get a greater understanding of the streaming phenomonon.

In order to make a better agreement between the experimental setup and the mathematical model, one could extend the two dimensional model to three dimensions. One of the problem with our two-dimensional model was that we could not actuate the whole system, but had to let a small actuator provide the acoustic waves. In a three dimensional analysis one could set the bottom boundary condition to normal acceleration as we did with the round actuator in the COMSOL simulations.

Another way to make the mathematical model agree with the experimental setup, one could change the latter. This could be done by solely actuate the silicon chip at certain points. This would be more similar to the COMSOL model used so far.

Appendix A

Material parameters

Material	Density	Speed of sound	Impedance
Water	1000	343	1.5×10^6
Silicon	2300	8500	2.0×10^7
Air	1.2	340	4.1×10^2

Table A.1: Typical parameter values for 20 °C, and normal atmospheric pressure.

Appendix B

Check If c_a Is The Speed Of Sound

As mentioned before we strongly suspect c_a in equation (2.30) to be the speed of sound. To verify this we will do a few calculations on a known problem which is sound waves in air where we know that the speed of sound is $343m/s$ [1, Table 15.2].
First we recall that

$$c_a^2 = \frac{\partial p}{\partial \rho} \tag{B.1}$$

Next we have ideal gas law

$$p(\rho) = \frac{nRT}{V} = \rho \frac{RT}{M} \tag{B.2}$$

where n is the number of atoms in mol, R is the gas constant, T is the temperature, V is the volume and M is the mass per mol.

A soundwave is air expanding and compressing thus changing the density ρ and the pressure p. We now see from the ideal gas law that such a change in pressure will change the temperature, but soundwaves are ocsillating so fast that we assume that no heat transfer will take place due to the short time intervals of difference in temperature. As there is no heat transfer we have a isentropic process and thus

$$pV^\gamma = \text{constant} \tag{B.3}$$

where $\gamma = \frac{c_p}{c_v} = \frac{c_v + R}{c_v}$ where c_p and c_v are the specific heat capacity at constant pressure and constant volumen, respectively [10].
From equation (B.3) and (B.2) we get

$$\frac{\partial}{\partial \rho} p \quad = \quad \frac{\partial}{\partial \rho} \frac{\text{constant}}{V^\gamma} \tag{B.4a}$$

$$= \quad \frac{\partial}{\partial \rho} \rho^\gamma \frac{\text{constant}}{\text{m}^\gamma} \tag{B.4b}$$

$$= \quad \frac{\gamma}{\rho} \rho^\gamma \frac{\text{constant}}{\text{m}^\gamma} \tag{B.4c}$$

$$= \quad \frac{\gamma}{\rho} \frac{\text{constant}}{V^\gamma} \tag{B.4d}$$

$$= \quad \frac{\gamma}{\rho} p \tag{B.4e}$$

$$= \quad \gamma \frac{RT}{M} \tag{B.4f}$$

Air mostly consist of N_2 and O_2 molecules and is therefor a diatomic gas. For a diatomic gas we have $c_v = \frac{5}{2}R$ [10] and thus $\gamma = \frac{7}{5}$. The temperature is taken to be the normal room temperature and so $T = 293K$. The Gas

Constant is $R = 8.3145 \frac{J}{K \cdot mol}$ [10]. We take the air to be 79% Nitrogen and 21% Oxygen and so the molar mass are

$$
\begin{aligned}
M &= 0.79 \, M_{N_2} + 0.21 \, M_{O_2} & \text{(B.5)} \\
&= 0.79 \cdot 2 \cdot 0.01401 \frac{kg}{mol} + 0.21 \cdot 2 \cdot 0.01600 \frac{kg}{mol} & \text{(B.6)} \\
&= 0.029 \frac{kg}{mol} & \text{(B.7)}
\end{aligned}
$$

From equation (B.1) and (B.4f) using the found values we get

$$
c_a = \sqrt{\frac{\partial p}{\partial \rho}} = \sqrt{\gamma \frac{RT}{M}} = \sqrt{\frac{7}{5} \cdot \frac{8.3145 \frac{J}{K \cdot mol} \cdot 293K}{0.029 \frac{kg}{mol}}} = 343 \frac{m}{s} \tag{B.8}
$$

Note that this gives us the expected value for the speed of sound in air which convince us that c_a is in fact the speed of sound.

Appendix C

Derivation of the continuity equation for compressible fluids

The first governing equating to derive is the continuity equation that expresses the conversation of mass.

We begin by expressing the mass M of a arbitrary, fixed region Ω as the volume integral over the mass density ρ which can vary as a function of time and space. We get

$$M(\Omega, t) = \int_\Omega \mathrm{d}\mathbf{r}\, \rho(\mathbf{r}, t) \tag{C.1}$$

Notice that the integral is expressed as and integral operator.

The change of mass may then be expressed as

$$\partial_t M(\Omega, t) = \partial_t \int_\Omega \mathrm{d}\mathbf{r}\, \rho(\mathbf{r}, t) = \int_\Omega \mathrm{d}\mathbf{r}\, \partial_t \rho(\mathbf{r}, t) \tag{C.2}$$

The derivative can be moved inside the integral as the integral is fixed in time.

Another way to express the change of mass requires the mass current density $\mathbf{J}$ which is defined by the mass density and the convection velocity $\mathbf{v}$. It reads

$$\mathbf{J}(\mathbf{r}, t) = \rho(\mathbf{r}, t)\mathbf{v}(\mathbf{r}, t) \tag{C.3}$$

In our case that mass can neither appear nor disappear spontaneously, and so the mass will only changes by the mass flux that passes through the surface $\partial\Omega$ which has the outward pointing normal vector $\mathbf{n}$. Thus the change of mass can be expressed as

$$\partial_t M(\Omega, t) = -\int_{\partial\Omega} \mathrm{d}a\, \mathbf{n} \cdot \mathbf{J} = -\int_\Omega \mathrm{d}a\, \nabla \cdot \mathbf{J} \tag{C.4}$$

The last equal sign is obtained by applying Gauss' Theorem.

Combining equation (C.2), (C.3) and (C.4) we get

$$\int_\Omega \mathrm{d}\,\mathbf{r}\, \partial_t \rho(\mathbf{r}, t) = -\int_\Omega \mathrm{d}a\, \nabla \cdot (\rho\mathbf{v}) \tag{C.5}$$

As this should hold for an arbitrary region Ω the integrands must be the same and thereby we get the continuity equation

$$\partial_t \rho(\mathbf{r}, t) = -\nabla \cdot (\rho\mathbf{v}) \tag{C.6}$$

Appendix D

Derivation of the Navier–Stokes equation for compressible fluids

In this section we are going to derive the generel equation of motion for the Eulerian velocity field of a viscous fluid. This equation can for Newtonian fluids be rewritten as the Navier–Stokes equation for compressible viscous fluids.

We begin by considering the rate of change of the total momentum $\mathbf{P}$ of the fluid inside an arbitrary shaped, but fixed in time, region Ω. The momentum can be expressed as the volume integral over the momentum density $\rho\mathbf{v}$. So the rate of change of the total momentum can in index notation, when applying the chain rule, be expressed as

$$\partial_t P_i = \partial_t \int_\Omega \mathrm{d}\mathbf{r}\rho v_i = \int_\Omega \mathrm{d}\mathbf{r}\partial_t(\rho v_i) = \int_\Omega \mathrm{d}\mathbf{r}[(\partial_t\rho)v_i + \rho\partial_t v_i] \tag{D.1}$$

The total momentum can change both by convection and by the action of forces given by Newton's second law. The forces can be divided into contact forces that act on the surface $\partial\Omega$ of Ω, e.g. pressure and viscosity forces, and body forces that act on the interior of Ω, e.g. gravitational and electrical forces. These forces can be written as the time derivatives of the corresponding parts of the total momentum. So the rate of change of the total momentum can be found as

$$\partial_t P_i = \partial_t P_i^{\mathrm{conv}} + \partial_t P_i^{\mathrm{press}} + \partial_t P_i^{\mathrm{visc}} + \partial_t P_i^{\mathrm{body}} \tag{D.2}$$

Convection of momentum

One way the total momentum $\mathbf{P}$ can change is by convection of the momentum described by the vector $\rho\mathbf{v}$. It means that we have a momentum current passing through the surface $\partial\Omega$ thus changing the total momentum in Ω. Just as in equation (C.3), where convection was obtained by multiplying with the velocity vector $\mathbf{v}$ and thus given by $\rho\mathbf{v}$, the convection of momentum is described as a tensor Π' which is given by

$$\Pi' = \rho\mathbf{v}\mathbf{v} = \rho v_i v_j \tag{D.3}$$

The change of the total momentum is given by the surface integral over the momentum density flux going inwards through the surface given by $-\mathbf{n}\cdot\Pi' = -\rho\mathbf{v}(\mathbf{n}\cdot\mathbf{v}) = -n_j\,\rho v_i v_j$ where $\mathbf{n}$ is dotted with the velocity of the convection. Thus the change of the total momentum becomes

$$\partial_t P_i^{conv} = -\int_{\partial\Omega} \mathrm{d}a\, n_j\,\rho v_i v_j \tag{D.4}$$

Pressure forces

As mentioned the total momentum will change due to forces. One of these forces are the pressure force from the surroundings acting on the surface $\partial\Omega$. At each infinitesimal area $\mathrm{d}a$ the pressure force on the surface is

given by $-p\mathbf{n}\mathrm{d}a$. Notice that the pressure force is simply proportial with the the pressure p pointing in the opposite direction as $\mathbf{n}$. The total change of momentum due to pressure forces on the surface is therefor given by

$$\partial_t P_i^{pres} = -\int_{\partial\Omega} \mathrm{d}a \, n_i \, p = -\int_{\partial\Omega} \mathrm{d}a \, n_j \, p\delta_{ij} \tag{D.5}$$

The last equal sign is made in order to give $\mathbf{n}$ the same index as in equation (D.4).

Viscous forces

Due to the viscosity of the fluid, the region Ω is also affected by fritional forces on the surface $\partial\Omega$ from the flow from the surrounding fluid. The frictional force is determined by two vectors: the vector of the force and the surface normalvector. Therefor the force $\mathrm{d}\mathbf{F}$ on a surface element $\mathrm{d}a$ is characterized by a second rank tensor σ'_{ij} which expressed the ith component of the friction force per area acting on the surface with its normalvector n_j. Thus the force is given by

$$\mathrm{d}F_i = \sigma_{ij} n_j \, \mathrm{d}a \tag{D.6}$$

As previous the total change in momentum is given by the sum of forces affecting the region Ω and we get

$$\partial_t P_i^{\mathrm{visc}} = \int_{\partial\Omega} \mathrm{d}F_i = \int_{\partial\Omega} \mathrm{d}a \, n_j \, \sigma'_{ij} \tag{D.7}$$

σ'_{ij} is the so-called viscous stress tensor and can be shown to have the following approximated expression:

$$\sigma'_{ij} = \eta \left(\partial_j v_i + \partial_i v_j\right) + (\zeta - \frac{2}{3}\eta)(\partial_k v_k)\delta_{ij} \tag{D.8}$$

where η and ζ are material parameters, dynamic viscosity and second visosity respectivily. The dynamic viscosity η is determined by the internal friction due to shear stress and the second viscosity ζ is determined by internal friction due to compression.

Body forces

The body forces are external forces that act throughout the entire body of the fluid. The most importent body forces are the gravitational force and the electrical force. The resulting change in the momentum of the fluid due to these two body forces is

$$\partial_t P_i^{body} = \int_\Omega \mathrm{d}\mathbf{r} \, (\rho\mathbf{g} + \rho_{\mathrm{el}}\mathbf{E})_i = \int_\Omega \mathrm{d}\mathbf{r} \, (\rho g_i + \rho_{\mathrm{el}} E_i) \tag{D.9}$$

Note that ρ_{el} is the charge density of the fluid, $\mathbf{g}$ is the acceleration of gravity, and $\mathbf{E}$ is the external electrical field.

The Navier–Stokes equation

The generel equation of motion for a viscous fluid can now be found from equation (D.2) by applying equation (D.1),(D.4),(D.5),(D.7), and (D.9). So we obtain the following equation

$$\int_\Omega \mathrm{d}\mathbf{r}[(\partial_t\rho)v_i + \rho\partial_t v_i] = \int_{\partial\Omega} \mathrm{d}a \, n_j \, [\sigma'_{ij} - \rho v_i v_j - p\delta_{ij}] + \int_\Omega \mathrm{d}\mathbf{r} \, (\rho g_i + \rho_{\mathrm{el}} E_i) \tag{D.10}$$

Utilizing Gauss's theorem the surface integral involving n_j can be rewritten as a volume integral involving ∂_j. Since the resulting volume integrals is taken over the same arbitrary region Ω the integrands must be equal. Hence we obtain the following partial differential equation

$$(\partial_t\rho)v_i + \rho\partial_t v_i = -\partial_j(\rho v_i v_j) - \partial_j(p\delta_{ij}) + \partial_j\sigma'_{ij} + \rho g_i + \rho_{\mathrm{el}} E_i \tag{D.11}$$

This expression can be simplified by using the chain rule $-\partial(\rho v_j v_i) = -\partial_j(\rho v_j) - \rho v_j \partial_j v_i$, of which according to the continuity equation (C.6) the first term cancels out with the term $(\partial_t \rho)v_i$ on the left-hand side in equation (D.11). In addition the term $\partial_j(p\delta_{ij})$ can be simplified to $\partial_i p$ according to the properties of the delta function. Assuming that we have a Newtonian fluid the viscosity coefficients η and ζ will only vary a little and so we take them as constants. Making this assumption we get

$$
\begin{aligned}
\partial_j \sigma'_{ij} &= \partial_j \eta \left(\partial_j v_i + \partial_i v_j\right) + \partial_j(\zeta - \frac{2}{3}\eta)(\partial_k v_k)\delta_{ij} & \text{(D.12)} \\
&= \eta\partial_j^2 v_i + \eta\partial_i\partial_j v_j + (\zeta - \frac{2}{3}\eta)\partial_i(\partial_k v_k) & \text{(D.13)} \\
&= \eta\partial_j^2 v_i + (\zeta + \frac{\eta}{3}\eta)\partial_i(\partial_j v_j) & \text{(D.14)}
\end{aligned}
$$

Substituting this result into equation (D.11) and making the discussed simplifications we arrive at the Navier–Stokes equation

$$
\begin{aligned}
\rho[\partial_t v_i + v_j\partial_j v_i] &= -\partial_i p + \eta\partial_j^2 v_i + (\zeta + \frac{\eta}{3})\partial_i(\partial_k v_k) + \rho g_i + \rho_{el}E_i & \text{(D.15)} \\
&\Leftrightarrow \\
\rho[\partial_t \mathbf{v} + (\mathbf{v}\cdot\nabla)\mathbf{v}] &= -\nabla p + \eta\nabla^2\mathbf{v} + (\zeta + \frac{\eta}{3})\nabla(\nabla\cdot\mathbf{v}) + \rho\mathbf{g} + \rho_{\mathbf{el}}\mathbf{E} & \text{(D.16)}
\end{aligned}
$$

This equation is seen to be a three dimensional, second order, non-linear, and inhomogeneus partial differential equation.

Simplification of the Navier–Stokes equation

In the futher treatment of the Navier-Stoke equation we discard the contribution from the external electromagnetic fields, and thus the term $\rho_{el}\mathbf{E}$. In addition the pressure p can be divided into two terms, one due to gravity and one due to everything else. This implies that the gradient of the pressure can be found as

$$
\begin{aligned}
\nabla p &= \nabla p_{fluid} + \nabla p_{grav.} & \text{(D.17)} \\
&= \nabla p_{fluid} + \nabla\rho\mathbf{g}(z - z_0) & \text{(D.18)} \\
&= \nabla p_{fluid} + \rho\mathbf{g} & \text{(D.19)}
\end{aligned}
$$

By inserting this expression for the gradient of the pressure in the Navier–Stokes equation, the terms $\rho\mathbf{g}$ and $-\rho\mathbf{g}$ cancel out. So in conclusion we arrive at the following simplified Navier–Stokes equation after these simplifications

$$
\rho[\partial_t\mathbf{v} + (\mathbf{v}\cdot\nabla)\mathbf{v}] = -\nabla p_{fluid} + \eta\nabla^2\mathbf{v} + (\zeta + \frac{\eta}{3})\nabla(\nabla\cdot\mathbf{v}) \tag{D.20}
$$

p_{fluid} will just be denoted as p.

Appendix E

Matlab script which locates the resonance in pressure

```
clear all
flclear fem

% COMSOL version
clear vrsn
vrsn.name = 'COMSOL 3.3';
vrsn.ext = '';
vrsn.major = 0;
vrsn.build = 405;
vrsn.rcs = '$Name:  $';
vrsn.date = '$Date: 2006/08/31 18:03:47 $';
fem.version = vrsn;

flbinaryfile='EIGENMODEDEPENDENCE.mphm';

% Geometry
clear draw
g17=flbinary('g17','draw',flbinaryfile);
draw.s.objs = {g17};
draw.s.name = {'CO2'};
draw.s.tags = {'g17'};
fem.draw = draw;
fem.geom = geomcsg(fem);

% Initialize mesh
fem.mesh=meshinit(fem, ...
                  'hauto',1, ...
                  'hmaxsub',[1,5e-4,2,5e-5]);

% Create a grid of points:
xx=linspace(-1.5e-4,0.00255,1000);
yy=linspace(-0.00155,0.00115,1000);
[xx,yy] = meshgrid(xx, yy);
d = [xx(:)'; yy(:)'];

%initialize
ii=0;
```

```
%start frequency
f_0=1.692898e6;

%eleminate zeroes in matrix to save memory
f_tom=1.69e6;

%impedance loop
for imp=[1.2*343]
ii=ii+1;

imp

%start frequency is set
frekvens=f_0;

% Application mode 1
clear appl
fem .dim = {'p'};
appl.mode.class = 'Acoustics';
appl.assignsuffix = '_aco';
clear bnd
bnd.Z = {imp};
bnd.type = {'IMP','cont','NA'};
bnd.nacc = {0,0,1};
bnd.ind = [1,1,1,2,2,2,2,2,2,2,2,2,2,2,2,1,3,3,3,3];
appl.bnd = bnd;
clear equ
equ.cs = {8500,1483};
equ.rho = {2300,1000};
equ.ind = [1,2];
appl.equ = equ;
appl.var = {'freq','5689'};
fem.appl{1} = appl;
fem.frame = {'ref'};
fem.border = 1;
clear units;
units.basesystem = 'SI';
fem.units = units;

% Global expressions
fem.globalexpr = {'v2x','real(p*conj(vx_aco))','v2y','real(p*conj(vy_aco))'};

% Multiphysics
fem=multiphysics(fem);

% Extend mesh
fem.xmesh=meshextend(fem);

% Solve problem
fem.sol=femstatic(fem, ...
                  'solcomp',{'p'}, ...
                  'outcomp',{'p'}, ...
                  'pname','freq_aco', ...
```

```
                      'plist',[frekvens], ...
                      'oldcomp',{}, ...
                      'ntol',1.0E-7, ...
                      'maxiter',50);

% get the solution only in chamber
u = postinterp(fem, 'abs(p)', d);

%save maximum pressure value in f-imp-matrix
p1(frekvens-f_tom,ii)=max(u);

%maximum pressure value
pmax=max(u);

n=1;

while n==1

    count=0;

    for step=[3 3]

    count=count+1;

    %defining the frequency to solve for, counting upwards
    frekvens=frekvens+step;

    % Solve problem
    fem.sol=femstatic(fem, ...
                  'solcomp',{'p'}, ...
                  'outcomp',{'p'}, ...
                  'pname','freq_aco', ...
                  'plist',[frekvens], ...
                  'oldcomp',{}, ...
                  'ntol',1.0E-7, ...
                  'maxiter',50);

    % get the solution only in chamber
    u = postinterp(fem, 'abs(p)', d);

    %save maximum pressure value in f-imp-matrix
    p1(frekvens-f_tom,ii)=max(u);

    %maximum pressure value
    maxx(count)=max(u);
    end

    max5=max(maxx);

    clear maxx

    if max5<pmax
        n=0;
    end
```

```
pmax=max5;

end

%the center frequency
frekvens=f_0;

% Solve problem
fem.sol=femstatic(fem, ...
                  'solcomp',{'p'}, ...
                  'outcomp',{'p'}, ...
                  'pname','freq_aco', ...
                  'plist',[frekvens], ...
                  'oldcomp',{}, ...
                  'ntol',1.0E-7, ...
                  'maxiter',50);

% get the solution only in chamber
u = postinterp(fem, 'abs(p)', d);

%save maximum pressure value in f-imp-matrix
p1(frekvens-f_tom,ii)=max(u);

%maximum pressure value
pmax=max(u);

n=1;

while n==1

    count=0;

    for step=[3 3]

    count=count+1;

    %defining the frequency to solve for, counting upwards
    frekvens=frekvens-step;

    % Solve problem
    fem.sol=femstatic(fem, ...
                  'solcomp',{'p'}, ...
                  'outcomp',{'p'}, ...
                  'pname','freq_aco', ...
                  'plist',[frekvens], ...
                  'oldcomp',{}, ...
                  'ntol',1.0E-7, ...
                  'maxiter',50);

    % get the solution only in chamber
    u = postinterp(fem, 'abs(p)', d);

    %save maximum pressure value in f-imp-matrix
```

```
        p1(frekvens-f_tom,ii)=max(u);

        %maximum pressure value
        maxx(count)=max(u);
        end

        max5=max(maxx);

        clear maxx

        if max5<pmax
            n=0;
        end

pmax=max5;

end

%find the frequency with the highes pressure and
%define this as the new center frequency
%this will be the start frequency for the next impedans
f_0=find(p1(:,ii)==max(p1(:,ii)))+f_tom;

frekvens=f_0;

% Solve problem
fem.sol=femstatic(fem, ...
                  'solcomp',{'p'}, ...
                  'outcomp',{'p'}, ...
                  'pname','freq_aco', ...
                  'plist',[frekvens], ...
                  'oldcomp',{}, ...
                  'ntol',1.0E-7, ...
                  'maxiter',50);

% get the solution only in chamber
u = postinterp(fem, 'abs(p)', d);

%save maximum pressure value in f-imp-matrix
p1(frekvens-f_tom,ii)=max(u);

%maximum pressure value
pmax=max(u);

n=1;

while n==1

    count=0;

    for step=[1 1 1]

    count=count+1;
```

```
    %defining the frequency to solve for, counting upwards
    frekvens=frekvens+step;

    % Solve problem
    fem.sol=femstatic(fem, ...
                'solcomp',{'p'}, ...
                'outcomp',{'p'}, ...
                'pname','freq_aco', ...
                'plist',[frekvens], ...
                'oldcomp',{}, ...
                'ntol',1.0E-7, ...
                'maxiter',50);

    % get the solution only in chamber
    u = postinterp(fem, 'abs(p)', d);

    %save maximum pressure value in f-imp-matrix
    p1(frekvens-f_tom,ii)=max(u);

    %maximum pressure value
    maxx(count)=max(u);
    end

    max5=max(maxx);

    clear maxx

    if max5<pmax
        n=0;
    end

pmax=max5;

end

%the center frequency
frekvens=f_0;

% Solve problem
fem.sol=femstatic(fem, ...
                'solcomp',{'p'}, ...
                'outcomp',{'p'}, ...
                'pname','freq_aco', ...
                'plist',[frekvens], ...
                'oldcomp',{}, ...
                'ntol',1.0E-7, ...
                'maxiter',50);

% get the solution only in chamber
u = postinterp(fem, 'abs(p)', d);

%save maximum pressure value in f-imp-matrix
p1(frekvens-f_tom,ii)=max(u);
```

```
%maximum pressure value
pmax=max(u);

n=1;

while n==1

    count=0;

    for step=[1 1 1]

    count=count+1;

    %defining the frequency to solve for, counting upwards
    frekvens=frekvens-step;

    % Solve problem
    fem.sol=femstatic(fem, ...
                'solcomp',{'p'}, ...
                'outcomp',{'p'}, ...
                'pname','freq_aco', ...
                'plist',[frekvens], ...
                'oldcomp',{}, ...
                'ntol',1.0E-7, ...
                'maxiter',50);

    % get the solution only in chamber
    u = postinterp(fem, 'abs(p)', d);

    %save maximum pressure value in f-imp-matrix
    p1(frekvens-f_tom,ii)=max(u);

    %maximum pressure value
    maxx(count)=max(u);
    end

    max5=max(maxx);

    clear maxx

    if max5<pmax
        n=0;
    end

pmax=max5;

end

%find the frequency with the highes pressure and
%define this as the new center frequency
%this will be the start frequency for the next impedans
f_0=find(p1(:,ii)==max(p1(:,ii)))+f_tom;

% Solve problem for the center frequency
```

```matlab
fem.sol=femstatic(fem, ...
                  'solcomp',{'p'}, ...
                  'outcomp',{'p'}, ...
                  'pname','freq_aco', ...
                  'plist',[f_0], ...
                  'oldcomp',{}, ...
                  'ntol',1.0E-7, ...
                  'maxiter',50);

% get the solution only in chamber
u = postinterp(fem, 'abs(p)', d);

data(1,ii)=imp;
data(2,ii)=f_0;
data(3,ii)=max(u);

% Plot solution
figure(ii),
postplot(fem, ...
         'tridata',{'abs(p)','cont','internal','unit','Pa'}, ...
         'trimap','jet(1024)', ...
         'title','Surface: Pressure [Pa]   Arrow: [v2x, v2y] [kg*m/(m*s^3)]', ...
         'axis',[-0.02015242232920353,0.043825232757259816,-0.01801613712448399,0.019012946859382925,-1,1]

end

%identify the non-zero elements
[row,col]=find(p1);

%define new pressure matrix, only with the non-zero elements
minrow=min(row);
maxrow=max(row);
mincol=min(col);
maxcol=max(col);
p2=(p1(minrow:maxrow,mincol:maxcol)).^(1/5);

%plot max pressure in f-imp-coordinate system
figure(ii+1),
imagesc([mincol:maxcol],[minrow:maxrow],p2)
```

Appendix F

Matlab script which locates the resonance in rotation

```
clear all
flclear fem

% COMSOL version
clear vrsn
vrsn.name = 'COMSOL 3.3';
vrsn.ext = '';
vrsn.major = 0;
vrsn.build = 405;
vrsn.rcs = '$Name:  $';
vrsn.date = '$Date: 2006/08/31 18:03:47 $';
fem.version = vrsn;

flbinaryfile='EIGENMODEDEPENDENCE.mphm';

% Geometry
clear draw
g17=flbinary('g17','draw',flbinaryfile);
draw.s.objs = {g17};
draw.s.name = {'CO2'};
draw.s.tags = {'g17'};
fem.draw = draw;
fem.geom = geomcsg(fem);

% Initialize mesh
fem.mesh=meshinit(fem, ...
                  'hauto',1, ...
                  'hmaxsub',[1,5e-4,2,5e-5]);

% Create a grid of points:
xx=linspace(-1.5e-4,0.00255,1000);
yy=linspace(-0.00155,0.00115,1000);
[xx,yy] = meshgrid(xx, yy);
d = [xx(:)'; yy(:)'];

%initialize
ii=0;
```

```
%start frequency
f_0=1.195957e6;

%eleminate zeroes in matrix to save memory
f_tom=1.19e6;

%impedance loop
for imp=[2e2 3e2 4e2 5e2 6e2 7e2 8e2 9e2]
ii=ii+1;

imp

%start frequency is set
frekvens=f_0;

% Application mode 1
clear appl
fem .dim = {'p'};
appl.mode.class = 'Acoustics';
appl.assignsuffix = '_aco';
clear bnd
bnd.Z = {imp};
bnd.type = {'IMP','cont','NA'};
bnd.nacc = {0,0,1};
bnd.ind = [1,1,1,2,2,2,2,2,2,2,2,2,2,2,2,1,3,3,3,3];
appl.bnd = bnd;
clear equ
equ.cs = {8500,1483};
equ.rho = {2300,1000};
equ.ind = [1,2];
appl.equ = equ;
appl.var = {'freq','5689'};
fem.appl{1} = appl;
fem.frame = {'ref'};
fem.border = 1;
clear units;
units.basesystem = 'SI';
fem.units = units;

% Global expressions
fem.globalexpr = {'v2x','real(p*conj(vx_aco))','v2y','real(p*conj(vy_aco))'};

% Multiphysics
fem=multiphysics(fem);

% Extend mesh
fem.xmesh=meshextend(fem);

% Solve problem
fem.sol=femstatic(fem, ...
                  'solcomp',{'p'}, ...
                  'outcomp',{'p'}, ...
                  'pname','freq_aco', ...
```

```
                        'plist',[frekvens], ...
                        'oldcomp',{}, ...
                        'ntol',1.0E-7, ...
                        'maxiter',50);

% get the solution only in chamber
u=max(max(rotation(fem)));
%u = postinterp(fem, 'abs(p)', d);

%save maximum pressure value in f-imp-matrix
p1(frekvens-f_tom,ii)=u;

%maximum pressure value
pmax=u;

n=1;

while n==1

    step=5;

    %defining the frequency to solve for, counting upwards
    frekvens=frekvens+step;

    % Solve problem
    fem.sol=femstatic(fem, ...
                    'solcomp',{'p'}, ...
                    'outcomp',{'p'}, ...
                    'pname','freq_aco', ...
                    'plist',[frekvens], ...
                    'oldcomp',{}, ...
                    'ntol',1.0E-7, ...
                    'maxiter',50);

    % get the solution only in chamber
    %u = postinterp(fem, 'abs(p)', d);
    u=max(max(rotation(fem)));

    %save maximum pressure value in f-imp-matrix
    p1(frekvens-f_tom,ii)=u;

    if u<pmax
        n=0;
    end

pmax=max(u);

end

%the center frequency
frekvens=f_0;

% Solve problem
fem.sol=femstatic(fem, ...
```

```
                  'solcomp',{'p'}, ...
                  'outcomp',{'p'}, ...
                  'pname','freq_aco', ...
                  'plist',[frekvens], ...
                  'oldcomp',{}, ...
                  'ntol',1.0E-7, ...
                  'maxiter',50);

% get the solution only in chamber
%u = postinterp(fem, 'abs(p)', d);
u=max(max(rotation(fem)));

%save maximum pressure value in f-imp-matrix
p1(frekvens-f_tom,ii)=(u);

%maximum pressure value
pmax=(u);

n=1;

while n==1

    step=5;

    %defining the frequency to solve for, counting upwards
    frekvens=frekvens-step;

    % Solve problem
    fem.sol=femstatic(fem, ...
                  'solcomp',{'p'}, ...
                  'outcomp',{'p'}, ...
                  'pname','freq_aco', ...
                  'plist',[frekvens], ...
                  'oldcomp',{}, ...
                  'ntol',1.0E-7, ...
                  'maxiter',50);

    % get the solution only in chamber
    %u = postinterp(fem, 'abs(p)', d);
    u=max(max(rotation(fem)));

    %save maximum pressure value in f-imp-matrix
    p1(frekvens-f_tom,ii)=(u);

    if(u)<pmax
        n=0;
    end

pmax=(u);

end

%find the frequency with the highes pressure and
%define this as the new center frequency
```

```
%this will be the start frequency for the next impedans
f_0=find(p1(:,ii)==max(p1(:,ii)))+f_tom;

frekvens=f_0;

% Solve problem
fem.sol=femstatic(fem, ...
                  'solcomp',{'p'}, ...
                  'outcomp',{'p'}, ...
                  'pname','freq_aco', ...
                  'plist',[frekvens], ...
                  'oldcomp',{}, ...
                  'ntol',1.0E-7, ...
                  'maxiter',50);

% get the solution only in chamber
%u = postinterp(fem, 'abs(p)', d);
u=max(max(rotation(fem)));

%save maximum pressure value in f-imp-matrix
p1(frekvens-f_tom,ii)=(u);

%maximum pressure value
pmax=(u);

n=1;

while n==1

    count=0;

    for step=[1 1 1 1 1]

    count=count+1;

    %defining the frequency to solve for, counting upwards
    frekvens=frekvens+step;

    % Solve problem
    fem.sol=femstatic(fem, ...
                      'solcomp',{'p'}, ...
                      'outcomp',{'p'}, ...
                      'pname','freq_aco', ...
                      'plist',[frekvens], ...
                      'oldcomp',{}, ...
                      'ntol',1.0E-7, ...
                      'maxiter',50);

    % get the solution only in chamber
    %u = postinterp(fem, 'abs(p)', d);
    u=max(max(rotation(fem)));

    %save maximum pressure value in f-imp-matrix
    p1(frekvens-f_tom,ii)=(u);
```

```matlab
    %maximum pressure value
    maxx(count)=(u);
    end

    max5=max(maxx);

    clear maxx

    if max5<pmax
        n=0;
    end

pmax=max5;

end

%the center frequency
frekvens=f_0;

% Solve problem
fem.sol=femstatic(fem, ...
                  'solcomp',{'p'}, ...
                  'outcomp',{'p'}, ...
                  'pname','freq_aco', ...
                  'plist',[frekvens], ...
                  'oldcomp',{}, ...
                  'ntol',1.0E-7, ...
                  'maxiter',50);

% get the solution only in chamber
%u = postinterp(fem, 'abs(p)', d);
u=max(max(rotation(fem)));

%save maximum pressure value in f-imp-matrix
p1(frekvens-f_tom,ii)=(u);

%maximum pressure value
pmax=(u);

n=1;

while n==1

    count=0;

    for step=[1 1 1 1 1]

    count=count+1;

    %defining the frequency to solve for, counting upwards
    frekvens=frekvens-step;

    % Solve problem
```

```
    fem.sol=femstatic(fem, ...
                'solcomp',{'p'}, ...
                'outcomp',{'p'}, ...
                'pname','freq_aco', ...
                'plist',[frekvens], ...
                'oldcomp',{}, ...
                'ntol',1.0E-7, ...
                'maxiter',50);

    % get the solution only in chamber
    %u = postinterp(fem, 'abs(p)', d);
    u=max(max(rotation(fem)));

    %save maximum pressure value in f-imp-matrix
    p1(frekvens-f_tom,ii)=(u);

    %maximum pressure value
    maxx(count)=(u);
    end

    max5=max(maxx);

    clear maxx

    if max5<pmax
        n=0;
    end

pmax=max5;

end

%find the frequency with the highes pressure and
%define this as the new center frequency
%this will be the start frequency for the next impedans
f_0=find(p1(:,ii)==max(p1(:,ii)))+f_tom

% Solve problem for the center frequency
fem.sol=femstatic(fem, ...
                'solcomp',{'p'}, ...
                'outcomp',{'p'}, ...
                'pname','freq_aco', ...
                'plist',[f_0], ...
                'oldcomp',{}, ...
                'ntol',1.0E-7, ...
                'maxiter',50);

% get the solution only in chamber
%u = postinterp(fem, 'abs(p)', d);
u=max(max(rotation(fem)))

rotV=rotation(fem);

data(1,ii)=imp;
```

```
data(2,ii)=f_0;
data(3,ii)=max(u);

N=1000;
x=linspace(-1.5e-4,0.00255,N);
y=linspace(-0.00155,0.00115,N);
xx=x;
yy=y;
[x,y] = meshgrid(x, y);

%Plot the computed values:
figure(ii),
pcolor(xx(30:N-30),yy(30:N-30),abs(rotV(30:N-30,30:N-30)))
shading interp
axis equal
colorbar
hold on

postplot(fem, ...
         'arrowdata',{'v2x','v2y'}, ...
         'arrowxspacing',300, ...
         'arrowyspacing',300, ...
         'arrowtype','arrow', ...
         'arrowstyle','proportional', ...
         'arrowcolor',[0.0,0.0,0.0], ...
         'title','Arrow: [v2x, v2y] [kg*m/(m*s^3)]', ...
         'axis',[-0.0032054798904736217,0.007525619374142739,-0.00327846273863774,0.0025557168419289562,-1
hold off
shg
end

%identify the non-zero elements
[row,col]=find(p1);

%define new pressure matrix, only with the non-zero elements
minrow=min(row);
maxrow=max(row);
mincol=min(col);
maxcol=max(col);
p2=(p1(minrow:maxrow,mincol:maxcol));

%plot max pressure in f-imp-coordinate system
figure(ii+1),
imagesc([mincol:maxcol],[minrow:maxrow],p2)

shg
```

Appendix G

Matlab script which calculates the maximum rotation in the water champer

```
clear all
flclear fem

% COMSOL version
clear vrsn
vrsn.name = 'COMSOL 3.3';
vrsn.ext = '';
vrsn.major = 0;
vrsn.build = 405;
vrsn.rcs = '$Name:  $';
vrsn.date = '$Date: 2006/08/31 18:03:47 $';
fem.version = vrsn;


flbinaryfile='EIGENMODEDEPENDENCE.mphm';

% Geometry
clear draw
g17=flbinary('g17','draw',flbinaryfile);
draw.s.objs = {g17};
draw.s.name = {'CO2'};
draw.s.tags = {'g17'};
fem.draw = draw;
fem.geom = geomcsg(fem);

% Initialize mesh
fem.mesh=meshinit(fem, ...
                  'hauto',1, ...
                  'hmaxsub',[1,5e-4,2,5e-5]);


%impedans
imp=1.25*343;

%start frekvens
```

```matlab
f0=1.46719e6;

%resonansfrekvenser fundet vha.eigenfrequency solveren
fR1=9.51869e5;

%counter
j=0;

% Application mode 1
clear appl
fem .dim = {'p'};
appl.mode.class = 'Acoustics';
appl.assignsuffix = '_aco';
clear bnd
bnd.Z = {imp};
bnd.type = {'IMP','cont','NA'};
bnd.nacc = {0,0,1};
bnd.ind = [1,1,1,2,2,2,2,2,2,2,2,2,2,2,2,1,3,3,3,3];
appl.bnd = bnd;
clear equ
equ.cs = {8500,1483};
equ.rho = {2300,1000};
equ.ind = [1,2];
appl.equ = equ;
appl.var = {'freq','5689'};
fem.appl{1} = appl;
fem.frame = {'ref'};
fem.border = 1;
clear units;
units.basesystem = 'SI';
fem.units = units;

% Global expressions
fem.globalexpr = {'v2x','real(p*conj(vx_aco))','v2y','real(p*conj(vy_aco))'};

% Multiphysics
fem=multiphysics(fem);

% Extend mesh
fem.xmesh=meshextend(fem);

f=fR1
    j=j+1;
    % Solve problem
     fem.sol=femstatic(fem, ...
                  'solcomp',{'p'}, ...
                  'outcomp',{'p'}, ...
                  'pname','freq_aco', ...
                  'plist',[f], ...
                  'oldcomp',{}, ...
                  'ntol',1.0E-7, ...
                  'maxiter',50);

rotation(fem)
```

Appendix H

Calculates the rotation

```
function rotV = rotation(fem)


%   Programstump der kan finde rotationen af <v2>

% Create a grid of points:
N=1000;
x=linspace(-1.5e-4,0.00255,N);
y=linspace(-0.00155,0.00115,N);
xx=x;
yy=y;
[x,y] = meshgrid(x, y);
d = [x(:)'; y(:)'];
% Evaluate the solution u at these points:
V2x = postinterp(fem, 'v2x', d);
V2x = reshape(V2x, size(x));
HX=(1.5e-4+0.00255)/N;
HY=(0.00155+0.00115)/N;
[V2xX,V2xY] = GRADIENT(V2x,HX,HY);   %finder gradienten af <v_2x>


V2y = postinterp(fem, 'v2y', d);
V2y = reshape(V2y, size(x));
[V2yX,V2yY] = GRADIENT(V2x,HX,HY);   %finder gradienten af <v_2y>


%rotationen er nu givet ved
rotV=V2yX-V2xY;
% Plot the computed values:
% % figure(1),
% % pcolor(xx(30:N-30),yy(30:N-30),abs(rotV(30:N-30,30:N-30)))
% % shading interp
% % axis equal
% % colorbar
% % hold on
% %
% % postplot(fem, ...
% %          'arrowdata',{'v2x','v2y'}, ...
% %          'arrowxspacing',300, ...
% %          'arrowyspacing',300, ...
% %          'arrowtype','arrow', ...
```

```
% %             'arrowstyle','proportional', ...
% %             'arrowcolor',[0.0,0.0,0.0], ...
% %             'title','Arrow: [v2x, v2y] [kg*m/(m*s^3)]', ...
% %             'axis',[-0.0032054798904736217,0.007525619374142739,-0.00327846273863774,0.00255571684192895
% % hold off
% % shg
```

Bibliography

[1] Henrik Bruus,
Theoretical Microfluidics, Oxford master series in condensed matter physics number 18,
Oxford University Press, Great Clarendon Street, Oxford OX2 6DP, 2008.

[2] Peder Skafte-Pedersen,
Acoustic forces on particles and liquids in microfluidic systems
Master's thesis, DTU Nanotech - Department of Micro- and Nanotechnology, DTU — Technical University
of Denmark, January 2008.

[3] *http://en.wikipedia.org/wiki/Reynolds_number*

[4] *http://www.maths.manchester.ac.uk/ suzanne/teaching/BLT/sec1.pdf*
The University of Manchester

[5] Nakhlé H. Asmar,
Partiel Differential Equations with Fourier Series and Boundary Value Problems, second edition,
Pearson Prentice Hall, Pearson Education Inc., Upper Saddle River, NJ 07458, 2005.

[6] COMSOL AB, *Heat Transfer Module User's Guide*, Version: August 2006 COMSOL 3.3,
COPYRIGHT 1994-2006 by COMSOL AB.

[7] Thomas Glasdam Jensen,
Acoustic radiation in microfluidic systems
Master's thesis, MIC — Department of Micro and Nanotechnology, DTU — Technical University of
Denmark, April 2007.

[8] S. M. Hagsäter,
Micro-PIV development and applications
Master's thesis, MIC — Department of Micro and Nanotechnology, DTU — Technical University of
Denmark, April 2007.

[9] Lifshitz and Landau, *Course of theoretical fluid mechanics*

[10] Charles kittel and Herbert Kroemer,
Thermal Physics, second edition,
W. H. Freeman and Company, New York, 1980.